Development of a Neurostimulation Method Using Pulsed Ultrasound

by

Yusuf Zahid Tufail

A Dissertation Presented in Partial Fulfillment
of the Requirements for the Degree
Doctor of Philosophy

Approved March 2011 by the
Graduate Supervisory Committee:

William Tyler, Chair
Carsten Duch
Jitendran Muthuswamy
Marco Santello
Stephen Tillery

ARIZONA STATE UNIVERSITY

May 2011

UMI Number: 3453551

All rights reserved

INFORMATION TO ALL USERS
The quality of this reproduction is dependent upon the quality of the copy submitted.

In the unlikely event that the author did not send a complete manuscript
and there are missing pages, these will be noted. Also, if material had to be removed,
a note will indicate the deletion.

UMI®
Dissertation Publishing

UMI 3453551
Copyright 2011 by ProQuest LLC.
All rights reserved. This edition of the work is protected against
unauthorized copying under Title 17, United States Code.

ProQuest®

ProQuest LLC
789 East Eisenhower Parkway
P.O. Box 1346
Ann Arbor, MI 48106-1346

ABSTRACT

Neurostimulation methods currently include deep brain stimulation (DBS), optogenetic, transcranial direct-current stimulation (tDCS), and transcranial magnetic stimulation (TMS). TMS and tDCS are noninvasive techniques whereas DBS and optogenetic require surgical implantation of electrodes or light emitting devices. All approaches, except for optogenetic, have been implemented in clinical settings because they have demonstrated therapeutic utility and clinical efficacy for neurological and psychiatric disorders. When applied for therapeutic applications, these techniques suffer from limitations that hinder the progression of its intended use to treat compromised brain function. DBS requires an invasive surgical procedure that surfaces complications from infection, longevity of electrical components, and immune responses to foreign materials. Both TMS and tDCS circumvent the problems seen with DBS as they are noninvasive procedures, but they fail to produce the spatial resolution required to target specific brain structures. Realizing these restrictions, we sought out to use ultrasound as a neurostimulation modality. Ultrasound is capable of achieving greater resolution than TMS and tDCS, as we have demonstrated a ~2mm lateral resolution, which can be delivered noninvasively. These characteristics place ultrasound superior to current neurostimulation methods. For these reasons, this dissertation provides a developed protocol to use transcranial pulsed ultrasound (TPU) as a neurostimulation technique. These investigations

implement electrophysiological, optophysiological, immunohistological, and behavioral methods to elucidate the effects of ultrasound on the central nervous system and raise questions about the functional consequences. Intriguingly, we showed that TPU was also capable of stimulating intact sub-cortical circuits in the anesthetized mouse. These data reveal that TPU can evoke synchronous oscillations in the hippocampus in addition to increasing expression of brain-derived neurotrophic factor (BDNF). Considering these observations, and the ability to noninvasively stimulate neuronal activity on a mesoscale resolution, reveals a potential avenue to be effective in clinical settings where current brain stimulation techniques have shown to be beneficial. Thus, the results explained by this dissertation help to pronounce the significance for these protocols to gain translational recognition.

DEDICATION

This is for the individuals that have provided me with the time and tools to uncover my path in this life. This is especially dedicated to those young minds that have witnessed my growth, one day you too will have it. Thank you all.

ACKNOWLEDGMENTS

My greatest thanks must go to Dr. Jamie Tyler. As a mentor and a vital advisor, Jamie has played an integral role throughout the progression of my dissertation and in my advancement as a young scientist. I would like to extend my appreciation to Jamie for creating the opportunity for me to pursue my doctoral degree, and the invaluable advice and unique exposure to my scientific training and research that he has endlessly provided.

For their openness, support, and excitement throughout the culmination of my research, I would like to thank and lend my appreciation to Dr. Steve Helms-Tillery, especially for the time he spent teaching and advising during my early non-degree seeking year. I would also like to thank Dr. Carsten Duch for his rigor and honest input, and the remainder of my thesis committee Dr. Marco Santello and Dr. Jitendran Muthuswamy for sharing their scientific knowledge and support for my dissertation.

My progress would not have been conceivable if it wasn't for Dr. Brian Smith and everyone involved with the Bridge to the Doctorate and MGE@MSA fellowship for providing essential career training, and financial support throughout my graduate career.

Additionally, great thanks are due to my lab mates who are my best friends and dear colleagues. If it was not for the supportive and team driven atmosphere they provided none of this would have been possible. I

would like to thank Monica Li for her true faith and never ending support, Joseph Georges who will one day return to being a medical student, Anna Yoshihiro for her dedication and perseverance and Liliana Rincon for her patience and honest advice.

My unique experience in graduate school was heavily influenced by my life outside the lab, a critical balance difficult to maintain. For that I would like to thank Stephen Woo, Christopher Blockwitz, and Amanda Ferrao for providing a supportive, exciting, and stress free lifestyle outside the lab.

Finally, I acknowledge my parents, Zahid Tufail and Yolanda Tufail for the wisdom they have imparted on me and the life they have worked so hard for so that I may pursue my goals.

TABLE OF CONTENTS

Page

LIST OF TABLES viii

LIST OF FIGURES ix

CHAPTER

1 INTRODUCTION 1

2 REMOTE EXCITATION OF NEURONAL CIRCUITS USING LOW-INTENSITY, LOW-FREQUENCY ULTRASOUND 10

Introduction 11

Materials and Methods 15

Results 21

Discussion 35

Conclusion 43

References 43

3 TRANSCRANIAL PULSED ULTRASOUND STIMULATES INTACT BRAIN CIRCUITS 50

Introduction 51

Experimental Procedures 54

Results 64

Discussion 92

References 97

4 ULTRASONIC NEUROMODULATION: BRAIN STIMULATION WITH TRANSCRANIAL ULTRASOUND 104

CHAPTER Page

Introduction 105

Development of the Protocol 107

Experimental Design and Considerations 118

Materials and Methods 127

Procedure 130

Anticipated Results 166

References 169

5 DISCUSSION 176

Mechanismsm Behind Ultrasound Induced Neuronal Activity 178

Biosafety of Ultrasound 181

Innovative Technology 185

Applications for Clinical Models 187

REFERENCES 192

LIST OF TABLES

Table Page

1. Potential problems and solutions to achieving UNMOD success 149

LIST OF FIGURES

Figure Page

1. Generation and propagation of LILFU waveforms through neuronal tissue 24
2. LILFU stimulates sodium transients mediated by voltage-gated sodium channels in hippocampal neurons 25
3. LILFU triggers voltage-dependent somatic and presynaptic Ca^{2+} transients in neurons 28
4. LILFU waveforms transmitted through whole brains are capable of stimulating calcium transients 29
5. LILFU stimulates SNARE-mediated synaptic vesicle exocytosis and central synaptic transmission 33
6. Influence of LILFU on putative excitatory hippocampal CA3-CA1 synapses 34
7. Construction and characterization of low-intensity ultrasound stimulus waveforms for the transcranial stimulation of intact brain circuits 66
8. Low-intensity pulsed US stimulates neuronal activity in the intact mouse motor cortex 69
9. Transcranial stimulation of motor cortex with pulsed US functionally activates descending corticospinal motor circuits in intact mice 70

10. Interactions of the acoustic frequency and acoustic intensity of stimulus waveforms on descending corticospinal circuit activation 76

11. Spatial distribution of neuronal activation triggered by transcranial pulsed US 85

12. Transcranial stimulation of mouse cortex with low-intensity pulsed US is safe 86

13. Transcranial stimulation of the intact mouse hippocampus with pulsed ultrasound 91

14. Basic ultrasonic brain stimulation rig and UNMOD waveform generation 162

15. Preparation of electromyographic recordings to monitor US-evoked stimulation of intact motor cortex 164

16. Electrophysiological recordings in response to brain stimulation with transcranial pulsed ultrasound 165

17. Induction and disruption of electrographic seizure activity using UNMOD 166

Chapter 1

INTRODUCTION

The search for answers to questions about our biology has inspired and challenged fields of science to produce technology that can meet such demands. Neuroscience, a fast-paced emerging field has done just that. Neuroscience has brought molecular, physiological, and imaging techniques to the leading edge of research. Congruently, neurostimulation techniques have helped to unveil the adaptive and dynamic nature of the nervous system, formally known as neuronal plasticity.

A hallmark of neuronal plasticity was discovered in 1973, when Tim Bliss, Terje Lømo, and Tony Gardner-Medwin discovered that high frequency stimulation could produce lasting changes of synaptic weights to the dentate gyrus of the hippocampus (Bliss and Gardner-Medwin 1973; Bliss and Lomo 1973). This was achieved using electrolyticaly sharpened tungsten wire to stimulate the axons of the perforant pathway while recording with NaCl filled glass electrodes.

It was their deciphering protocols that elucidated a fundamental neuronal property which grew into a dogma that has become a lasting basis for learning and memory.

The technique became a conventional means to stimulate nervous tissue. Since then, neurostimulation techniques have developed into more manipulative yet elegant means, and have continued to unveil intriguing properties of the nervous system.

Advances in molecular and genetic techniques have developed a superb means to stimulate nervous tissue using photons of particular wavelengths. From the unicellular green alga *Chlamydomonas reinhardtii*, a rhodopsin deemed Channelrhodopsin-2 (ChR2) had been isolated. The nature of this light-gated cation channel permits its incorporation into specific populations of neurons through the customizing of plasmids and viral vectors providing unrivaled spatial and genetic isolation. It has provided investigators with millisecond temporal precision of neuronal depolarization and synaptic events (Boyden, Zhang et al. 2005; Zhang, Wang et al. 2007).

This technology has birthed revolutionizing techniques that have provided mechanisms to answer and reaffirm some of neuroscience's intriguing questions, a field now known as optogenetics. Such examples include the use of ChR2 to more effectively and precisely map motor cortex *in vivo* (Ayling, Harrison et al. 2009). It has even demonstrated potential clinical efficacy for neurological and psychiatric disorders such as Parkinson's, major depression, and epilepsy (Gradinaru, Thompson et al. 2007; Tonnesen, Sorensen et al. 2009). The light induced excitation of ChR2 pyramidal cells of M1 layer V has given new insight into the therapeutic effects observed with deep brain stimulation (DBS) for patients with refractory Parkinson's disease (Gradinaru, Thompson et al. 2007). Through a series of trials designed to dissect the physiology and circuitry involved with rodents observing Parkinsonian-like motor behaviors, it was

found that discrete high-frequency stimulation (HFS) of afferents to the subthalamic nucleus (STN) from M1 produced robust ameliorating effects on rodent motor behavior (Gradinaru, Thompson et al. 2007).

The robust symptoms of motor-related neurological disorders provide a model that can be sufficiently manipulated and studied, another such model is epilepsy. Epileptic activity can be described as the excessive and uncontrollable discharging of neuronal populations. It was hypothesized that control could be regained over such pathologic conditions through optical means (Tonnesen, Sorensen et al. 2009). By transducing the halorhodopsin isolated from the archaebacterium *Natronomonas pharaonis* (NpHR) into the hippocampal formation, this light-gated chloride ion pump would bias the membrane polarization and quell the overactivation of neurons. Using protocols to induce epileptic activity, Tønnesen et al. demonstrated just that. Electrically induced epileptiform activity using stimulation train-induced bursting (STIB) was suppressed while slices were simultaneously exposed to light activating the halorhodopsin (573-613 nm) (Tonnesen, Sorensen et al. 2009).

In addition to providing novel insight into the functional circuitry of normal and compromised neural tissue, optogenetics has provided evidence to assist in controversial neurophysiological phenomena. One such issue is the interpretation of the blood-oxygen level dependent (BOLD) signal acquired through functional magnetic resonance imaging (fMRI). fMRI is a noninvasive imaging tool used to observe and quantify

brain activity through the magnetic detection of hemoglobin in its oxygenated and deoxygenated states, otherwise known as the BOLD signal. The BOLD signal has been loosely used to interpret changes in neuronal activity, minding the assumption that general activity elicits a metabolic demand that is satiated by increased delivery of oxygen through the vascular system. Combining the noninvasive imaging power of fMRI with the optogenetic control of specific neuronal populations, Lee et al. were able to soundly demonstrate that the photonic stimulation of excitatory neurons could elicit BOLD signals with classical kinetics (Lee, Durand et al.).

Despite the immense advantages optogenetic approaches may provide, the requirement of introducing foreign genes into a human brain has remained an obstacle for the expansion of this technology to clinical practice. One approach that has gained extensive clinical utility is deep brain stimulation (DBS). Used for the treatment of chronic pain since the 1960's (Hosobuchi, Rossier et al. 1979), DBS is a procedure that uses surgically implanted electrodes to focally stimulate specific brain regions. Despite the vague understanding of the mechanisms behind its therapeutic utility, DBS was approved by the Food and Drug Administration (FDA) for tremor in 1997, followed by approval in 2002 for the targeted stimulation of the subthalamic nucleus (STN) and the globus pallidus interna for other movement disorders (Andrews 2003). Moreover, the investigations into psychiatric illnesses that are thought to be

manifested by the dysfunction of specific brain region(s) have implicated such regions as the subcallosal cingulate (SCC) gyrus as a DBS target for treatment resistant depression (TRD) (Lozano and Snyder 2008; Holtzheimer and Mayberg 2011).

One of the many concerns that arise from using DBS as a neurologic or psychiatric intervention is that most cases have provided evidence for only acute remission, lacking permanence for the intended treatment. This is partly because we lack the understanding of how DBS specifically works and what it means to electrically stimulate isolated regions of the brain. While these concerns are currently under tremendous investigation, other means for stimulating the central nervous system have been developed.

More efficacious procedures that may obtain a broader clinical impact because of its noninvasive nature include both transcranial magnetic stimulation (TMS) and transcranial direct current stimulation (tDCS). TMS manipulates the principles of electromagnetic induction to evoke current densities in the brain (Wagner, Valero-Cabre et al. 2007). In 1985, A.T. Barker et al. successfully demonstrated that magnetic stimulation of the motor cortex in humans could produce muscle action potentials (Barker, Jalinous et al. 1985). This report stressed that the pain-free, lack of contact with the scalp, noninvasive, and straightforward application of magnetic stimulation rendered this procedure superior to electrical stimulation. Since then, this technique has been applied to

investigating cognitive tasks in search of functional networks using a combination of TMS and fMRI (Driver, Blankenburg et al. 2009). Additionally, TMS has been used to investigate brain regions involved with mental state reasoning, reward choice, treatment of schizophrenia, brain injury and stroke (Bashir, Mizrahi et al. 2010; Figner, Knoch et al. 2010; Poulet, Haesebaert et al. 2010; Young, Camprodon et al. 2010).

Recently gaining prominence and greater clinical attention, tDCS is another noninvasive technique that has shared similar utility as TMS. tDCS consists of attaching electrodes of different polarity to the surface of the scalp in various locations in order to excite neural tissue (Utz, Dimova et al. 2010). Used as a neuromodulation tool, tDCS can generate both immediate and long lasting changes in neuronal excitability (Wagner, Valero-Cabre et al. 2007). It is hypothesized that anodal stimulation (surface-positive) increases spontaneous firing rate and the excitability of cortical neurons, whereas cathodal (surface-negative) stimulation induces hyperpolarization of cortical neurons and thus produces the opposite, a decrease in firing rate and excitability (Utz, Dimova et al. 2010). Other factors that have been considered to affect the delivery and design of tDCS are the spatial inhomogeneities of the brain and the differential sensitivity of neuronal and non-neuronal components (Creutzfeldt, Fromm et al. 1962; Purpura and McMurtry 1965; Utz, Dimova et al. 2010). During early investigations of topically manipulating electrical brain activity, I. B. Gartside conducted a clever set of experiments that produced strong

evidence for an “after effect” that allured the involvement of synaptic modifications (Gartside 1968; Gartside 1968) and perhaps arousing suspicion for cortical plasticity. Again, because of its noninvasive approach, the usage of tDCS in scientific and clinical applications has significantly preceded its fundamental research stages, an unconventional process that has resulted with concerns about fidelity and mechanisms behind the clinical benefits. As investigations continue, proposed mechanisms arise, and controversies persist, efforts towards implementing other modes of brain stimulation could diversify the interventional toolbox and create new avenues for neurostimulation, unveil neurophysiological properties, and spur innovative technologies.

It is the purpose of this dissertation to report the development of a novel neurostimulation method using pulsed ultrasound. Considering the extensive development and applications for current brain stimulation approaches, we have proposed a technique that demonstrates an ability to circumvent the limitations observed with the stimulation methods mentioned by using pulsed ultrasound.

The literature detailing the biological interactions with ultrasound is extensive, but mirroring the progression of other stimulation interventions, the research on ultrasound has mostly focused on the resulting phenomena and much less attention has been devoted to the underlying mechanisms. By maintaining a goal to advance the translation of our work, we aimed to elucidate some of the fundamental properties in efforts to

discover suitable applications. Specifically, my dissertation research addresses the following questions:

1) Can pulsed ultrasound alter the membrane polarization and ionic conductance in neurons? (Chapter 2)
2) Is pulsed ultrasound capable of noninvasively stimulating brain activity *in vivo*? (Chapter 3)
3) What are the neuromodulation capabilities of pulsed ultrasound with regards to neurological impairments such as epilepsy? (Chapter 4)

Using electrophysiology and optical techniques, chapter 2 employs a hippocampal slice culture model to investigate the effects of ultrasound on sodium and calcium ion conductance, and synaptic transmission.

Chapter 3 transcends observations collected in the previous chapter in order to apply them to an *in vivo* mouse model. This chapter explores the acoustic parameters that influence neuronal activity by direct cortical and subcortical electrical recordings. Additionally, we explored the functional output of acoustically stimulating cortico-spinal circuits and assessed safety qualities observed from using our waveforms.

Finally, chapter 4 provides a detailed protocol to achieve neurostimulation using our transcranial pulsed ultrasound (TPU) methods. In completion, we provide preliminary data that suggests the efficacious use of TPU for acute treatment during kainic acid induced (KA) epileptic episodes. The study of the effects of ultrasound on brain circuit

dysfunction has permitted us with the creation of ultrasonic neuromodulation (UNMOD) and a starting point for future applications using US for brain stimulation.

Chapter 2

REMOTE EXCITATION OF NEURONAL CIRCUITS USING LOW-INTENSITY, LOW-FREQUENCY ULTRASOUND

Possessing the ability to noninvasively elicit brain circuit activity yields immense experimental and therapeutic power. Most currently employed neurostimulation methods rely on the somewhat invasive use of stimulating electrodes or photonemitting devices. Due to its ability to noninvasively propagate through bone and other tissues in a focused manner, the implementation of ultrasound (US) represents a compelling alternative approach to current neuromodulation strategies. Here, we investigated the influence of low-intensity, low-frequency ultrasound (LILFU) on neuronal activity. By transmitting US waveforms through hippocampal slice cultures and ex vivo mouse brains, we determined LILFU is capable of remotely and noninvasively exciting neurons and network activity. Our results illustrate that LILFU can stimulate electrical activity in neurons by activating voltage-gated sodium channels, as well as voltage-gated calcium channels. The LILFU-induced changes in neuronal activity were sufficient to trigger SNARE-mediated exocytosis and synaptic transmission in hippocampal circuits. Because LILFU can stimulate electrical activity and calcium signaling in neurons as well as central synaptic transmission we conclude US provides a powerful tool for remotely modulating brain circuit activity.

Introduction

Neuromodulation techniques such as deep brain stimulation (DBS) and repetitive transcranial magnetic stimulation (rTMS) have gained widespread attention due to their therapeutic utility in managing numerous neurological/psychiatric diseases (Wagner, Valero-Cabre et al. 2007). The field of neural control has recently made significant advances by demonstrations of millisecond optical control of individual neurons and synapses in intact brain circuits (Zhang, Wang et al. 2007). Ultrasound (US) as a means of exciting (Gavrilov, Gersuni et al. 1976) and reversibly suppressing (Fry, Ades et al. 1958) neuronal activity was shown to be effective on a gross level several decades ago. Since then however, explorations into the use of US as a neurostimulation tool have been relatively sparse. The focus has instead been on employing more traditional approaches such as pharmacological, electrical, magnetic, and photonic stimulation of neuronal circuits. Coupling its ability to interact with biological tissues (ter Haar 2007) and its noninvasive transmission through skull bone and other biological tissues in a focused manner (Hynynen and Jolesz 1998; Clement and Hynynen 2002; Clement 2004), US holds promise as a potentially powerful neurostimulation tool (Fry 1968; Gavrilov, Tsirulnikov et al. 1996), which may be capable of replacing currently invasive DBS strategies. Ultrasound can produce bioeffects by acting through thermal and/or nonthermal mechanisms as it propagates through tissues in pulsed or continuous waveforms (Dinno, Crum et al.

1989; Dalecki 2004; O'Brien 2007; ter Haar 2007). Therapeutic US can be broadly characterized as low-power/low-intensity or high-power/high-intensity (Dinno, Crum et al. 1989; Dalecki 2004; O'Brien 2007; ter Haar 2007). High-intensity focused ultrasound (HIFU) used in the thermal ablation of tissue implements peak power levels often exceeding 1000 W/cm2, whereas non-thermal therapeutic effects of US have been well described at power levels ranging from 30–500 mW/cm2 (Dalecki 2004; ter Haar 2007). Modulation of ionic conductance produced by adiabatic processes as US propagates rapidly and transiently through cellular membranes may alter the activity of individual neurons due to the elastic nature of lipid bilayers and the spring-like mechanics of many transmembrane protein channels. In partial support of this hypothesis, low-power US has been shown to influence the membrane conductance of frog skin epidermis (Dinno, Crum et al. 1989). In addition, US exposure can induce a reversible increase in the internal Ca2+ concentration of fibroblasts (Mortimer and Dyson 1988). In rat thymocytes, stimulation with US can modulate K+ influx and efflux (Chapman, MacNally et al. 1980). Interestingly, many voltage-gated ion channels, as well as neurotransmitter receptors possess mechanosensitive properties that render their gating kinetics sensitive to transient changes in lipid bilayer tension (Sukharev and Corey 2004; Morris and Juranka 2007). Whether or not ion channels can be modulated by US in neurons has remained unknown. Several investigations have demonstrated however that US

modulates neuronal activity by enhancing and/or suppressing the amplitudes and/or conduction velocities of evoked nerve potentials (Fry, Wulff et al. 1950; Fry, Ades et al. 1958; Young and Henneman 1961; Gavrilov, Gersuni et al. 1976; Foster and Wiederhold 1978; Mihran, Barnes et al. 1990; Rinaldi, Jones et al. 1991; Bachtold, Rinaldi et al. 1998; Tsui, Wang et al. 2005). In a pioneering study, Fry and colleagues (1950) first demonstrated US is capable of modulating neuronal activity by reporting the temporary suppression of spontaneous activity following US transmission through crayfish ventral nerve cords (Fry, Wulff et al. 1950). Transmitting US through the lateral geniculate nucleus of intact cats, Fry and colleagues (1958) demonstrated that high-power US reversibly suppressed light-evoked potentials recorded in the visual cortex (Fry, Ades et al. 1958). Rinaldi and colleagues (1991) demonstrated that 2.5 to 15 min irradiation of hippocampal slices with0.75 MHz US (temporal average intensity; ITA: 80 W/cm2), significantly reduces the amplitude of evoked potentials in CA1 pyramidal neurons. In the dentate gyrus of hippocampal slices, focused US pulses have been shown to both enhance and suppress electrically evoked field potentials (Bachtold, Rinaldi et al. 1998). In cat saphenous nerve bundles it has been demonstrated that focused US is capable of differentially effecting Ad- and C-fibers depending on the intensity and duration of US irradiation (Young and Henneman 1961). In excised frog sciatic nerve bundles, Tsui and colleagues (2005) reported that a temporal average intensity of 1 W/cm2

continuous wave (5 min) US (3.5 MHz) increased the amplitude of compound action potentials (CAP), while both 2 and 3 W/cm2 intensities decreased CAP amplitudes. Mihran and colleagues (1990) also reported differential excitatory and inhibitory effects of US on frog sciatic CAPs using relatively short irradiation times by delivering 500 ms US pulses (2.0–7.0 MHz) with peak intensities ranging from 100–800 W/cm2. Direct activation of the cat auditory nerve has been achieved in vivo using 5-MHz US pulses (68 msec; ,30 W/cm2) (Foster and Wiederhold 1978). In human subjects, focused US pulses have been shown to activate deep nerve structures in the hand by differentially producing tactile, thermal, and pain sensations (Gavrilov, Gersuni et al. 1976). Although numerous intriguing studies examining the influence of US on neuronal activity have been conducted, these previous investigations have implemented high-intensity US, which can destroy nervous tissue. Thus, we decided to investigate the influence of low-intensity ultrasound on neuronal activity. Most of the prior investigations examining the effect of US on neuronal activity also used high-frequency US (.1 MHz; for exceptions see (Gavrilov, Gersuni et al. 1976; Rinaldi, Jones et al. 1991; Bachtold, Rinaldi et al. 1998), which has larger attenuation coefficients compared to lower frequency ultrasound. Medical diagnostic US typically operates from 1 to 15 MHz while therapeutic US is usually conducted using acoustic frequencies around 1 MHz (O'Brien 2007). We chose to pursue our investigations here using low-frequency US (0.44–0.67 MHz) since both mathematical models and

experimental data indicate the optimal gain between transcranial transmission and brain absorption for US is ,0.60–0.70 MHz (Hayner and Hynynen 2001; White, Clement et al. 2006). Detailed cellular investigations into the influence of US on neuronal activity are lacking and the mechanisms underlying US modulation of neuronal activity remain unknown. By optically monitoring changes in ionic conductance in individual neurons and synaptic transmission from individual release sites we investigated the influence of low-intensity, low-frequency ultrasound (LILFU) on central nervous system activity.

Materials and Methods

Preparation of slice cultures and ex vivo brains

All procedures involving mice were conducted in accordance with federal guidelines and protocols approved by the Institutional Animal Care and Use Committee at Arizona State University. Hippocampal slice cultures were prepared from postnatal day 7–8 thy-1-spH, thy-1-YFP, or wild-type mice similar to previously described methods (Stoppini, Buchs et al. 1991). Briefly, transverse hippocampal slices (,400 mm thick) were made using a wire slicer (MX-TS, Siskiyou, Inc., Grants Pass, Oregon, USA) and maintained in vitro on Millicell CM filter inserts (PICMORG50, Millipore, Bedford, MA) in a 36uC, 5% CO2, humidified (99%) incubator. Slices were used for experiments between 7 and 12 days in vitro. In some experiments to cleave SNARE-proteins, BoNT/A (250 ng/mL) was added

to the slice culture media 24–36 h prior to use. We prepared ex vivo brains using the following approach. Following CO2 inhalation, wild-type mice were rapidly decapitated and their brains were removed. The dura was carefully removed and the brains were then placed in ice-cold artificial CSF (aCSF) containing (in mM) 83 NaCl, 2.5 KCl, 3.3 MgSO4, 1 NaH2PO4, 26.2 NaHCO3, 22 glucose, 72 sucrose, and 0.5 CaCl2, and equilibrated with 95% O2/5% CO2. Brains were allowed to recover for 5 min in the ice-cold aCSF before recovering for, 20 min at 37°C. Following this recovery period, ex vivo brains were bulk loaded with OGB-1 AM (Invitrogen, Carlsbad,
California, USA).

Loading of slice cultures and ex vivo brains with fluorescent ion indicators

In order to load slice cultures prepared from wild-type mice with CoroNa Green AM (Invitrogen, Carlsbad, California, USA), 5 mL 20% Pluronic F-127 in DMSO (Invitrogen) was added to a 50 mg vial of CoroNa Green AM. The dye solution was then vortexed for 15 min before adding 100 mL culture medium. We then added 5 mL of the dye containing solution to 1 mL culture medium underneath culture inserts, as well as adding 5 mL to the surface of slices. Following a 10 min incubation time at 36°C, slices were washed three times with slice culture medium, allowed to recover an additional 10 min, and then used for experiments. To load slice cultures with OGB-1 AM, we added 2 mL 20% Pluronic F-127 in

DMSO and 8 mL DMSO to a 50 mg vial of OGB-1 AM. The dye-containing solution was then vortexed for 30 M before adding 90 mL culture media. We next added 20 mL of this dye-containing solution to 3 mL culture medium and incubated slices in this solution for 30–40 min at 37uC. Slices were washed three times with slice culture medium, then loaded with sulforhodamine 101 (Invitrogen; 10 mM in slice culture medium for 15 min) or allowed to recover for 30 min prior to an experiment. To load ex vivo brains with OGB-1 AM we used a procedure similar to above, but substituted the slice culture medium for dissection aCSF (see above)–we added 60 mL of the dye-containing solution to 9 mL dissection aCSF. Brains were loaded for 30 min at room temperature then rinsed three times and allowed to recover for an additional 30 min in dissection aCSF at room temperature before use.

Confocal imaging and whole-cell patch-clamp recordings

Slice cultures or whole ex vivo brains were transferred to recording chambers containing recording aCSF (in mM) 136 NaCl, 2.5 KCl, 1.3 MgSO4, 10 HEPES, 10 glucose, and 2.5 CaCl2, pH 7.4 at room temperature. Recording chambers were affixed above US transducers on a custom built-stage on an Olympus Fluoview FV-300 laser-scanning confocal microscope (Olympus America, Inc., Center Valley, Pennsylvania, USA). Excitation of spH, OGB-1 AM, and CoroNa Green AM was performed using the 488 nm laser-line of an argon laser and in

some experiments DiI was excited using a 546 nm HeNe laser. Time-series images were acquired using 20x (0.5 NA) or 40x (0.8 NA) Olympus UMPlanFL water-immersion lens. Slice recording chambers consisted of culture inserts placed inside an aCSF reservoir held in place with either vacuum grease on the silicon face of the transducer. This approach produced a 4.5 mm standoff distance between the face of the transducer and the imaging plane on the surface of slices. In a subset of experiments, slice cultures (n=5) were mounted near the top of an aCSF column in a 500 mL beaker containing immersed US transducers, which were affixed to the bottom beakers to provide a 45 mm standoff distance. To image ex vivo brains, the ventral surface of whole ex vivo brains were glued to the bottom of polystyrene 6-well plates using superglue, which were filled with aCSF and mounted above US transducers using ultrasonic coupling gel. Confocal imaging of OGB-1 fluorescence was conducted on the superficial dorsal surface of ex vivo brains during transmission of LILFU waveforms from the ventral surface of the brain. In a subset of experiments we performed whole-cell current clamp recordings from visually identified CA1 pyramidal neurons using standard approaches. Briefly, patch electrode pipettes filled with an intracellular solution containing (in mM) 130 KCl, 10 Na-HEPES, 10 Di-Tris-P-creatine, 0.2 EGTA, 3 Mg-ATP, and 0.5 Na-GTP, 280–290 mOsm, pH 7.2; the final resistance of these unpolished patch electrodes was 5–7 MΩ. Current clamp recordings were performed using a MultiClamp 700B patchclamp amplifier with pCLAMP 10 software

(Molecular Devices, Sunnyvale, California, USA). Following 5–10 min of whole-cell access, changes in membrane voltage were recorded in response to stimulation with LILFU waveforms.

Generation and characterization of LILFU waveforms

In our studies we used custom built PZT ultrasound transducers (d = 35 mm) having a single quarter-wave matching layer, a center frequency of 0.53 MHz, and a 26 dB fractional bandwidth of 65% with two peaks (0.44 MHz, 0.66 MHz). LILFU waveforms used as stimuli were generated by repeating pulse trains of US tone bursts at a pulse repetition frequency until a desired number of tone bursts had been generated (Figure 1B). Ultrasound tone bursts were generated by trains of square waves (0.2 msec) with variable amplitudes using an Agilent 33220A function generator. To produce final plate voltages delivered to transducers, square waves were further amplified (50 dB gain) using an ENI 240L RF amplifier. Square waves were delivered between 0.44–0.67 MHz depending on the acoustic frequency desired, while the number of square waves driving each US tone burst equaled the number of acoustic cycles desired for a given US tone burst. Each US tone burst (pulse) contained between 1 and 50,000 acoustic cycles depending on the LILFU waveform generated. US tone bursts (Figure 1B) were repeated at a pulse repetition frequency by triggering the above referenced function generator with a second Agilent 33220A function generator. Pulse

repetition frequencies were either a constant frequency or a swept waveform. Our primary LILFU waveform (LILFU-1) had the following properties: f= 0.44 MHz, TBD= 22.7 ms, c/tb = 10, PRF = 5 sec sweep 0–100 Hz, and Ntb= 250. To characterize LILFU power levels, we recorded voltage waveforms produced by US pressure waves using a hydrophone (HNR 500, Onda Corporation, Sunnyvale, California, USA) and an Agilent DSO6012A 100 MHz digital oscilloscope (Agilent Technologies, Inc., Santa Clara, California, USA). To confirm transducers were operating at the intended acoustic frequency, we performed an FFT on hydrophone voltage traces recorded in response to US tone bursts. All pressure waves produced by LILFU waveforms were measured at points corresponding to tissue positions in the actual recording chambers by positioning the hydrophone face using a xyz micromanipulator (MP-225, Novato, CA, USA) mounted on the vibration isolation table attached to the microscope stage. The position of slices in recording chambers was held consistent across experiments. We measured acoustic intensities with and without slices in the recording chamber and found no effect of the presence of a slice on the acoustic waveform. The acoustic pressure and ultrasonic intensities (IPA and ITA) were calculated using published equations and technical standards established by the American Institute of Ultrasound in Medicine and the National Electrical Manufacturers Association (NEMA 2004).

Data analysis

Confocal images were analyzed offline using ImageJ (http://rsb.info.nih.gov/ij/) or the Olympus Fluoview 5.0 software. We express changes in spH fluorescence as a percent change from baseline fluorescence levels. For OGB-1 and CoroNa Green signals, we calculated DF/F0 using standard approaches where DF=F2F0. LILFU waveforms and electrophysiological analyses were performed offline using Igor Pro (WaveMetrics, Lake Oswego, Oregon, USA). Data shown are mean ± S.E.M.

Results

LILFU activates voltage-gated sodium channels in neurons

We transmitted LILFU waveforms through hippocampal slice cultures from remotely positioned tissue-matched piezoelectric (PZT) transducers (Figure 1A). We constructed LILFU waveforms by repeating US tone bursts at variable pulse repetition frequencies (Figure 1B). Measured using a needle hydrophone a points in the recording chamber, which corresponded to slice positions, the predominant LILFU waveform used in our studies (LILFU-1) had a pulse average intensity (IPA) of 2.9 W/cm2 and a temporal average intensity (ITA) of 23 mW/cm2. Figure 1C illustrates a typical pressure wave obtained for a single US tone burst used in the construction of LILFU-1.

By imaging organotypic hippocampal slice cultures bath-loaded with the Na+ indicator CoroNa Green AM [27], we found LILFU-1 triggered Na+ transients in hippocampal CA1 pyramidal neurons ($\Delta F/F0$ = 0.05±0.006, n = 24, 6 slices; Figure 2A). Addition of the voltage-gated Na+ channel pore blocker tetrodotoxin (TTX; 1 μm), blocked Na+ transients evoked by LILFU-1 (Figure 2A). These observations indicate that LILFU-1 increased the Na+ conductance in hippocampal neurons by stimulating the opening of voltage-gated Na+ channels. We next aimed to determine if LILFU waveforms were also capable of triggering action potentials in CA1 pyramidal neurons. Indeed, we observed single action potentials in response to the delivery of individual LILFU tone bursts during whole-cell current clamp recordings of CA1 pyramidal neurons (n = 4, 4 slices; Figure 2B). We determined however, whole-cell electrophysiological approaches were not very useful in studying the influence of US on neuronal activity since electrode resonances typically cause the loss of whole-cell seals during stimulation with LILFU. Thus, we continued our investigations using standard optophysiological approaches.

Cavitation is one of the best studied non-thermal effects of US on biological tissue (Miller, Pislaru et al. 2002; Dalecki 2004). Acoustic cavitation can occur when the intensity of US is sufficient to induce the resonation, expansion, and collapse of gas bodies present in some biological tissue. These microexplosions can influence membrane porosity (Dinno, Dyson et al. 1989; Dalecki 2004). Monitored using optical

microscopy during LILFU stimulation, we did not observe cavitation in our studies. Additionally, at the acoustic intensities used in our studies, we did not observe other evidence of membrane damage produced by LILFU stimulation. To examine the effect of LILFU on membrane integrity, we chronically stimulated slice cultures prepared from thy-1-YFP mice (Feng, Mellor et al. 2000) with LILFU-1 every 8 min for 36–48 hours. We observed no difference in the membrane structures of YFP+ neurons undergoing chronic stimulation compared to unstimulated controls (n = 9 slices each; Figure 2C, 2D).

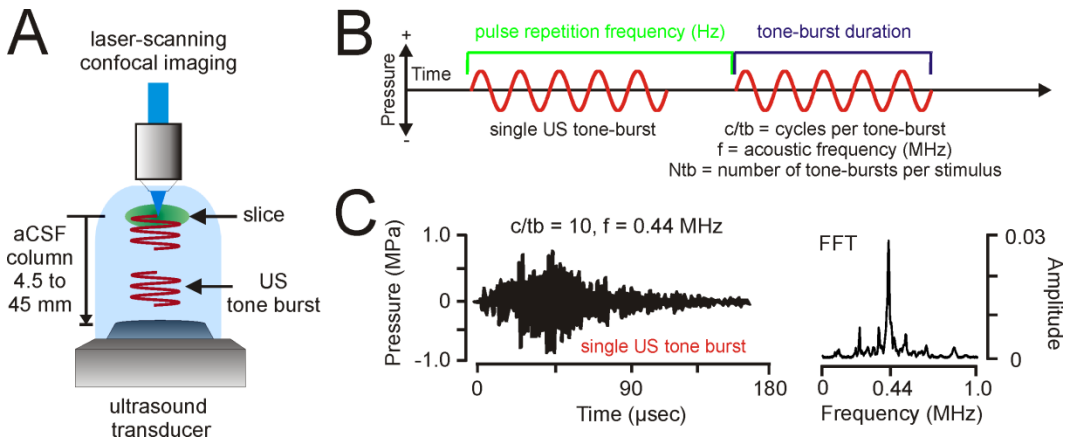

Figure 1. Generation and propagation of LILFU waveforms through neuronal tissue. (A) General experimental configuration implemented to transmit LILFU waveforms through slice cultures while optically monitoring neuronal activity. (B) Graphical illustration of some of the variables involved in constructing LILFU waveforms. These variables include acoustic frequency (f), the number of acoustic cycles per tone burst (c/tb), tone burst duration (TBD), pulse repetition frequency (PRF), and number of tone bursts per stimulus (Ntb). (C) Acoustic pressure wave (left) produced by a typical US tone burst consisting of 10 acoustic cycles at f = 0.44 MHz and FFT of this US tone burst (right). For the construction of our primary US stimulus waveform (LILFU-1), we used a linearly sweeping PRF by repeating the illustrated tone burst from 0–100 Hz over a 5 sec period.

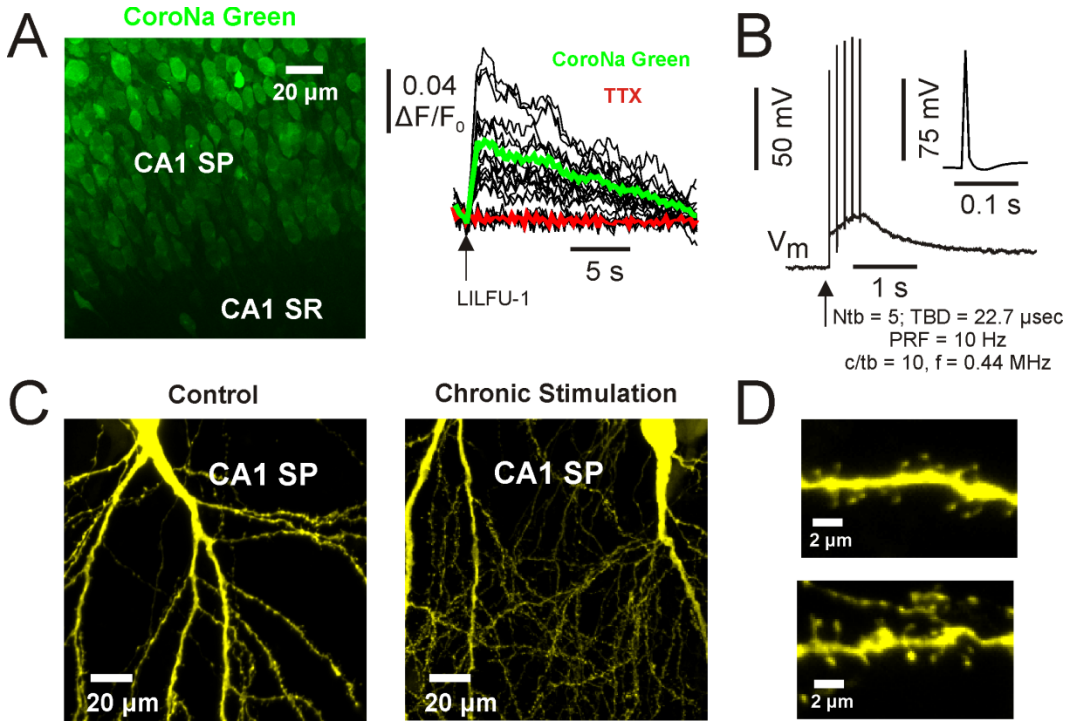

Figure 2. LILFU stimulates sodium transients mediated by voltage-gated sodium channels in hippocampal neurons. (A) Confocal image (left) of a slice culture loaded with CoroNa Green AM. Hippocampal regions CA1 stratum pyramidale (SP) and stratum radiatum (SR) are illustrated. Individual (black) and averaged (color) Na+ transients (right) triggered in CA1 pyramidal neuron somas by LILFU-1 under control conditions and in the presence of TTX. (B) Voltage trace of membrane voltage in response to five US tone bursts delivered at a PRF of 10 Hz during whole-cell current clamp recordings of a CA1 pyramidal neuron. (C) Neuronal membrane integrity is preserved following chronic in vitro stimulation with LILFU. Confocal images of CA1 pyramidal neurons from hippocampal slice cultures prepared from thy-1-YFP mice. The images shown are from a control slice culture (left) and a slice culture following chronic stimulation (right) with LILFU-1 every 8 min for 48 h (360 LILFU-1 stimuli). (D) Similar to (C), but higher magnification images of regions in CA1 SR, which more clearly illustrate the presence of fine membrane structures such as dendritic spines for control (top) and chronic LILFU stimulation conditions (bottom).

LILFU stimulates voltage-dependent calcium transients in neurons

To determine if LILFU waveforms were capable of activating Ca2+ transients, we bath-loaded slice cultures prepared from wild-type mice with the Ca2+ indicator Oregon Green 488 BAPTA-1 AM)OGB-1 AM) and Sulforhodamine 101 (to differentiate between neurons and glial cells) as previously described (Nimmerjahn, Kirchhoff et al. 2004). We found that LILFU-1 activated Ca2+ transients in both hippocampal pyramidal neurons ($\Delta F/F_0$ = 1.14±0.10, n = 61, 10 slices) and glial cells ($\Delta F/F_0$ = 1.40±0.12, n = 55, 10 slices; Figure 3A). Highlighting temporal specificity, stimulation with more brief LILFU waveforms (f = 0.44 MHz, TBD = 0.18 msec, c/tb = 80, PRF = 10Hz, and Ntb = 3), elicitied neuronal Ca2+ transients ($\Delta F/F_0$ = 0.38±0.02, n = 24, 5 slices) with faster kinetics as expected (Figure 3B). In response to LILFU stimulation, we observed that Ca2+ transients could be repeatedly obtained from neurons across multiple LILFU stimulation trials (Figure 3B). While we primarily focused on small regions of interest during stimulation, when we imaged large fields of view we observed that approximately 30% of the neurons respond to LILFU-1. Stimulation with LILFU-1 also induced presynaptic Ca2+ transients in *en passant* boutons located in CA1 SR ($\Delta F/F_0$ = 0.76±0.07, n =31 from 4 slices; Figure 3C). Addition of Cd2+ (500μM) nearly abolished OGB-1 signals in response to LILFU-1, indicating Ca2+ transients triggered by LILFU are primarily mediated by voltage-gated Ca2+ channels (Figure 3D). Likewise, the addition of TTX blocked ~85% of the OGB-1 signal produced by LILFU-1

(Figure 3D). Residual Ca2+transients not blocked by Cd2+ or TTX are likely to involve other hippocampal neuron Ca2+ sources such as NMDA or TRPC1 receptors, which is consistent with both channels possessing mechanosensitive properties (Paoletti and Ascher 1994; Maroto, Raso et al. 2005) and being expressed in hippocampal neurons.

We were able to observe Ca2+ transients in response to pulsed US even when transducers were placed as far as 45 mm away from slices (n = 5; data not shown). Similar to water and aqueous buffers, soft biological tissues (including brain) have relatively low acoustic absorption coefficients. Therefore, we sought to determine if LILFU propagated through whole brain tissue was also capable of stimulating neuronal activity. We imaged OGB-1 signals on the dorsal superficial surface of ex vivo brains (n = 3) obtained from wild-type adult mice while transmitting LILFU waveforms through their ventral surfaces (Figure 4A). In these ex vivo brain preparations, we observed Ca2+ transients similar to those observed in thinner and less intact slice culture preparations in response to stimulation with LILFU (Figure 4B, 4C).

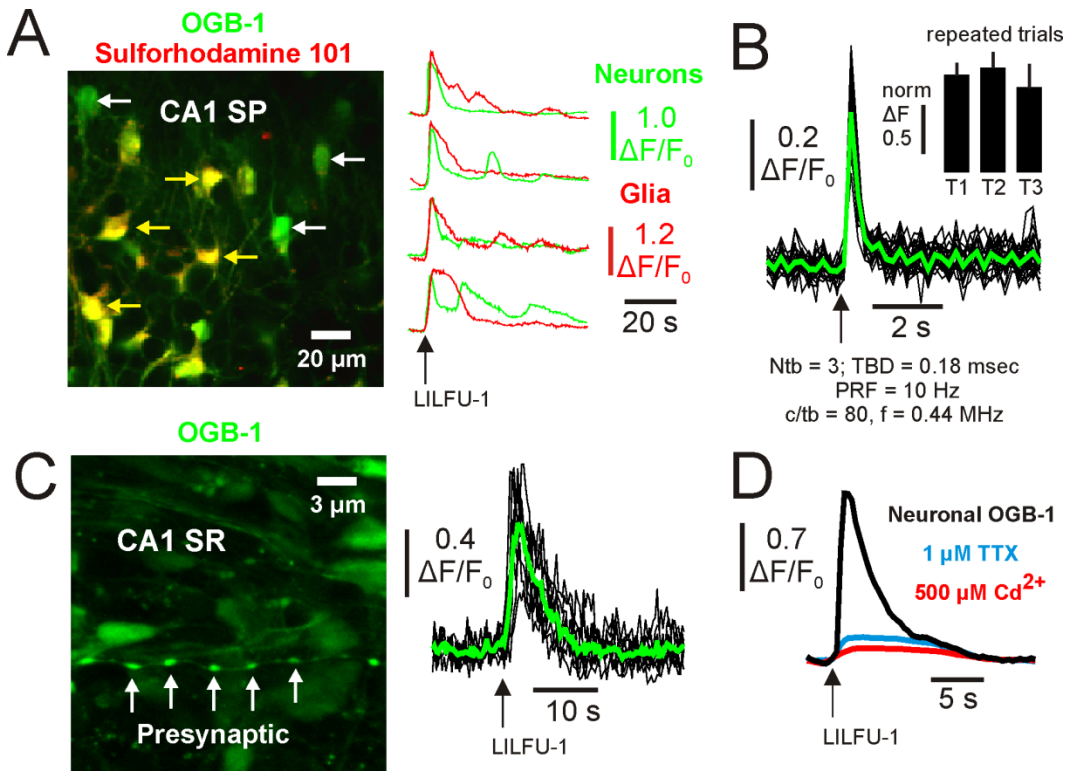

Figure 3. LILFU triggers voltage-dependent somatic and presynaptic Ca^{2+}transients in neurons. (A) Confocal image (left) of a slice culture loaded with OGB-1 AM (green) to monitor Ca2+ activity and Sulforhodamine 101 (red) to identify glial cells (yellow). Representative LILFU-triggered Ca2+ transients observed in the somas of neurons and glial cells are illustrated (right). (B) Individual (black) and averaged (green) Ca2+transients observed in the somas of neurons in response to a brief LILFU waveform. The histogram (inset) illustrates trial 1 normalized mean Ca2+ transient amplitudes in response to repeated trials of LILFU stimulation (n = 19 cells from 3 slices). (C) Confocal image (left) of a slice culture loaded with OGB-1 AM illustrating en passant boutons located in CA1 SR. Individual (black) and averaged (green) presynaptic Ca2+ transients (right) produced by stimulation with LILFU-1. (D) Averaged somatic Ca2+ transients obtained from neurons under control conditions or in the presence of either TTX (n = 36 from 4 slices) or Cd2+ (n = 30 from 4 slices) in response to stimulation with LILFU-1.

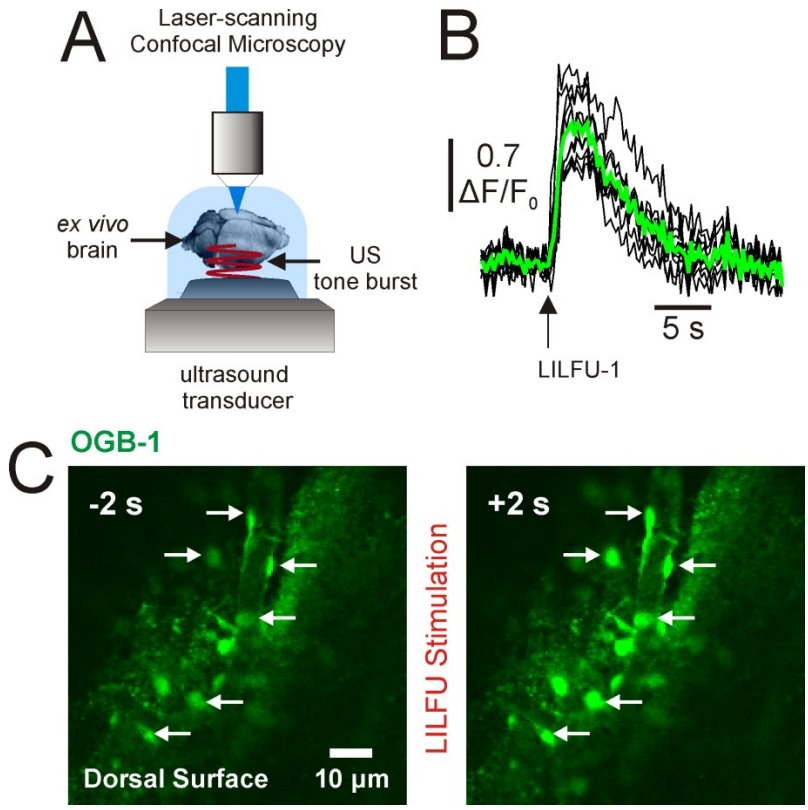

Figure 4. LILFU waveforms transmitted through whole brains are capable of stimulating Ca^{2+}transients. (A) Illustration of basic experimental procedure we developed to transmit LILFU waveforms through whole ex vivo brains prepared from adult wild-type mice and bath-loaded with OGB-1 AM. As depicted, LILFU waveforms were transmitted from the ventral surface of the brain through the tissue to the dorsal surface where we performed confocal imaging. (B) Individual (black) and averaged (green) Ca2+transients observed in the somas of cells on the dorsal surface of an ex vivo brain in response to stimulation with LILFU-1, which was transmitted through the brain from the ventral surface. (C) Confocal images illustrating OGB-1 loaded cells on the dorsal surface of the brain. The image on left illustrates cells during baseline, while the image on the right illustrates cells two-seconds after stimulation with LILFU-1 ensued.

LILFU triggers SNARE-mediated synaptic vesicle exocytosis and synaptic transmission

To investigate the influence of LILFU on synaptic transmission we focused on studying a well-characterized synapse in the mammalian central nervous system, the hippocampal CA3-CA1 synapse. We transmitted LILFU waveforms through hippocampal slice cultures prepared from thy-1-synaptopHluorin (spH) mice (Li, Burrone et al. 2005). The pH-dependent optical probe of synaptic vesicle exocytosis spH reflects neurotransmitter release through an increase in fluorescence when protons are released from synaptic vesicles during fusion (Miesenbock, De Angelis et al. 1998). Transmission of LILFU-1 through slices triggered synaptic vesicle exocytosis producing a ΔFspH of 18.52±2.2% at individual release sites (n = 148 from 15 slices) in CA1stratum radiatum, which primarily represent CA3-CA1 synapses (Figures 5A, 5B). We identified several other LILFU waveforms, which were also effective at triggering synaptic vesicle release. For example, a LILFU waveform composed of different US tone bursts (f = 0.67 MHz, TBD = 74.5 msec, c/tb = 50,000; Figure 5C) delivered at PRF = 10 Hz with Ntb = 5 also stimulated synaptic vesicle release (ΔFspH = 12.86±2.6%, n = 74 from 6 slices; Figure 5D). Figure 5E illustrates spH responses obtained as a function of acoustic intensity across several different LILFU waveforms used in this study. To more specifically examine excitatory CA3-CA1 hippocampal synapses, we implemented a DiOlistic labeling

approach (Gan, Grutzendler et al. 2000) to visualize dendritic spines on CA1 apical dendrites inthy-1-spH slices cultures. Indeed, LILFU-1 stimulated synaptic vesicle release in this population of spine synapses (Figure 6).

Hyperosmotic shock produced by application of sucrose to hippocampal synapses is capable of stimulating the release of a small pool of primed synaptic vesicles (~10 vesicles) in a Ca2+-independent manner and is thought to occur from mechanical processes (Rosenmund and Stevens 1996). Due to the nature of mechanical energy conferred by acoustic waves, we questioned whether some part of the synaptic vesicle release we observed in response to LILFU might be due to mechanical interactions on vesicle release machinery or between the lipid bilayers of active zones and synaptic vesicles. Since hypertonic sucrose application is still capable of triggering neurotransmitter release at hippocampal synapses lacking the SNARE-protein SNAP-25 (Bronk, Deak et al. 2007), we aimed to determine if LILFU-1 was capable of stimulating neurotransmitter release after cleaving SNAP-25 by treating slice cultures with botulinum neurotoxin type-A (BoNT/A; 24–36 h). Indicating that pulsed US-induced exocytosis is SNARE-mediated and not likely due to mechanisms similar to those produced by hyperosmotic shock, treatment of slice cultures with BoNT/A nearly abolished spH responses produced by LILFU-1 stimulation (Figure 5F).

Addition of TTX almost completely blocked vesicular release in response to LILFU-1 highlighting the importance of Na+ conductance and action potentials in LILFU-triggered synaptic vesicle release (Figure 5F). Blocking excitatory network activity with CNQX (20 μM) and APV (100 μM) reduced the ΔFspH by ~50% compared to controls indicating that LILFU stimulates synaptic transmission (network activity) and not merely exocytosis (Figure 5F). Interestingly, the kinetics and amplitudes of LILFU-triggered spH signals were nearly identical to those obtained in response to electrical stimulation of CA3 Schaffer collaterals using monopolar electrodes (Figure 5G), as well as those spH responses previously reported (Sankaranarayanan, De Angelis et al. 2000; Li, Burrone et al. 2005). Since spH typically produces a ΔF of ~1–2% per released vesicle (Sankaranarayanan, De Angelis et al. 2000; Burrone, Li et al. 2006), we estimated LILFU-1 to stimulate the release of ~15 vesicles per release site.

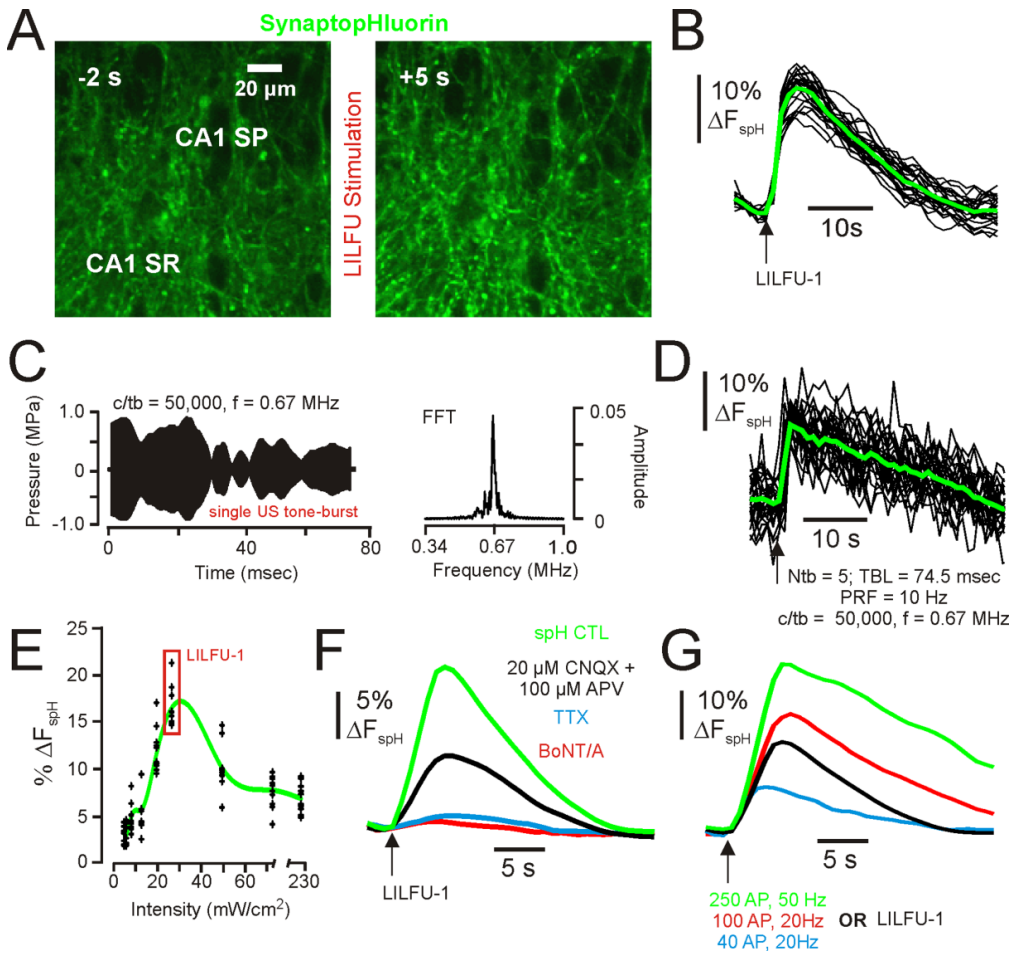

Figure 5. LILFU stimulates SNARE-mediated synaptic vesicle exocytosis and central synaptic transmission. (A) Confocal images illustrating spH signals obtained before (left) and during (right) stimulation with LILFU-1. (B) Individual (black) and averaged (green) spH signals typically obtained in response to stimulation with LILFU-1. (C) Acoustic pressure wave (left) produced by a single LILFU tone burst consisting of 50,000 acoustic cycles at f = 0.67 MHz and FFT of LILFU tone burst (right). (D) Individual (black) and averaged (green) spH signals obtained in response to stimulation with the LILFU tone burst shown in (C) delivered at a PRF = 10 Hz for 0.5 s to produce Np = 5. (E) Histogram of spH responses obtained as a function of acoustic intensity. Responses from individual experiments are indicated by black crosses while the average response is indicated by the green line. (F) Averaged spH signals illustrating the effect of CNQX+APV (n = 84 from 4 slices), TTX (n = 108 from 4 slices), or BoNT/A (n = 60 from 4 slices) on synaptic vesicle exocytosis induced by LILFU-1. (G) Averaged spH signals obtained from buttons in response to field stimulation of Schaffer collaterals with 250 AP, 50 Hz (n = 48), 100 AP, 20 Hz (n = 63), 40 AP, 20 Hz (n = 51), or by LILFU-1 (n = 148).

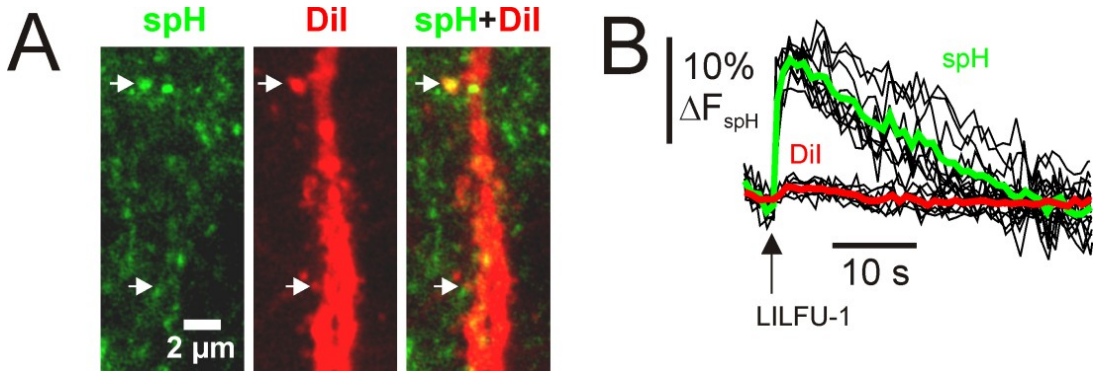

Figure 6. Influence of LILFU on putative excitatory hippocampal CA3-CA1 synapses. (A) Confocal images illustrating spH expression in CA1 SR (left) and an apical dendritic branch of a CA1 pyramidal neuron, which was labeled with DiI using a DiOlistic labeling technique (middle). The two-channel confocal image (right) illustrates putative excitatory synapses indicated by apposition of spH+ puncta and dendritic spines. (B) Individual (black), mean spH (green), and mean DiI (red) signals obtained from terminals impinging on dendritic spines in response to stimulation with LILFU-1.

Discussion

In this study we tested whether LILFU was capable of directly stimulating the activity of neurons in the central nervous system. We made several novel observations in our study. From a mechanistic view, we observed that US stimulates neuronal activity at least partially by triggering voltage-gated Na+transients and voltage-dependent Ca2+ transients. We further observed the US-induced changes in neuronal activity were sufficient to trigger SNARE-mediated synaptic vesicle exocytosis and synaptic transmission at central synapses thereby driving network activity. The mechanisms underlying US activation of voltage-sensitive channels in neurons are presently unknown. We postulate however the mechanical nature of US and its interactions with neuronal membranes leads to the opening of mechanically sensitive voltage-gated channels. Supporting this hypothesis, we observed that TTX a voltage-gated Na+ channel pore-blocker attenuated LILFU-triggered Na+ transients. Further, many voltage-gated Na+ channels (i.e. NaV 1.2, 1.4, 1.5, and 1.6) are known to possess varying degrees of mechanical sensitivity (Sukharev and Corey 2004; Morris and Juranka 2007). The addition of TTX also blocked a large portion of LILFU-induced Ca2+ transients indicating the primary action of LILFU may be on voltage-gated Na+ channels. However, the addition of Cd2+ further reduced LILFU-activated Ca2+transients, which suggests at least some voltage-gated Ca2+ channels may be sensitive to LILFU. Indeed, L-type, N-type,

T-type, and P-type Ca2+ channels have been shown to be mechanically sensitive under various conditions (Sukharev and Corey 2004; Morris and Juranka 2007).

Further studies are required to identify which ion channels are sensitive to US, as well as to characterize how these channels respond to US as a function of acoustic intensity. By imaging large fields of view and monitoring the responses from large populations of neurons, we observed that LILFU-1 stimulated activity in ~30% of the neurons in a given field. These observations raise several interesting issues. We question for instance whether neurons, which have been recently active, are less susceptible to US stimulation. In other words, the kinetic states of a neuron's ion channels may shape how responsive a given cell is to US stimulation. It could also be the case that recently active neurons are more responsive to US stimulation. We are currently in the process of investigating these issues. The individual properties of US waveforms (peak and temporal average intensity, tone burst/pulse duration, pulse repetition frequency, etc.) will also likely determine how effective a given waveform is at stimulating neuronal activity. With respect to acoustic intensity for example, we observed that US waveforms having moderate intensities were more robust in triggering synaptic transmission compared to US waveforms possessing lower or higher intensities. Future studies investigating the influence of US on neuronal activity should consider interactions among waveform parameters such as tone-burst duration

(pulse length), pulse repetition frequency, exposure time, acoustic frequency, and acoustic intensity. Understanding how waveform characteristics contribute to the actions of US on neuronal activity will be an important issue to resolve. One particularly interesting question is can LILFU be used in a molecularly specific manner–perhaps by inducing protein specific resonances using an optimal acoustic frequency or particular LILFU waveform?

Potential Biohazard effects of US

Having a long and proven safety record, US is widely used for diagnostic medical imaging, as well as in an array of noninvasive therapies (Dalecki 2004). Ultrasound is however quite capable of destroying biological tissues, so when employing US to stimulate neuronal activity the potential for biohazardous effects must be carefully considered. Many of the hazards associated with US stem from its ability to induce large thermal fluctuations and/or cavitational damage in soft tissues. Although many groups have previously demonstrated an effect of US on neuronal activity (Fry, Wulff et al. 1950; Fry, Ades et al. 1958; Young and Henneman 1961; Gavrilov, Gersuni et al. 1976; Foster and Wiederhold 1978; Mihran, Barnes et al. 1990; Rinaldi, Jones et al. 1991; Bachtold, Rinaldi et al. 1998; Tsui, Wang et al. 2005), these results are unique in that we found US is capable of stimulating neuronal activity at lower acoustic intensities than those previously reported. Some groups

have utilized acoustic intensities as low as 1 W/cm2 to modulate neuronal activity in hippocampal brain slices (Tsui, Wang et al. 2005), whereas other groups have used intensities exceeding 1000 W/cm2 to trigger peripheral pain sensations in humans (Gavrilov, Gersuni et al. 1976). In this study we implemented a range of acoustic intensities where the nonthermal effects of US have been well documented in other tissues (30–500 mW/cm2) (Dinno, Crum et al. 1989; Dalecki 2004; O'Brien 2007; ter Haar 2007). Further, the US intensities we found sufficient for stimulating neuronal activity are below the output power limits set by the United States Food and Drug Administration for diagnostic imaging.

Due to the lack of gas bodies in most soft tissues including brain (Dalecki 2004), we do not expect cavitation to pose significant problems when using LILFU to stimulate brain activity in vivo. In most soft tissues, cavitation rarely induces damage at pressures <40 MPa (except for lung, intestinal, and cardiac tissues in which cavitational damage can occur at pressures ~2 MPa due to the presence of naturally occurring gas bodies) (Dalecki 2004). The peak rarefaction pressure used in our studies was <1 MPa. At the US power levels we studied, cavitational damage was not induced in hippocampal slice cultures. Besides the potential biohazards of acute US transmission into brain tissue, the possibility for damage arising from repeated, long-term US exposure needs to be evaluated. Few studies have examined the effects of chronic US administration on brain function. We found that chronic LILFU stimulation

(36–48 h) did not alter the fine structure of neuronal membranes. Demonstrating the need for caution however, a recent study reported that repeated US exposure is capable of producing some disruption of neuronal migration in the cortex of developing mouse embryos (Ang, Gluncic et al. 2006).

The effects of ultrasound on molecular signal transduction pathways

While we have studied the actions of US on neuronal activity by monitoring ionic conductance and synaptic vesicle exocytosis, we recognize US may influence signaling molecules capable of influencing neuronal function. In other tissues, the activity of several signaling molecules also present in neuronal tissues are known to be influenced by US. For example, low-intensity pulsed US stimulates TGF-β signaling, which triggers the differentiation of human mesynchymal stem cells into chondrocytes (Ebisawa, Hata et al. 2004). Low-intensity pulsed US has also been shown to stimulate the production of bFGF, TGF-β, BMP-7, VEGF, and IGF-1 (Reher, Doan et al. 1999; Naruse, Miyauchi et al. 2003; Mukai, Ito et al. 2005; Sant'Anna, Leven et al. 2005). Certainly bFGF, TGF-β, BMP-7, VEGF, and IGF-1 have differential yet significant effects on the nervous system by affecting processes involved in synaptic transmission, neuronal growth/survival (Abe and Saito 2001; Molteni, Fumagalli et al. 2001), cell fate specification, tissue patterning, axon guidance in the nervous system (Charron and Tessier-Lavigne 2007), and

angiogenesis in the brain (Gora-Kupilas and Josko 2005). Moreover, VEGF (Jin, Mao et al. 2000; Gora-Kupilas and Josko 2005), TGF-β (Flanders, Ren et al. 1998; Tesseur and Wyss-Coray 2006), and bFGF (Abe and Saito 2001) are neuroprotective against hypoxic-ischemic injury and neurodegeneration. These observations prompt the intriguing question of whether it is possible for US to trigger these pathways in the brain or the production and secretion of growth factors such as brain-derived neurotrophic factor, neurotrophin-3, or nerve growth factor.

Additional actions on conserved cell signaling pathways further support explorations into the use of US as a neuromodulation tool. NF-κB is known to regulate neuronal survival and plasticity (Mattson 2005). Integrin-linked kinase (ILK) and Akt are known to be important signals in establishing neuronal polarity (Guo, Jiang et al. 2007). The PI3K-Akt signaling pathway is capable of blocking cell death and promoting cell survival of many neuronal cell types (Brunet, Datta et al. 2001). Ultrasound induces cyclooxegynase-2 expression in human chondrocytes by activating the integrin/ILK/Akt/NF-κB/ and p300 signaling pathway (Hsu, Fong et al. 2007), while in murine osteoblasts US stimulates COX-2 expression via the integrin/FAK/PI3K/Akt and ERK signaling pathway (Tang, Yang et al. 2006). It should be determined if US is also capable of stimulating ILK, PI3K, Akt, and or NF-κB signaling in neurons as these signaling molecules may become important targets for future ultrasonic neuromodulation strategies.

Feasibility for delivering LILFU to intact nervous systems and brains for neuromodulation

As a tool for modulating neuronal function, US has been studied and considered across a range of uses from thermal ablation of nervous tissues to its ability to produce sensory perceptions (Fry 1968; Gavrilov, Tsirulnikov et al. 1996; Hynynen and Jolesz 1998). Gavrilov and colleagues (1976) were the first to show that US is capable of activating both superficial and deep peripheral nerve structures in humans, which lead to different thermal, tactile, and pain sensations. In these studies however, US was only transmitted through soft tissues such as the skin to stimulate neuronal activity. Whether US will be effective in the noninvasive transcranial regulation of neuronal circuits in the intact nervous system remains to be determined.

Transcranial ultrasonography of the basilar artery has been shown to trigger auditory sensations in human subjects (Magee and Davies 1993). Other studies have reported similar observations in animals during delivery of transcranial US and at least one underlying mechanism is thought to involve the direct stimulation of auditory nerve fibers by US (Gavrilov, Tsirulnikov et al. 1996). Collectively, these observations demonstrate transcranial US is capable of evoking sensory stimuli even in humans. Despite these exciting observations, the skull is a major obstacle when considering the transmission of US into intact brains for neurostimulation purposes. The skull reflects, refracts, absorbs, and

diffracts US fields. Acoustic impedance mismatches between the skin, skull, and skull-brain interfaces also present a challenge for transmitting US through the skull into the intact brain. The frequency of US we chose for the construction of LILFU waveforms (0.44–0.67 MHz) represents a range where optimal gains have been previously reported between transcranial US transmission and brain absorption. Based on modeling data of transmission and attenuation coefficients, as well as experimental data examining the transmission of US through ex vivo human skulls, the optimal gain for the transcranial US transmission and brain absorption is between 0.60 and 0.70 MHz (Hayner and Hynynen 2001; White, Clement et al. 2006). Based on our observations and the findings of others, it is likely that LILFU fields can be transmitted through skulls into the intact brain for gross neurostimulation purposes similar to methods using rTMS. In order to achieve targeted neurostimulation however, it will be necessary to focus LILFU fields.

It is possible to focus US fields using a variety of approaches. Pulsed US (<1 MHz) can be focused through human skulls to points within 1 mm of intended loci using phased US transducer arrays (Hynynen and Jolesz 1998; Clement and Hynynen 2002; Hynynen, Clement et al. 2004). Based on observations reported in studies designed to investigate US field focusing through human skulls (Hynynen and Jolesz 1998; Clement and Hynynen 2002; Hynynen, Clement et al. 2004), US may be able to confer a spatial resolution similar to those achieved by currently implemented

neuromodulation strategies such as vagal nerve stimulation and DBS, which have been shown to possess high therapeutic value (Andrews 2003; Wagner, Valero-Cabre et al. 2007). Before the feasibility of using focused LILFU for targeted neurostimulation purposes can be properly determined, future studies must directly address how focused US fields influence the activity of neuronal populations in vivo.

Conclusion

Our observations demonstrate that LILFU can be used to remotely stimulate the activity of central nervous system neurons and circuits in vitro. We have provided the first direct evidence that US modulates the ionic conductance of neurons and astrocytes to increase cellular activity and synaptic transmission in a manner sufficient to stimulate neuronal circuits. Several issues need to be resolved before the full potential of US in controlling neuronal activity can be realized. Since US is capable of being focused through the human skull however, one tantalizing possibility is that LILFU may permit deep-brain stimulation without the need for surgically implanted devices or other invasive procedures.

References

Abe K, Saito H (2001) Effects of basic fibroblast growth factor on central nervous system functions. Pharmacol Res 43: 307–312.

Andrews RJ (2003) Neuroprotection trek–the next generation: neuromodulation I. Techniques–deep brain stimulation, vagus nerve

stimulation, and transcranial magnetic stimulation. Ann N Y Acad Sci 993: 1–13; discussion 48-53.

Ang ES, Jr, Gluncic V, Duque A, Schafer ME, Rakic P (2006) Prenatal exposure to ultrasound waves impacts neuronal migration in mice. Proc Natl Acad Sci U S A 103: 12903–12910.

Bachtold MR, Rinaldi PC, Jones JP, Reines F, Price LR (1998) Focused ultrasound modifications of neural circuit activity in a mammalian brain. Ultrasound Med Biol 24: 557–565.

Bronk P, Deak F, Wilson MC, Liu X, Sudhof TC, et al. (2007) Differential effects of SNAP-25 deletion on Ca2+ -dependent and Ca2+ -independent neurotransmission. J Neurophysiol 98: 794–806.

Brunet A, Datta SR, Greenberg ME (2001) Transcription-dependent and -independent control of neuronal survival by the PI3K-Akt signaling pathway. Curr Opin Neurobiol 11: 297–305.

Burrone J, Li Z, Murthy VN (2006) Studying vesicle cycling in presynaptic terminals using the genetically encoded probe synaptopHluorin. Nat Protoc 1:2970–2978.

Chapman IV, MacNally NA, Tucker S (1980) Ultrasound-induced changes in rates of influx and efflux of potassium ions in rat thymocytes in vitro. Ultrasound Med Biol 6: 47–58.

Charron F, Tessier-Lavigne M (2007) The Hedgehog, TGF-beta/BMP and Wnt families of morphogens in axon guidance. Adv Exp Med Biol 621: 116–133.

Clement GT (2004) Perspectives in clinical uses of high-intensity focused ultrasound. Ultrasonics 42: 1087–1093.

Clement GT, Hynynen K (2002) A non-invasive method for focusing ultrasound through the human skull. Phys Med Biol 47: 1219–1236.

Dalecki D (2004) Mechanical bioeffects of ultrasound. Annu Rev Biomed Eng 6:229–248.

Dinno MA, Dyson M, Young SR, Mortimer AJ, Hart J, et al. (1989) The significance of membrane changes in the safe and effective use of therapeutic and diagnostic ultrasound. Phys Med Biol 34: 1543–1552.

Ebisawa K, Hata K, Okada K, Kimata K, Ueda M, et al. (2004) Ultrasound enhances transforming growth factor beta-mediated chondrocyte differentiation of human mesenchymal stem cells. Tissue Eng 10: 921–929.

Feng G, Mellor RH, Bernstein M, Keller-Peck C, Nguyen QT, et al. (2000) Imaging neuronal subsets in transgenic mice expressing multiple spectral variants of GFP. Neuron 28: 41–51.

Flanders KC, Ren RF, Lippa CF (1998) Transforming growth factor-betas in neurodegenerative disease. Prog Neurobiol 54: 71–85.

Foster KR, Wiederhold ML (1978) Auditory responses in cats produced by pulsed ultrasound. J Acoust Soc Am 63: 1199–1205.

Fry FJ, Ades HW, Fry WJ (1958) Production of reversible changes in the central nervous system by ultrasound. Science 127: 83–84.

Fry WJ (1968) Electrical stimulation of brain localized without probes–theoretical analysis of a proposed method. J Acoust Soc Am 44: 919–931.

Fry WJ, Wulff VJ, Tucker D, Fry FJ (1950) Physical factors involved in ultrasonically induced changes in living systems: I. Identification of nontemperature effects. J Acoust Soc Am 22: 867–876.

Gan WB, Grutzendler J, Wong WT, Wong RO, Lichtman JW (2000) Multicolor ‘‘DiOlistic’’ labeling of the nervous system using lipophilic dye combinations. Neuron 27: 219–225.

Gavrilov LR, Gersuni GV, Ilyinsky OB, Sirotyuk MG, Tsirulnikov EM, et al. (1976) The effect of focused ultrasound on the skin and deep nerve structures of man and animal. Prog Brain Res 43: 279–292.

Gavrilov LR, Tsirulnikov EM, Davies IA (1996) Application of focused ultrasound for the stimulation of neural structures. Ultrasound Med Biol 22: 179–192.

Gora-Kupilas K, Josko J (2005) The neuroprotective function of vascular endothelial growth factor (VEGF). Folia Neuropathol 43: 31–39.

Guo W, Jiang H, Gray V, Dedhar S, Rao Y (2007) Role of the integrin-linked kinase (ILK) in determining neuronal polarity. Dev Biol 306: 457–468.

Hayner M, Hynynen K (2001) Numerical analysis of ultrasonic transmission and absorption of oblique plane waves through the human skull. J Acoust Soc Am 110: 3319–3330.

Hsu HC, Fong YC, Chang CS, Hsu CJ, Hsu SF, et al. (2007) Ultrasound induces cyclooxygenase-2 expression through integrin, integrin-linked kinase, Akt, NF-kappaB and p300 pathway in human chondrocytes. Cell Signal 19:2317–2328.

Hynynen K, Clement GT, McDannold N, Vykhodtseva N, King R, et al. (2004) 500-element ultrasound phased array system for noninvasive focal surgery of the brain: a preliminary rabbit study with ex vivo human skulls. Magn Reson Med52: 100–107.

Hynynen K, Jolesz FA (1998) Demonstration of potential noninvasive ultrasound brain therapy through an intact skull. Ultrasound Med Biol 24:275–283.

Jin KL, Mao XO, Greenberg DA (2000) Vascular endothelial growth factor: direct neuroprotective effect in vitro ischemia. Proc Natl Acad Sci U S A 97:10242–10247.

Li Z, Burrone J, Tyler WJ, Hartman KN, Albeanu DF, et al. (2005) Synaptic vesicle recycling studied in transgenic mice expressing synaptopHluorin. Proc Natl Acad Sci U S A 102: 6131–6136.

Magee TR, Davies AH (1993) Auditory phenomena during transcranial Doppler insonation of the basilar artery. J Ultrasound Med 12: 747–750.

Maroto R, Raso A, Wood TG, Kurosky A, Martinac B, et al. (2005) TRPC1 forms the stretch-activated cation channel in vertebrate cells. Nat Cell Biol 7:179–185.

Mattson MP (2005) NF-kappaB in the survival and plasticity of neurons. Neurochem Res 30: 883–893.

Meier SD, Kovalchuk Y, Rose CR (2006) Properties of the new fluorescent Na+ indicator CoroNa Green: comparison with SBFI and confocal Na+ imaging. J Neurosci Methods 155: 251–259.

Miesenbock G, De Angelis DA, Rothman JE (1998) Visualizing secretion and synaptic transmission with pH-sensitive green fluorescence proteins. Nature 394:192–195.

Mihran RT, Barnes FS, Wachtel H (1990) Temporally-specific modification of myelinated axon excitability in vitro following a single ultrasound pulse. Ultrasound Med Biol 16: 297–309.

Miller DL, Pislaru SV, Greenleaf JE (2002) Sonoporation: mechanical DNA delivery by ultrasonic cavitation. Somat Cell Mol Genet 27: 115–134.

Molteni R, Fumagalli F, Magnaghi V, Roceri M, Gennarelli M, et al. (2001) Modulation of fibroblast growth factor-2 by stress and corticosteroids: from developmental events to adult brain plasticity. Brain Res Brain Res Rev 37: 249–258.

Morris CE, Juranka PF () Lipid Stress at Play: Mechanosensitivity of Voltage-Gated Channels, Current Topics in Membranes: Academic Press 2007. Pp 297–338.

Mortimer AJ, Dyson M (1988) The effect of therapeutic ultrasound on calcium uptake in fibroblasts. Ultrasound Med Biol 14: 499–506.

Mukai S, Ito H, Nakagawa Y, Akiyama H, Miyamoto M, et al. (2005) Transforming growth factor-beta1 mediates the effects of low-intensity pulsed ultrasound in chondrocytes. Ultrasound Med Biol 31: 1713–21.

Naruse K, Miyauchi A, Itoman M, Mikuni-Takagaki Y (2003) Distinct anabolic response of osteoblast to low-intensity pulsed ultrasound. J Bone Miner Res 18:360–369.

NEMA (2004) Acoustic Output Measurement Standard for Diagnostic Ultrasound Equipment. Washington, DC: National Electrical Manufacturers Association.

O'Brien WD Jr (2007) Ultrasound-biophysics mechanisms. Prog Biophys Mol Biol 93: 212–255.

Paoletti P, Ascher P (1994) Mechanosensitivity of NMDA receptors in cultured mouse central neurons. Neuron 13: 645–655.

Reher P, Doan N, Bradnock B, Meghji S, Harris M (1999) Effect of ultrasound on the production of IL-8, basic FGF and VEGF. Cytokine 11: 416–423.

Rinaldi PC, Jones JP, Reines F, Price LR (1991) Modification by focused ultrasound pulses of electrically evoked responses from an in vitro hippocampal preparation. Brain Res 558: 36–42.

Rosenmund C, Stevens CF (1996) Definition of the readily releasable pool of vesicles at hippocampal synapses. Neuron 16: 1197–1207.

Sankaranarayanan S, De Angelis D, Rothman JE, Ryan TA (2000) The use of pHluorins for optical measurements of presynaptic activity. Biophys J 79:2199–2208.

Sant'Anna EF, Leven RM, Virdi AS, Sumner DR (2005) Effect of low intensity pulsed ultrasound and BMP-2 on rat bone marrow stromal cell gene expression. J Orthop Res 23: 646–652.

Stoppini L, Buchs PA, Muller D (1991) A simple method for organotypic cultures of nervous tissue. J Neurosci Methods 37: 173–182.

Sukharev S, Corey DP (2004) Mechanosensitive channels: multiplicity of families and gating paradigms. Sci STKE 219: re4.

Tang CH, Yang RS, Huang TH, Lu DY, Chuang WJ, et al. (2006) Ultrasound stimulates cyclooxygenase-2 expression and increases bone formation through integrin, focal adhesion kinase, phosphatidylinositol 3-kinase, and Akt pathway in osteoblasts. Mol Pharmacol 69: 2047–2057.

ter Haar G (2007) Therapeutic applications of ultrasound. Prog Biophys Mol Biol 93: 111–129.

Tesseur I, Wyss-Coray T (2006) A role for TGF-beta signaling in neurodegeneration: evidence from genetically engineered models. Curr Alzheimer Res 3:505–513.

Trevelyan AJ, Sussillo D, Watson BO, Yuste R (2006) Modular propagation of epileptiform activity: evidence for an inhibitory veto in neocortex. J Neurosci 26:12447–12455.

Tsui PH, Wang SH, Huang CC (2005) In vitro effects of ultrasound with different energies on the conduction properties of neural tissue. Ultrasonics 43:560–565.

Wagner T, Valero-Cabre A, Pascual-Leone A (2007) Noninvasive Human Brain Stimulation. Annu Rev Biomed Eng 9: 527–565.

White PJ, Clement GT, Hynynen K (2006) Local frequency dependence in transcranial ultrasound transmission. Phys Med Biol 51: 2293–2305.

Young RR, Henneman E (1961) Functional effects of focused ultrasound on mammalian nerves. Science 134: 1521–1522.

Zhang F, Wang LP, Brauner M, Liewald JF, Kay K, et al. (2007) Multimodal fast optical interrogation of neural circuitry. Nature 446: 633–639.

Chapter 3

TRANSCRANIAL PULSED ULTRASOUND STIMULATES INTACT BRAIN CIRCUITS

Electromagnetic-based methods of stimulating brain activity require invasive procedures or have other limitations. Deep-brain stimulation requires surgically implanted electrodes. Transcranial magnetic stimulation does not require surgery, but suffers from low spatial resolution. Optogenetic-based approaches have unrivaled spatial precision, but require genetic manipulation. In search of a potential solution to these limitations, we began investigating the influence of transcranial pulsed ultrasound neuronal activity in the intact mouse brain. In motor cortex, ultrasound-stimulated neuronal activity was sufficient to evoke motor behaviors. Deeper in subcortical circuits, we used targeted transcranial ultrasound to stimulate neuronal activity and synchronous oscillations in the intact hippocampus. We found that ultrasound triggers TTX-sensitive neuronal activity in the absence of a rise in brain temperature (<0.01°C). Here, we also report that transcranial pulsed ultrasound for intact brain circuit stimulation has a lateral spatial resolution of approximately 2 mm and does not require exogenous factors or surgical invasion.

Introduction

All currently implemented approaches to the stimulation of brain circuits suffer from a limitation or weakness. Pharmacological and chemical methods lack brain target specificity and have numerous metabolic requirements. Electrical methods, such as deep-brain stimulation offer a higher targeting specificity, but require surgery and brain impalement with electrodes (Ressler and Mayberg 2007). Optogenetic-based methods using light-activated ion channels or transporters offer unrivaled spatial resolution, but require genetic alteration (Szobota, Gorostiza et al. 2007; Zhang, Aravanis et al. 2007). Transcranial magnetic stimulation (TMS) and transcranial direct current stimulation do not require invasive procedures, but suffer from poor spatial resolutions of ≈ 1 cm (Barker 1999; Wagner, Valero-Cabre et al. 2007). Considering the above limitations, a remaining challenge for neuroscience is to develop improved stimulation methods for use in intact brains. To address this need, we began studying the influence of pulsed ultrasound (US) on neuronal activity in mice.

Ultrasound is a mechanical pressure wave (sound wave) having a frequency above the range of human hearing (> 20 kHz). Due to its physical properties, specifically its ability to be transmitted long distances through solid structures including bone and soft tissues, US is used in a wide range of medical and industrial applications. Diagnostic imaging US has a frequency range from 1 to 15 MHz, while therapeutic US tends to

employ a frequency of about 1 MHz (O'Brien 2007). Ultrasound can be transmitted into tissues in either pulsed or continuous waveforms and can influence physiological activity through thermal and/or nonthermal (mechanical) mechanisms (Dinno, Dyson et al. 1989; Dalecki 2004; O'Brien 2007; ter Haar 2007). The potential of using US for brain stimulation has been largely overlooked in comparison to chemical, electrical, magnetic, or photonic methods. Surprisingly, this is in lieu of the fact that US was shown capable of exciting nerve and muscle more than eight decades ago (Harvey 1929).

Edmund Newton Harvey first published a set of ground-breaking observations, which clearly described that US can stimulate nerve and muscle fibers in neuromuscular preparations (Harvey 1929). Since then, US has been shown to stimulate and inhibit neuronal activity under various conditions. For example, US has been reported to reversibly suppress sensory-evoked potentials in the cat primary visual cortex following treatment of the lateral geniculate nucleus with US transmitted through a cranial window (Fry, Ades et al. 1958). Conversely, US has been shown to stimulate auditory nerve responses in the craniotomized cat brain (Foster and Wiederhold 1978). In cat saphenous nerve preparations, US was shown to differentially modulate the activity of Aδ- and C-fibers depending on the fiber diameter, US intensity, and US exposure time (Young and Henneman 1961).

Ultrasound can be defined as low-intensity or high-intensity (ter Haar 2007). High-intensity US (> 1 W/cm^2) influences neuronal excitability by producing thermal effects (Tsui, Wang et al. 2005). In addition to the initial studies cited above, high-intensity US has been reported to modulate neuronal activity in peripheral nerves (Lele 1963; Mihran, Barnes et al. 1990; Tsui, Wang et al. 2005), craniotomized cat and craniotomized rabbit cortex (Velling and Shklyaruk 1988), peripheral somatosensory receptors in humans (Gavrilov, Gersuni et al. 1976), cat spinal cord (Shealy and Henneman 1962), and rodent hippocampal slices (Rinaldi, Jones et al. 1991; Bachtold, Rinaldi et al. 1998). While these prior studies support the general potential of US for neurostimulation, high-intensity US can readily produce mechanical and/or thermal tissue damage (Dalecki 2004; Hynynen and Clement 2007; O'Brien 2007; ter Haar 2007) precluding it from use in noninvasive brain circuit stimulation. At acoustic intensities < 500 mW/cm^2 pulsed US can produce mechanical bioeffects without producing thermal effects or tissue damage (Dinno, Dyson et al. 1989; Dalecki 2004; O'Brien 2007; ter Haar 2007). In hippocampal slices, we previously reported low-intensity US (< 300 mW/cm^2), low-frequency US (< 0.65 MHz) is capable of stimulating action potentials and synaptic transmission (Tyler, Tufail et al. 2008). Since low-frequency US can be reliably transmitted through skull bone (Hynynen, Clement et al. 2004; Hynynen and Clement 2007), the motivation for the present study was to investigate the influence of low-frequency, low-

intensity transcranial pulsed US on intact brain circuits in pursuit of a novel brain stimulation method. We report that transcranial US is capable of safely and reliably stimulating *in vivo* brain circuits, such as the motor cortex and intact hippocampus of mice.

Experimental Procedures

Generation and Characterization of Pulsed US Waveforms

We used immersion-type US transducers having a center frequency of 0.5 MHz (V301-SU, Olympus NDT, Waltham, MA) or 0.3 MHz (GS-300-D19, Ultran, State College, PA) to produce US waveforms. US pulses were generated by brief bursts of square waves (0.2 μsec; 0.5 mV peak-to-peak) using an Agilent 33220A function generator (Agilent Technologies, Inc., Santa Clara, California, USA). Square waves were further amplified (50 dB gain) using a 40 W ENI 240L RF amplifier. Square waves were delivered between 0.25 – 0.50 MHz depending on the acoustic frequency desired. US pulses were repeated at a pulse repetition frequency by triggering the above referenced function generator with square waves produced using a second Agilent 33220A function generator (Figure S1).

To characterize the intensity characteristics of pulsed US stimulus waveforms, we recorded voltage traces produced by US pressure waves using a calibrated needle hydrophone (HNR 500, Onda Corporation, Sunnyvale, California, USA) and an Agilent DSO6012A 100 MHz digital

oscilloscope connected to a PC. Intensity measurements were made from targeted points inside fresh *ex vivo* mouse heads corresponding to the brain region targeted. The transcranial US waveforms were transmitted to intact brain circuits from US transducers using custom-designed acoustic collimators consisting of 3.0 or 4.7 mm (1 mL syringe) diameter polyethylene tubing or 5.0 mm diameter tubing tapered to a 2.0 mm diameter output aperture (Figure S2C). Collimating guides were constructed so stimulated regions of the brain were in the far-field of US transmission paths and filled with ultrasound coupling gel.

Using measurements recorded from calibrated hydrophones (described above), we calculated several acoustic intensity characteristics of pulsed US stimulus waveforms based on published and industry accepted standards (NEMA 2004).

The pulse intensity integral (*PII*) was defined as:

$$PII = \int \frac{p^2(t)}{Z_0} dt$$

where p is the instantaneous peak pressure, Z_0 is the characteristic acoustic impedance in Pa·s/m defined as ρc where ρ is the density of the medium, and c is the speed of sound in the medium. We estimated ρ to be 1028 kg/m^3 and c to be 1515 m/s for brain tissue based on previous reports (Ludwig 1950). The spatial-peak, pulse-average intensity (I_{SPPA}) was defined as:

$$I_{\mathrm{SPPA}} = \frac{PII}{\mathrm{PD}}$$

where PD is the pulse duration defined as (t)(0.9PII – 0.1PII) ·1.25 as outlined by technical standards established by AIUM and NEMA (NEMA 2004).

The spatial-peak temporal-average intensity (I_{SPTA}) was defined as:

$$I_{\mathrm{SPTA}} = PII(\mathrm{PRF})$$

where PRF is equal to the pulse repetition frequency in hertz.

The mechanical index (MI; see Table S1) was defined as:

$$\mathrm{MI} = \frac{p_r}{\sqrt{f}}$$

In Vivo US Stimulation

In this study we used wild-type mice in accordance with animal use protocols approved by the Institutional Animal Care and Use Committee at Arizona State University. To conduct transcranial US stimulation of intact motor cortex, mice were anesthetized using a ketamine-xylazine cocktail (70 mg/kg ketamine, 7 mg/kg xylazine) administered intraperitoneally. The hair on the dorsal surface of the head over regions corresponding to targeted brain regions was trimmed. Mice were then placed in a custom-designed or Cunningham mouse stereotax. US transducers with affixed collimators were lowered to points above the skin corresponding to brain regions using standard stereotactic coordinates. Collimators or transducers were then placed on the surface of the skin above the

targeted brain region and coupled to the skin using ultrasound gel. Transcranial pulsed US stimulus waveforms were delivered to the targeted motor cortex or hippocampus using standard TTL triggering protocols (Figure S1). Digital signal markers indicated the onset and length of US stimulus waveforms. During some experiments, simultaneous electrophysiological data were acquired were acquired (*see below*). Only in experiments where we conducted *in vivo* extracellular recordings of brain activity or brain temperature was a craniotomy performed. Since cranial windows and electrode insertions were made at sites adjacent to angled US projection lines targeting specific brain regions, in these cases the US was still transmitted through skull bone although not covered by overlying skin. All other experiments were conducted in wholly intact mice except for some mapping experiments which required retraction of the skin to identify landmarks on the mouse skull. Following stimulation, animals were either allowed to recover from anesthesia or processed as described below.

In Vivo US Stimulation

In this study we used wild-type mice in accordance with animal use protocols approved by the Institutional Animal Care and Use Committee at Arizona State University. To conduct transcranial US stimulation of intact motor cortex, mice were anesthetized using a ketamine-xylazine cocktail (70 mg/kg ketamine, 7 mg/kg xylazine) administered intraperitoneally. The

hair on the dorsal surface of the head over regions corresponding to targeted brain regions was trimmed. Mice were then placed in a custom-designed or Cunningham mouse stereotax. US transducers with affixed collimators were lowered to points above the skin corresponding to brain regions using standard stereotactic coordinates. Collimators or transducers were then placed on the surface of the skin above the targeted brain region and coupled to the skin using ultrasound gel. Transcranial pulsed US stimulus waveforms were delivered to the targeted motor cortex or hippocampus using standard TTL triggering protocols (Figure S1). Digital signal markers indicated the onset and length of US stimulus waveforms. During some experiments, simultaneous electrophysiological data were acquired were acquired (*see below*). Only in experiments where we conducted *in vivo* extracellular recordings of brain activity or brain temperature was a craniotomy performed. Since cranial windows and electrode insertions were made at sites adjacent to angled US projection lines targeting specific brain regions, in these cases the US was still transmitted through skull bone although not covered by overlying skin. All other experiments were conducted in wholly intact mice except for some mapping experiments which required retraction of the skin to identify landmarks on the mouse skull. Following stimulation, animals were either allowed to recover from anesthesia or processed as described below.

EMG Recordings

Fine-wire EMG recordings were made using standard approaches and a four-channel differential AC amplifier (model 1700, A-M Systems, Inc., Sequim, WA, USA) with 10-1000 Hz band-pass filter and a 100 X gain applied. Electrical interference was rejected using a 60 Hz notch filter. EMG signals were acquired at 2 kHz using a Digidata 1440A and pClamp or a 16-channel DataWave Experimenter and SciWorks. Briefly, small barbs were made in a 2 mm uncoated end of teflon coated steel wire (California Fine Wire, Co., Grover Beach, CA, USA). Single recording wires were then inserted into the appropriate muscles using a 30 gauge hypodermic syringe before being connected to the amplifier. Ground wires were similarly constructed and subcutaneously inserted into the dorsal surface of the neck.

Brain Temperature Recordings and Estimated Changes

Prior to US stimulation in some experiments we performed a small craniotomy (d ≈ 2 mm) on mouse temporal bone. Following removal of dura, we inserted a 0.87 mm diameter thermocouple (TA-29, Warner Instruments, LLC, Hamden, CT, USA) into motor cortex through the cranial window. The thermocouple was connected to a monitoring device (TC-324B, Warner Instruments) and to a Digidata 1440A to record temperature (calibrated voltage signal = 100 mV/°C) using pClamp.

We also estimated the influence of US stimulus waveforms on brain temperature change using a set of previously described equations valid for short exposure times (O'Brien 2007). Briefly, we estimated the maximum temperature change (ΔT_{max}) to be:

$$\Delta t_{max} = \frac{\dot{Q}\,\Delta t}{C_v}$$

where Δt is the pulse exposure time, where C_v is the specific heat capacity for brain tissue ≈ 3.6 J/g/K (Cooper and Trezek 1972) and where $\dot{Q}$ is the rate at which heat is produced defined by (Nyborg 1981):

$$\dot{Q} = \frac{\alpha p_0^2}{\rho c}$$

where ρ is the density of the medium, c is the speed of sound in the medium as described above, where α is the absorption coefficient of brain (≈ 0.03 Np/cm for 0.5 MHz US (Goss, Johnston et al. 1978)), and p_0 is the pressure amplitude of US stimulus waveforms.

Transmission Electron Microscopy

Following stimulation, animals were transcardially perfused with 2% glutaraldehyde, 2.5% formaldehyde in sodium cacodylate buffer. Brains were subsequently removed and post-fixed in 2% glutaraldehyde, 2.5% formaldehyde in sodium cacodylate buffer overnight in 4°C. Following post-fixation, and sodium cacodylate buffer rinsing secondary fixation was performed with 0.2% osmium textroxide in sodium cacodylate for 1 hr.

Sections were then block-stained overnight at 4°C with 0.25% uranyl acetate before being dehydrated in a graded ethanol series followed by 100% acetone. Samples were infiltrated Spur's resin during the next 3 d and flat embedded on Teflon coated glass slides before being polymerized overnight at 60°C. Motor cortex regions of interest were then identified and trimmed prior to block mounting. Trimmed sections were then ultra-thin sectioned at 70 nm on an ultramicrotome (Leica Ultra Cut R, Leica Microsystems, Inc., Bannockburn, IL, USA). Samples were collected on formvar coated copper slot grids and post-stained with 1% uranyl acetate in ethanol and Sato's lead citrate. Samples were imaged at 80 kV on a Phillips CM12 transmission electron microscope and images acquired with a Gatan CCD camera (model 791, Gatan, Inc., Warrendale, PA, USA). Images were acquired at 8,000x for analysis of overall ultrastructure, 19,500x for analysis of synaptic density and 40,000x quantitative analysis of synapse specific parameters.

Histological Evaluation

In some experiments we performed histological investigations of stimulated and unstimulated brain regions of mice receiving transcranial US stimulation of motor cortex. To prepare tissue for histology, mice were transcardially perfused using 4% paraformaldehyde in PBS. Mouse brains were removed and post-fixed in 4% paraformaldehyde at 4°C overnight. Coronal slices of stimulated and adjacent unstimulated motor cortex were

then made using a vibratome or a cryotome. For mapping studies, coronal cryosections were immunolabeled using antibodies against c-fos (1:250; SC-253, Santa Cruz Biotechnology, Inc., Santa Cruz, CA, USA) and standard processing techniques with Vectastain Elite ABC kits (Vector Laboratories, Burlingame, CA) before being imaged using transmitted light microscopy. In other histological analyses, brain sections (50 μm) were double-labeled using standard immunocytochemistry techniques with antibodies against cleaved Caspase-3 (1:250; Asp 175-9661, Cell Signaling Technology, Beverly, MA, USA), BDNF (1:1000, AB1534SP, Millipore, Billerica, MA), and/or NeuN (1:1000, MAB377, Millipore). Following overnight primary antibody incubation, sections were washed and incubated in appropriate Alexa Fluor 488, Alexa Fluor 568, or Alexa Fluor 633 secondary antibodies (1:500; Invitrogen, Carlsbad, CA, USA) for two hours at room temperature. One- or two-channel fluorescence images were acquired on an Olympus Fluoview FV-300 laser-scanning confocal microscope (Olympus America, Inc., Center Valley, Pennsylvania, USA).

Prior to US stimulation trials, some animals received an intravenous infusion of 5% fluorescein isothiocyanate-dextran (10 kDa; Sigma, St. Louis, MO, USA) in a 0.9% sodium chloride solution (0.35 mL). Coronal sections (75 μm) of these brains were prepared using a vibratome. Floating sections were then labeled with TO-PRO-3 (1:1000; Invitrogen) to identify cell bodies. Following washing and mounting, the cerebrovasculature was then examined using confocal microscopy. In

additional positive control experiments, prior to US stimulation mice received an intravenous infusion of 5% fluorescein isothiocyanate-dextran in conjunction with an ultrasound contrast agent (Optison®; GE Healthcare, Piscataway, NJ, USA) known to elicit BBB disruption during US administration (Raymond, Treat et al. 2008). These brains were processed and examined as described above.

Behavioral Assays

US stimulated and sham-treated control mice were subjected to behavioral testing using a rotorod task and a wire-hanging task. On US stimulation treatment day, sham-treated controls and US stimulated animals were anesthetized with ketamine/xylazine and their hair was trimmed. Following US stimulation or sham-treatment, motor skill testing was administered on rotorod and wire-hanging tasks again at 24 h and 7 days later and compared against 24-h pre-stimulation control performance. On behavioral testing days, mice ran on the rotorod (25.4 cm circumference, 10.8 cm wide rod) until failure (time in seconds before falling from rotorod) for 5 trials each at two speeds (17 and 26 RPM). Following rotorod trials, animals performed wire-hanging tests until failure time (time in seconds before falling from suspended wire) for 5 trials.

Data Analyses

All electrophysiological data (MUA, LFP, and EMG) were processed and analyzed using custom-written routines in Matlab (The Mathworks, Natick, MA, USA) or Clampfit (Molecular Devices). Single spikes were isolated using a standard thresholding window. Ultrasound waveform characteristics were analyzed using hydrophone voltage traces and custom written routines in Matlab and Origin (OriginLab Corp., Northampton, MA, USA). All histological confocal and transmitted light images were processed and analyzed using *ImageJ* (http://rsb.info.nih.gov/ij/). Electron microscopy data were also quantified using *ImageJ*. All statistical analyses were performed using SPSS (SPSS, Inc., Chicago, IL, USA). Data shown are mean ± S.E.M unless indicated otherwise.

Results

Construction and Transmission of Pulsed Ultrasound Stimulus Waveforms into Intact Brain Circuits

We constructed US stimulus waveforms and transmitted them into the intact brains of anesthetized mice (n = 192; Figure 7A). The optimal gains between transcranial transmission and brain absorption occurs for US at acoustic frequencies (f) ≤ 0.65 MHz (Hayner and Hynynen 2001; White, Clement et al. 2006). Thus, we constructed transcranial stimulus waveforms with US having f = 0.25 to 0.50 MHz. Intensity characteristics

of US stimulus waveforms were calculated based on industry standards and published equations developed by the American Institute of Ultrasound Medicine, the National Electronics Manufacturers Association, and the United Stated Food and Drug Administration (NEMA 2004); see *Experimental Procedures*).

Single US pulses contained between 80 and 225 acoustic cycles per pulse (c/p) for pulse durations (PD) lasting 0.16 to 0.57 msec. Single US Pulses were repeated at pulse repetition frequencies (PRF) ranging from 1.2 to 3.0 kHz to produce spatial-peak temporal-average intensities (I_{SPTA}) of 21 to 163 mW/cm^2 for total stimulus duration ranging between 26 and 333 msec. Pulsed US waveforms had peak rarefactional pressures (p_r) of 0.070 to 0.097 MPa, pulse intensity integrals (*PII*) of 0.017 to 0.095 mJ/cm^2, and spatial-peak pulse-average intensities (I_{SPPA}) of 0.075 to 0.229 W/cm^2. Figures 7A, 7B, illustrate the strategy developed for stimulating intact brain circuits with transcranial pulsed US. The attenuation of US due to propagation through the hair, skin, skull, and dura of mice was < 10% (Figure 7C) and all intensity values reported were calculated from US pressure measurements acquired using a calibrated hydrophone positioned with a micromanipulator inside fresh *ex vivo* mouse heads at locations corresponding to the brain circuit being targeted.

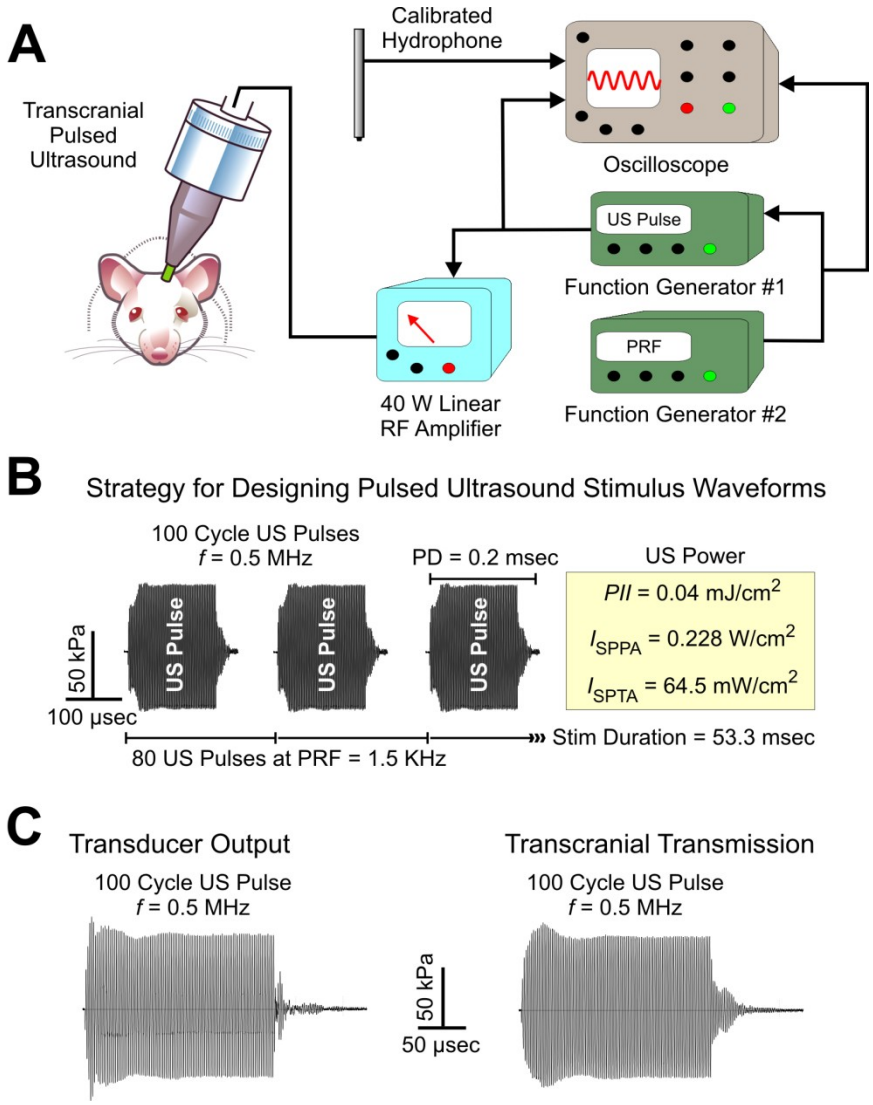

Figure 7. Construction and characterization of low-intensity ultrasound stimulus waveforms for the transcranial stimulation of intact brain circuits. (A) Illustration of the method used to construct and transmit pulsed US waveforms into the intact mouse brain. Two function generators were connected in series and used to construct stimulus waveforms. An RF amplifier was then used to provide final voltages to US transducers (see Figures S2.1-S2.2 and *Experimental Procedures*). (B) An example low-intensity US stimulus waveform is illustrated to highlight the parameters used in their construction. The acoustic intensities generated by the illustrated stimulus waveform are shown in the *yellow-box.* (C) Projected from a transducer surface to the face of a calibrated hydrophone, the acoustic pressure generated by a 100 cycle pulse of 0.5 MHz ultrasound is shown (*left*). The pressure generated by the same US pulse when transmitted from the face of the transducer through a fresh *ex vivo* mouse head to regions corresponding to motor cortex (0.8 mm deep) is shown (*right*).

Functional Stimulation of Intact Brain Circuits using Pulsed Ultrasound

We first studied the influence of pulsed US on intact motor cortex since it enables electrophysiological and behavioral measures of brain activation. We recorded local field potentials (LFP) and multi-unit activity (MUA) in primary motor cortex (M1) while transmitting pulsed US (0.35 MHz, 80 c/p, 1.5 kHz PRF, 100 pulses) having an I_{SPTA} = 36.20 mW/cm^2 through acoustic collimators (d = 4.7 mm) to the recording locations in anesthetized mice (*n* = 8; Figures 8A and 8B). Pulsed US triggered an LFP in M1 with a mean amplitude of -350.59 ± 43.34 μV (Figure 8B, 25 trials each). The LFP was associated with an increase in the frequency of cortical spikes (Figures 8C and 8D). This increase in spiking evoked by pulsed US was temporally precise and apparent within 50 msec of stimulus onset (Figure 8D). We found a broad range of pulsed US waveforms were equally capable of stimulating intact brain circuits as discussed below. Application of TTX (100 μM) to M1 (n = 4 mice) attenuated US-evoked increases in cortical activity, indicating transcranial US stimulates neuronal activity mediated by action potentials (Figure 8B). These data provide the first evidence that pulsed US can be used to directly stimulate neuronal activity and action potentials in intact brain circuits.

We next acquired fine-wire electromyograms (EMG) and videos of muscle contractions in response to US stimulation of motor cortex in skin- and skull-intact, anesthetized mice. Using transcranial US to stimulate

motor cortex, we evoked muscle contraction and movements in 92% of the mice tested. The muscle activity triggered by US stimulation of motor cortex produced EMG responses similar to those acquired during spontaneous muscle twitches (Figure 9A).

When using transducers directly coupled to the skin of mice, bilateral stimulation with transcranial US produced the near simultaneous activation of several muscle groups indicated by tail, forepaw, and whisker movements. By using acoustic collimators having an output aperture of d = 2.0, 3.0, or 4.7 mm and by making small (≈ 2 mm) adjustments to the positioning of transducers or collimators over motor cortex within a subject, we could differentially evoke the activity of isolated muscle groups. Despite these intriguing observations, we found it difficult to reliably generate fine maps of mouse motor cortex using US for brain stimulation. The likeliest explanation for this difficulty is that the topographical/spatial segregation of different motor areas represented on the mouse cortex are below the resolution limits of US (see *Spatial Resolution of Brain Circuit Activation with Transcranial Pulsed Ultrasound* below).

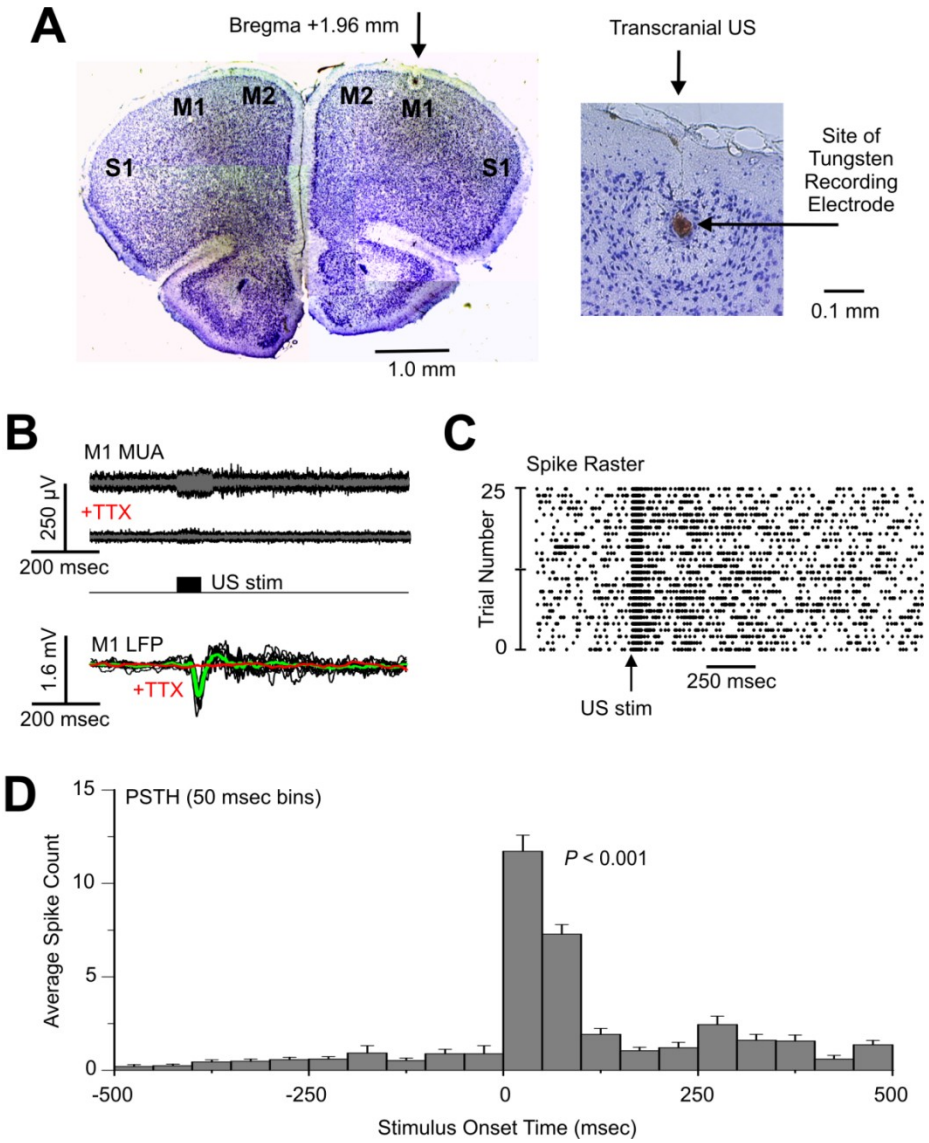

Figure 8. Low-intensity pulsed US stimulates neuronal activity in the intact mouse motor cortex. (A) The coronal brain section shows an electrolytic lesion illustrating a recording site from which US-evoked neuronal activity was acquired in M1. (B) *Top*, raw (*black*) and average (*grey*; 25 trials) US-evoked MUA recorded from M1 cortex in response to the delivery of pulsed US waveforms. *Middle*, addition of TTX to the cortex reduced synaptic noise and attenuated US-evoked MUA. *Bottom*, raw control (*black*), average control (*green*), and average TTX (*red*) LFP recorded from M1 cortex in response to 25 US stimulus waveforms delivered every 10 sec. (C) The spike raster plot illustrates the increase of cortical spiking as a function of time in response to 25 consecutive US stimulation trials. (D) A post-stimulus time histogram illustrates the average MUA spike count recorded 500 msec prior to and 500 msec following the delivery of US stimulus waveforms to motor cortex.

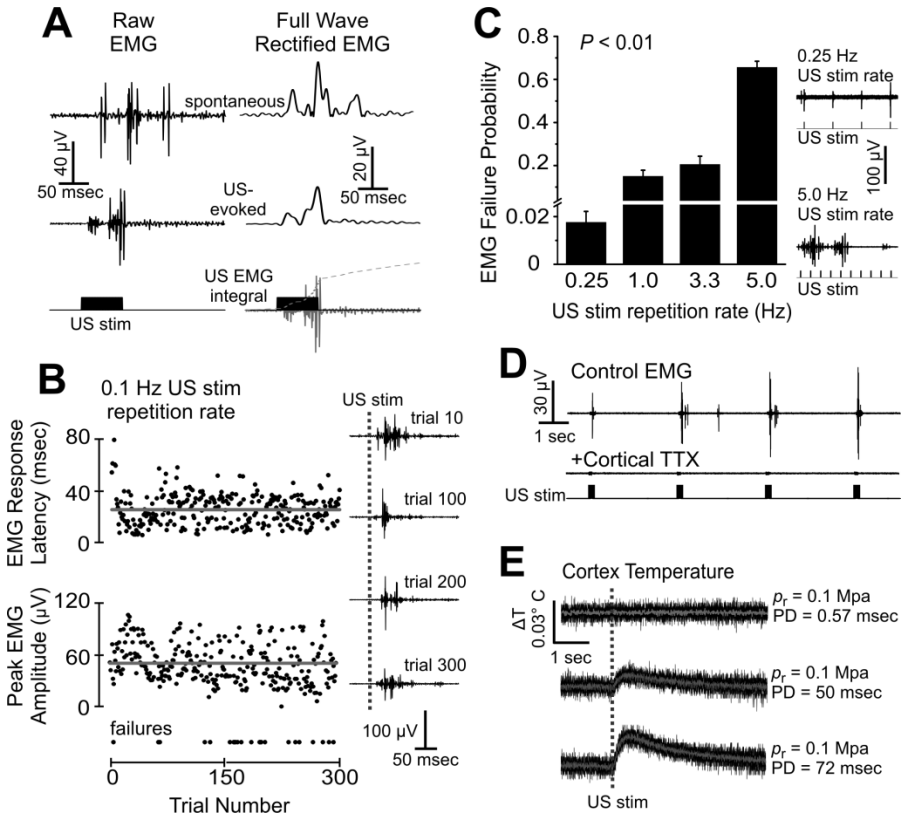

Figure 9. Transcranial stimulation of motor cortex with pulsed US functionally activates descending corticospinal motor circuits in intact mice. (A) Raw (*left*) and full-wave rectified (FWR; *right*) EMG traces obtained for a spontaneous muscle twitch (*top*) and average (10 trials) increase in muscle activity produced by transcranial US stimulation of motor cortex. The duration of the US stimulus waveform (*black*), average US-evoked EMG trace (*grey*), and EMG integral (*grey dashed-line*) are shown superimposed at *lower-right*. (B) EMG response latencies (*top*) and amplitudes (*bottom*) recorded from the left triceps brachii in response to right motor cortex stimulation are plotted as a function of trial number repeated at 0.1 Hz. Individual US-evoked raw EMG traces are shown for different trials (*right*). (C) EMG failure probability histograms are shown for four progressively increasing stimulus repetition frequencies. Raw US-evoked EMG traces are shown for two different stimulus repetition frequencies (*right*). (D) Raw EMG traces illustrating application of TTX to the motor cortex blocks US-evoked descending corticospinal circuit activity. (E) Raw (*black*) and averaged (*grey*; 10 trials) temperature recordings obtained from motor cortex in response to transmission of US waveforms with short pulse durations (PD) used in stimulus waveforms (*top*). Similarly, temperature recordings of cortex in response to waveforms having a PD approximately 100 times longer than those used in stimulus waveforms (*middle* and *bottom*).

The Influence of US Brain Stimulation Parameters on Motor Circuits Response Properties

When bilaterally targeted to motor cortex, pulsed US (0.50 MHz, 100 cycles per pulse, 1.5 kHz PRF, 80 pulses) having an I_{SPTA} = 64.53 mW/cm^2 triggered tail twitches and EMG activity in the lumbosacrocaudalis dorsalis lateralis muscle with a mean response latency of 22.65 ± 1.70 msec (*n* = 26 mice). When unilaterally transmitted to targeted regions of motor cortex using a collimator (d = 3 mm), pulsed US (0.35 MHz, 80 c/p, 2.5 kHz PRF, 150 pulses) having an I_{SPTA} = 42.90 mW/cm^2 triggered an EMG response in the contralateral triceps brachii muscle with a mean response with latency of 20.88 ± 1.46 msec (n = 17 mice). With nearly identical response latencies (21.29 ± 1.58 msec), activation of the ipsilateral triceps brachii was also observed in ~ 70% of these unilateral stimulation cases. Although consistent from trial-to-trial (Figure 9B), the EMG response latencies produced by US brain stimulation were ≈ 10 msec slower than those obtained using optogenetic methods and intracranial electrodes to stimulate motor cortex (Ayling, Harrison et al. 2009). Several reports show that TMS also produces response latencies slower than those obtained with intracranial electrodes (Barker 1999). Discrepancies among the response latencies observed between electrical and US methods of brain stimulation are possibly due to differences in the time-varying energy profiles that these methods impart on brain circuits. The underlying core mechanisms of action

responsible for mediating each brain stimulation method are additional factors likely to influence the different response times.

The baseline failure rate in obtaining US-evoked motor responses was < 5% when multiple stimulus trials were repeated once every four to ten seconds for time periods up to 50 min (Figure 9B). As observed for response latencies in acute experiments, the peak amplitudes of EMG responses evoked by transcranial pulsed US were stable across trial number (Figure 9B). In more chronic situations, we performed repeated US stimulation experiments within individual subjects (n = 5 mice) on days 0, 7, and 14 using a trial repetition frequency of 0.1 Hz for 12-15 min each day. In these experiments there were no differences in the peak amplitudes of the US-evoked EMG responses across days (day 0 mean peak EMG amplitude = 40.26 ± 0.99 μV, day 7 = 43.06 ± 1.52 μV, day 14 = 42.50 ± 1.42 μV; ANOVA $F_{2, 1303} = 1.47$, P = 0.23). These data demonstrate the ability of transcranial US to successfully stimulate brain circuit activity across multiple time periods spanning minutes (Figure 11A) to weeks.

By examining EMG failure rates in eight mice, we next studied how the success of achieving motor activation was affected when stimulus trials were repeated in more rapid succession. The mean EMG failure probability significantly increased ($P < 0.001$) as the rate of US stimulus delivery increased from 0.25 to 5 Hz (Figure 9C). This data suggest that brain stimulation with US may not be useful at stimulation frequencies

above 5 Hz. To confirm these observations and further explore this potential limitation, future investigations of an expanded US stimulus waveform space are required since it is not known how other US waveform profiles will influence the generation of sustained activity patterns.

We observed application of TTX to motor cortex blocked EMG activity, which indicates pulsed US triggers cortical action potentials to drive peripheral muscle contractions (n = 4 mice; Figure 3D). The intensities of US stimuli we studied were < 500 mW/cm^2, where mechanical bioeffects have been well documented in the absence of thermal effects (Dinno, Dyson et al. 1989; Dalecki 2004; O'Brien 2007; ter Haar 2007). To confirm these observations in brain tissue, we monitored the temperature of motor cortex in response to US waveforms having different pulse duration (PD) times. Equations for estimating thermal absorption of US in biological tissues indicate PD times are a critical factor for heat generation (O'Brien 2007) and predict 0.5 MHz US pulses exerting a p_r of 0.097 MPa for a PD of 0.57 msec should produce a temperature increase of 2.8 x 10^{-6} °C in brain (see *Experimental Procedures*). All US stimulus waveforms used in this study had p_r values < 0.097 MPa and PD times ≤ 0.57 msec. None of the US waveforms used to stimulate cortex elicited a significant change in cortical temperature within our 0.01 °C resolution limits (Figure 3E). We found US pulses with p_r

values of 0.1 MPa and PD times > 50 msec were required to produce a nominal temperature change (ΔT) of 0.02°C (Figure 9E).

We next examined how acoustic frequencies and intensities across the ranges studied here influenced US-evoked EMG responses from the triceps brachii of mice (n = 20). We stimulated motor cortex using 20 distinct pulsed US waveforms composed with different US frequencies (0.25, 0.35, 0.425, and 0.5 MHz) and having varied intensities. We randomized the sequence of which different waveforms were used in individual stimulus trials to avoid order effects. Relative comparisons of EMG amplitudes across animals can be influenced by many factors including electrode placement, number of fibers recorded from, variation in noise levels, and differential fiber recruitment, which can be handled using normalization techniques to reduce inter-subject variability (Yang and Winter 1984; Kamen and Caldwell 1996). To examine US-evoked EMG responses having the same dynamic range across animals, we normalized the peak amplitude of individual EMG responses to the maximum-peak amplitude EMG obtained for an animal and forced its minimum-peak amplitude EMG response through zero. A two-way ANOVA revealed a significant main effect of US frequency on EMG amplitude, where lower frequencies produced more robust EMG responses ($F_{3,\ 1085}$ = 3.95, P < 0.01; Figure 4A). The two-way ANOVA also revealed a significant main effect of intensity (I_{SPTA}) on EMG amplitudes ($F_{19,\ 1085}$ = 9.78, P < 0.001; Figure 4B), indicating lower intensities triggered more

robust EMG responses. The two-way ANOVA also revealed a significant frequency x intensity interaction ($F_{3, 1085} = 7.25$, $P < 0.01$; Figure 10C) indicating differential effects of US waveforms on neuronal activity as a function of frequency and intensity. Across the stimulus waveforms studied, we found the EMG response latencies were not affected by either frequency or intensity (*data not shown*).

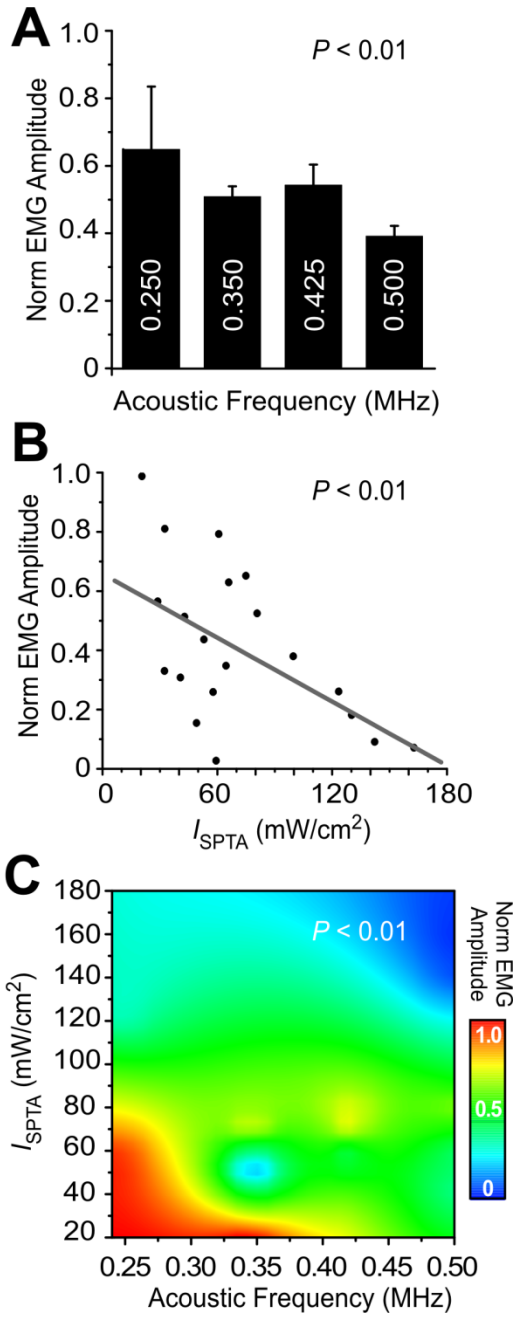

Figure 10. Interactions of the acoustic frequency and acoustic intensity of stimulus waveforms on descending corticospinal circuit activation. (A) Maximum-peak normalized (Norm) US-evoked EMG amplitude histograms are plotted for the four US frequencies used in the construction of stimulus waveforms. (B) Mean maximum-peak normalized US-evoked EMG amplitudes are plotted as a function of US intensities (I_{SPTA}) produced by 20 distinct stimulus waveforms (see Table S1). (C) The interaction between US intensity (I_{SPTA}) and US frequency is plotted as a function of maximum-peak normalized EMG amplitudes (*pseudocolor LUT*).

Spatial Distribution of Brain Circuit Activation with Transcranial Pulsed Ultrasound

To characterize the spatial distribution of US-evoked activity, we constructed functional activity maps using antibodies against *c-fos* (n = 4 mice). To facilitate data interpretation, we chose to stimulate intact brain tissue having a relatively planar surface and prominent subcortical structures. We centered the output of acoustic collimators (d = 2 mm) over the skull covering the right hemisphere from -1.2 mm to -3.2 mm of Bregma and 0.5 mm to 2.5 mm lateral of the midline using stereotactic coordinates (Figure 11A; (Franklin and Paxinos 2007). We used our smallest diameter collimator to characterize the minimal resolution of our brain stimulation method since it is expected larger collimators will produce larger areas of brain activation. Pulsed US (0.35 MHz, 50 c/p, 1.5 kHz PRF, 500 pulses) having an I_{SPTA} = 36.20 mW/cm^2 was transmitted along a vertical axis parallel to the sagittal plane through underlying brain regions once every 2 sec for 30 minutes. Following a 45-minute recovery period, mice were sacrificed and their brains were harvested for histology.

We prepared coronal sections from brain regions spanning +0.25 mm to -4.20 mm of Bregma (Figure 11A). Individual sections spaced every 125 µm were then immunolabeled using antibodies against *c-fos* and imaged using transmitted light microscopy. We quantified *c-fos*$^+$ cell densities in 250 x 250 µm squares for entire coronal sections, corrected for tissue shrinkage, and developed brain activity maps by plotting *c-fos*$^+$

cell densities in 250 x 250 μm pixels onto their corresponding anatomical locations using mouse brain atlas plates (Franklin and Paxinos 2007). Representative raw data and functional activity maps coding *c-fos*$^+$ cell density using a psuedo-color lookup table for visualization purposes are shown in Figure 11B-D. We estimated the lateral resolution of pulsed US along the rostral-caudal brain axis by analyzing regions of dorsal cortex (0.25 to 1.0 mm deep; 0.75 mm to 1.50 mm lateral of the midline) for each coronal section (Figures 11A-D). An ANOVA comparing the mean *c-fos*$^+$ cell densities for each 250 x 250 μm square region collapsed across animals revealed that pulsed US produced a significant increase in the density of *c-fos*$^+$ cells (ANOVA, $F_{1, 646} = 73.39$, $P < 0.001$; contralateral control hemisphere mean *c-fos*$^+$ cell density = 16.29 ± 0.20 cells/6.25 x 10^{-2} mm^2 compared to US stim = 19.82 ± 0.36 cells/6.25 x 10^{-2} mm^2). Subsequent pairwise comparisons of stimulated versus contralateral control cortex revealed US stimulation produced a significant increase in *c-fos*$^+$ cell densities for a 1.5 mm region along the rostral-caudal axis (-1.38 mm to -2.88 mm of Bregma) under the 2.0 mm diameter stimulation zone (Figure 11E). Similar analyses along the medial-lateral axis of dorsal cortex, revealed a significant increase ($P < 0.05$) in *c-fos*$^+$ cell densities for a 2.0 mm wide region of brain tissue under the stimulation zone. We observed a smearing of elevated *c-fos*$^+$ cell densities lateral to the stimulation zone, which could be attributed to nonlinearities in our acoustic

collimators, the corticocortical lateral spread of activity, and/or slight lateral variations in the positioning of our collimators.

By examining the effects of pulsed US along the dorsal-ventral axis within the stimulation zone (0.5 to 2.5 mm medial to lateral; -1.2 to -3.2 mm of Bregma), we found the density of *c-fos*$^+$ cells was significantly higher ($P < 0.05$) compared to contralateral controls in the superficial 1.0 mm of tissue. While there were trends of higher *c-fos*$^+$ cell densities in some deeper nuclei of stimulated hemispheres, we only observed one significant difference in a deep-brain region . The elevated *c-fos* here may have been produced by standing waves or reflections since higher *c-fos*$^+$ cell densities were generally observed near the skull base. Otherwise, we would have expected to observe elevated *c-fos*$^+$ levels uniformly along the dorsal-ventral axis of stimulated regions due to the transmission/absorption properties of US in brain tissue. For > 1.5 mm of the 2.0 mm diameter cortical area we targeted with US in these mapping studies, regions deeper than ≈ 1 mm were ventral to dense white matter tracts (corpus callosum) in the brain. Interestingly, unmyelinated C-fibers have been shown to be more sensitive to US than myelinated Aδ fibers (Young and Henneman 1961). Effectively blocking US-evoked activity in subcortical regions, we suspect low-intensity US fields may have been absorbed/scattered by dense white matter tracts in these mapping studies as a function of the US transmission path implemented. Despite these observations, we show below that it is indeed possible to stimulate

subcortical brain regions with transcranial US by employing different targeting approaches (see *Remote Stimulation of the Intact Hippocampus using Transcranial Pulsed US*).

Brain Stimulation with Low-Intensity Transcranial Pulsed Ultrasound is Safe in Mice

To assess the safety of transcranial US brain stimulation in mice, we first examined how pulsed US influenced blood-brain barrier (BBB) integrity. Prior to stimulation, mice received an intravenous administration of fluorescein isothiocyanate-dextran (10 kDa), which does not cross the BBB under normal conditions (Kleinfeld, Mitra et al. 1998). The motor cortex of mice (n = 5) was then unilaterally stimulated every 10 seconds for 30 minutes with pulsed US (0.50 MHz, 225 cycles per pulse, 1.5 kHz PRF, 100 pulses) having an I_{SPTA} = 142.20 mW/cm^2 using a collimator (d = 4.7 mm). We observed no evidence that US produced damage to the BBB as indicated by a complete lack fluorescein leakage (contralateral control = 179.6 mm vasculature length examined versus US Stim = 183.4 mm vasculature length examined; Figure 6A). In separate positive control experiments, we co-administered intravenous fluorescein-dextran with an US contrast agent (Optison®) shown to mediate *in vivo* BBB disruption in response to US (Raymond, Treat et al. 2008). Results from these positive control experiments (n = 3 mice) confirmed our ability to detect BBB damage had it occurred in response to pulsed US alone (Figure 12B).

We next probed the cellular-level consequences of pulsed US on brain tissues using antibodies against cleaved-caspase-3 to monitor cell death (Figure 12C). Using the same US waveform described above (I_{SPTA} = 142.2 mW/cm^2), we unilaterally stimulated the motor cortex of mice (n = 8) every 10 seconds for 30 minutes. Following a 24-hour recovery period to allow for peak caspase-3 activation, mice were sacrificed and their brains examined using confocal microscopy. In comparing stimulated cortex regions with their contralateral controls (2.81 mm^2 total area/hemisphere/mouse), we found pulsed US did not induce a change in the density of apoptotic glial cells (control = 0.40 ± 0.04 caspase-3$^+$ cells/0.56 mm^2 versus US Stim = 0.43 ± 0.06 caspase-3$^+$ cells/0.56 mm^2; P > 0.30) or apoptotic neurons (control = 0.08 ± 0.03 caspase-3$^+$ cells/0.56 mm^2 versus US stim = 0.07 ± 0.03 caspase-3$^+$ cells/0.56 mm^2; P > 0.50; Figure 12D). To further confirm this lack of an effect on cell death, we repeated the above experiment in mice (n = 4) using a higher intensity US waveform (I_{SPTA} = 300 mW/cm^2), which is 137 mW/cm^2 higher intensity than we used to evoke brain activity with any waveform in this study. We again observed no significant effects (2.81 mm^2 total area/hemisphere/mouse) of pulsed US on the density of apoptotic glial cells (control = 0.44 ± 0.16 caspase-3$^+$ cells/0.56 mm^2 versus US stim = 0.38 ± 0.13 caspase-3$^+$ cells/0.56 mm^2; P > 0.30) or apoptotic neurons (control = 0.06 ± 0.05 caspase-3$^+$ cells/0.56 mm^2 versus US stim = 0.07 ± 0.05 caspase-3$^+$ cells/0.56 mm^2; P > 0.50; Figure 12D).

To determine the effects of pulsed US on brain ultrastructure, we used quantitative transmission electron microscopy to examine stimulated and control brains. We compared excitatory synapses in the motor cortex from control unstimulated mice (n = 5 mice) with synapses in the stimulated regions of motor cortex from mice (n = 6), which underwent a US stimulus trial as described above (I_{SPTA} = 142.2 mW/cm^2) every 10 seconds for 30 minutes (Figure 12E). An independent samples *T*-test revealed no significant difference in the density of synapses between groups (control = 16.59 ± 0.81 synapses/100 μm^2 from 2.3 mm^2 versus US stim = 22.99 ± 4.07 synapses/100 μm^2 from 4.2 mm^2; $P > 0.10$; Figure 12F). There were also no significant differences in the postsynaptic density (PSD) length (control = 0.225 ± 0.009 μm from 99 synapses versus US stim = 0.234 ± 0.009 μm from 130 synapses; $P > 0.10$), the area of presynaptic terminals (control = 0.279 ± 0.02 μm^2 versus US stim = 0.297 ± 0.02 μm^2; $P > 0.10$), the density of vesicles in presynaptic boutons (control = 206.89 ± 9.52 vesicles/μm^2 versus US stim = 209.85 ± 8.14 vesicles/μm^2; $P > 0.10$), or the number of docked vesicles (DV) occupying active zones (control = 21.71 ± 0.91 DV/μm versus US stim = 20.26 ± 0.61 DV/μm; $P > 0.10$) between treatment groups (Figure 12F). There were no qualitative differences in the ultrastructure of cortical neuropil between treatment groups.

To determine if transcranial US stimulation of motor cortex produced any gross impairments in motor behavior, we assessed EMG

integrity the day before stimulation with pulsed US waveforms (I_{SPTA} = 142.2 mW/cm^2; every 10 seconds for 30 minutes), 24 hours post-stimulation, and again 7 days post-stimulation. Compared to sham-treated controls (n = 9 mice), a repeated measures ANOVA revealed no significant effect of US stimulation (n = 9 mice) on a rotorod running task ($F_{1,8}$ = 0.211, P > 0.1). We also measured motor function and grip strength by subjecting mice to wire-hanging task. Again, repeated measures ANOVA revealed no significant group effect on hang time ($F_{1,8}$ = 0.05; P > 0.1). During daily behavioral monitoring, we observed no differences in feeding behavior, grooming behavior, or startle reflexes between US stimulated mice and sham controls.

Through our development of the US brain stimulation method described above, we have stimulated the intact brains of more than 190 mice through > 92,000 US stimulus trails. We allowed > 50% of the mice to recover from anesthesia following stimulation procedures and never observed any neurological abnormalities such as paralysis, ataxia, or tremor in these mice. Even mice undergoing multiple repeated stimulation protocols spanning a two-week time period exhibited no visible behavioral impairments or signs of diminishing responsiveness to transcranial pulsed US. In our studies, fewer than 6% of the animals died during or immediately following a US stimulation experiment. This mortality rate was likely due to respiratory or cardiac complications associated with maintaining mice under ketamine/xylazine anesthesia for extended

periods of time (> 2 hrs). Based on the collective observations described above, we conclude that low-intensity transcranial pulsed US provides a safe and noninvasive method of stimulating intact brain circuit activity in mice. Whether similar safety margins hold true for other animal species must be directly evaluated and remains undetermined.

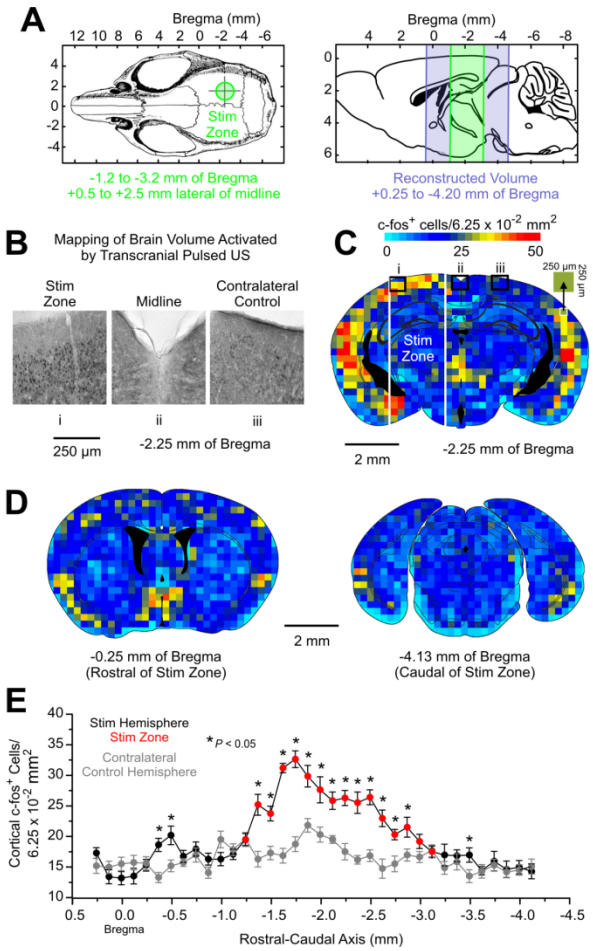

Figure 11. Spatial distribution of neuronal activation triggered by transcranial pulsed US. (A) Diagrams showing the anatomical locations where transcranial pulsed US was delivered through an acoustic collimator (*green*; d = 2 mm; Figure S2C) and the brain volume subsequently reconstructed (*blue*) to develop functional activity maps using antibodies against *c-fos* (Figure S3). (B) Light micrographs showing *c-fos* activity in a coronal brain section at different locations inside (i) and outside (ii and iii) the US transmission path. (C) A psuedo-colored map of *c-fos*$^+$ cell densities in 250 x 250 µm regions is shown for a reconstructed coronal section obtained from within the stimulus zone. Small regions inside (i) and outside (ii and iii) the US brain transmission path are highlighted and contain *c-fos* density data obtained from the corresponding images shown in *B*. (D) Similar psuedo-colored *c-fos* activity maps are shown for coronal brain sections rostral (*left*) and caudal (*right*) of the stimulated brain regions. (E) The line plots illustrate the mean *c-fos*$^+$ cell densities observed along the rostral-caudal axis of reconstructed brain volumes for stimulated (*black*) and contralateral control hemispheres (*grey*). Regions of cortex within the stimulation zone are indicated by *red*.

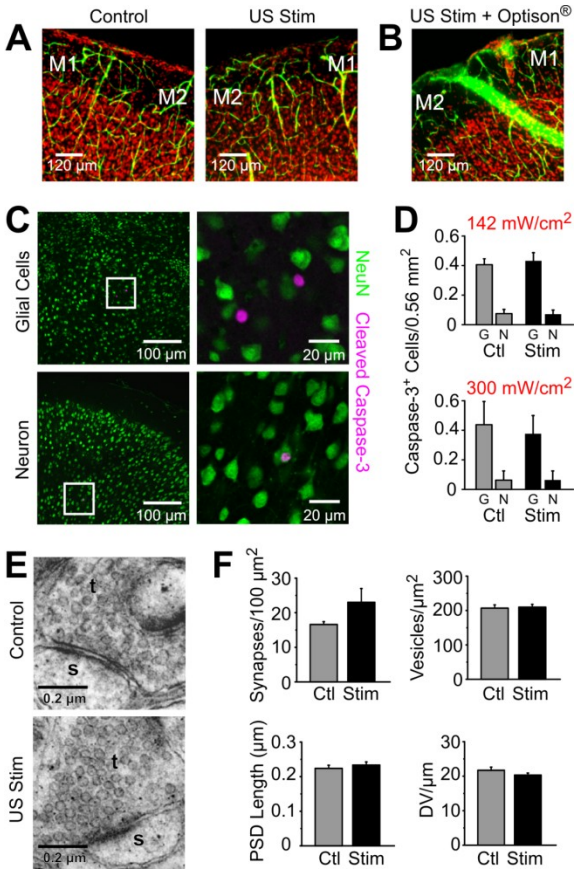

Figure 12. Transcranial stimulation of mouse cortex with low-intensity pulsed US is safe. (A) Confocal images of TO-PRO-3 labeled cells (*red*) and fluorescein-dextran filled cerebrovasculature (*green*) obtained from the motor cortex of a contralateral control hemisphere (*left*) and from the stimulated region of the US-treated hemisphere (*right*). (B) A similar confocal image is shown, but was obtained from a positive control treatment group where US-stimulation was performed in the presence of Optison® an ultrasound-microbubble contrast agent known to elicit cavitationally-mediated vasculature damage. (C) Confocal images of NeuN$^+$ (*green*) and cleaved-Caspase 3$^+$ (*magenta*) cells obtained from a US stimulated region show positive glial cells (*top*) and a neuron (*bottom*) at low-(*left*) and high-magnification (*right*). (D) Histograms illustrate the mean density of cleaved-Caspase 3$^+$ glial cells (*G*) and neurons (*N*) observed in the motor cortex of contralateral control and US-stimulated hemispheres for two different stimulus intensity waveforms. (E) Transmission electron microscopic images (*left*) of excitatory synapses from control (*top*) and US stimulated M1 cortex (*bottom*). (F) Histograms are shown for mean synaptic density (*top-left*), mean axonal bouton synaptic vesicle density (*top-right*), mean PSD length (*bottom-left*), and mean number of DV occupying active zones (*bottom-right*). Also see Figure S4.

Remote Stimulation of the Intact Mouse Hippocampus Using Transcranial Pulsed US

We finally aimed to determine if transcranial pulsed US can be used to stimulate subcortical brain circuits in intact mice. To address this issue, we focused our attention on the intact mouse hippocampus since pulsed US waveforms have been shown to elicit action potentials and synaptic transmission in hippocampal slices (Tyler, Tufail et al. 2008). We performed extracellular recordings of US-evoked activity in the CA1 *stratum pyramidale* (*s.p.*) cell body layer of dorsal hippocampus (n = 7 mice). Prompted by our observations regarding the potential disruption of US fields by dense white matter tracts, we implemented a targeting approach bypassing the dense white matter of the corpus callosum when transmitting pulsed US to the hippocampus.

We used an angled line of US transmission through the brain by positioning acoustic collimators 50° from a vertical axis along the sagittal plane. The output aperture of collimators (d = 2 mm) were unilaterally centered over -4.5 mm of Bregma and 1.5 mm lateral of the midline (Figure 13A). We used a 30° approach angle to drive tungsten microelectrodes to the CA1 *s.p.* region of hippocampus through cranial windows (d = 1.5 mm) centered approximately -1.0 mm of Bregma (Figure 13A). Pulsed US (0.25 MHz, 40 cycles per pulse, 2.0 kHz PRF, 650 pulses) having an I_{SPTA} = 84.32 mW/cm^2 reliably triggered an initial LFP with a mean amplitude of -168.94 ± 0.04 μV (50 trials each) and a mean

response latency of 123.24 ± 4.44 msec following stimulus onset (Figure 13B). This initial LFP was followed by a period of after-discharge activity lasting < 3 sec (Figure 13B). These short lived after-discharges did not appear to reflect abnormal circuit activity as observed during epileptogenesis (Racine 1972; McNamara 1994; Bragin, Penttonen et al. 1997). In fact, hippocampal after-discharges lasting more than ten seconds are indicative of seizure activity (Racine 1972).

Pulsed US produced a significant ($P < 0.01$) increase in spike frequency lasting 1.73 ± 0.12 seconds (Figure 13B). Natural activity patterns in the CA1 region of hippocampus exhibit gamma (40 - 100 Hz), sharp-wave (SPW) "ripple" (160 - 200 Hz), and other frequency-band oscillations reflecting specific behavioral states of an animal (Buzsaki 1989; Buzsaki, Horvath et al. 1992; Bragin, Jando et al. 1995; Buzsaki 1996). Sharp-wave ripples (≈ 20 msec oscillations at ≈ 200 Hz) in CA1 result from the synchronized bursting of small populations of CA1 pyramidal neurons (Buzsaki, Horvath et al. 1992; Ylinen, Bragin et al. 1995) and have recently been shown to underlie memory storage in behaving rodents (Girardeau, Benchenane et al. 2009; Nakashiba, Buhl et al. 2009). On the other hand, the consequences of gamma oscillations in the CA1 region of the hippocampus are not as well understood, but are believed to stem from the intrinsic oscillatory properties of inhibitory interneurons (Bragin, Jando et al. 1995; Buzsaki 1996). By decomposing the frequency components of wideband (1 to 10,000 Hz) activity patterns

evoked by pulsed US, we found all after-discharges contained both gamma oscillations and SWP ripple oscillations lasting < 3 sec (Figure 13C). These data demonstrate that pulsed US can stimulate intact mouse hippocampus while evoking synchronous activity patterns and network oscillations; hallmark features of intrinsic hippocampal circuitry.

We naturally questioned whether these effects were accompanied by the regulation of activity-mediated cellular molecular signaling cascades in the hippocampus. Brain-derived neurotrophic factor (BDNF) is one of the most potent neuromodulators of hippocampal plasticity and its expression/secretion is known to be regulated by neuronal activity (Poo 2001; Lessmann, Gottmann et al. 2003). We thus examined BDNF protein expression levels in the hippocampus following transcranscranial stimulation with pulsed US. Unilateral hippocampi of mice (n = 7) were targeted and stimulated with pulsed US (0.35 MHz, 50 cycles per pulse, 1.5 kHz PRF, 500 pulses) having an I_{SPTA} = 36.20 mW/cm^2 every two seconds for 30 minutes. Following a 45 minute recovery period, mice were sacrificed and their brains removed, sectioned, and immunolabeled with antibodies against BDNF. We observed pulsed US induced a significant increase in the density of BDNF$^+$ puncta in CA1 *s.p.* (contralateral control = 149.64 ± 11.49 BDNF$^+$ puncta/7.5 x 10^{-2} mm^2 from 0.61 mm^2 CA1 region/mouse versus US stim = 221.50 ± 8.75 BDNF$^+$ puncta/7.5 x 10^{-2} mm^2 from 0.61 mm^2 CA1region/mouse; *T*-test, $P < 0.001$; Figure 13D). Similar significant increases were observed in the CA3 *s.p*. region

(contralateral control = 206.20 ± 19.68 $BDNF^+$ puncta/7.5 x 10^{-2} mm^2 from 0.61 mm^2 CA3 region/mouse versus US stim = 324.82 ± 27.94 $BDNF^+$ puncta/7.5 x 10^{-2} mm^2 from 0.61 mm^2 CA3 region/mouse; *T*-test, $P < 0.005$; Figure 13D). These data demonstrate that pulsed US can be used to remotely stimulate neuronal activity in the intact mouse hippocampus. Posing captivating potential for broad applications in neuroscience, the increased synchronous activity and elevated BDNF expression patterns produced by pulsed US lend support to our hypothesis that transcranial US can be used to promote endogenous brain plasticity.

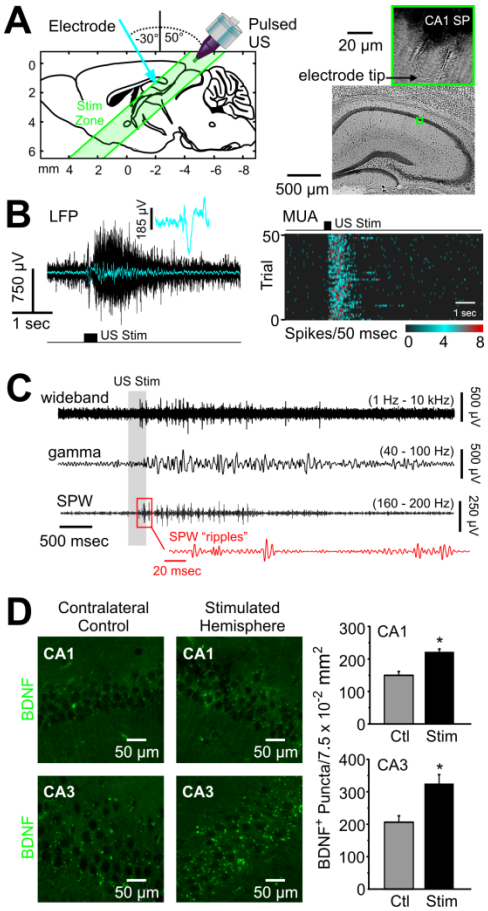

Figure 13. Transcranial stimulation of the intact mouse hippocampus with pulsed ultrasound. (A) Shown is an illustration of the geometrical configuration used for targeting the dorsolateral hippocampus with transcranial pulsed US while recording evoked electrophysiological responses in the dorsal hippocampus (*left*). A lesion illustrates the site of an electrophysiological recording location in the hippocampal CA1 *s.p.* region (*right*). (B) Raw (*black*) and average (*cyan*) hippocampal CA1 LFP recorded in response to 50 consecutive US stimulation trials (*left*). A psuedo-colored spike density plot illustrates the increase in CA1 *s.p.* spiking as a function of time in response to 50 consecutive pulsed US stimuli delivered at 0.1 Hz (*right*). (C) An individual recording trace of CA1 *s.p.* extracellular activity in response to a pulsed US waveform is shown in its wideband (*top*), gamma (*middle*), and SWP (*bottom*) frequency bands. An expanded 250 msec region of the SWP trace (*red*) illustrates SWP "ripples" (also see Figure S5). (D) Confocal images illustrating BDNF (*green*) expression in the CA1 *s.p.* (*top*) and CA3 *s.p.* (*bottom*) regions of hippocampus from contralateral control (*left*) and stimulated hemispheres (*right*). Histograms (*far-right*) illustrate the significant increase in the density of $BDNF^+$ puncta triggered by transcranial US stimulation for the CA1 *s.p.* (*top*) and CA3 *s.p.* (*bottom*) regions of hippocampus.

Discussion

To date, previous studies detailing the effects of US on neuronal activity have fallen short of providing methods for its practical implementation in stimulating intact brain function. Prior studies examined the effects of US on neuronal activity by pre-sonicating nervous tissues with US before examining its consequence on electrically-evoked activity. These studies indeed revealed how US differentially affects the amplitude and duration of compound action potentials/field potentials evoked with traditional stimulating electrodes (Mihran, Barnes et al. 1990; Rinaldi, Jones et al. 1991; Bachtold, Rinaldi et al. 1998; Tsui, Wang et al. 2005). In other words, previous studies showed US is capable of modulating electrically evoked activity, but not that it alone could stimulate neuronal activity. We have provided the first clear evidence that transcranial pulsed US can stimulate intact brain circuits without requiring exogenous factors or surgery.

Due to temperature increases < 0.01 °C in response to US stimulus waveforms (Figure 11D), we propose a predominantly nonthermal (mechanical) mechanism(s) of action. The nonthermal actions of US are best understood in terms of cavitation – for example radiation force, acoustic streaming, shock waves, and strain (Dalecki 2004; Leighton 2007; O'Brien 2007). Accordingly, we have proposed a continuum mechanics hypothesis of ultrasonic neuromodulation, where US produces fluid-mechanical effects on the cellular environments of neurons to

modulate their resting membrane potentials (Tyler 2010). The direct activation of ion channels by US may also represent a mechanism of action since many of the voltage-gated sodium, potassium, and calcium channels influencing neuronal excitability possess mechanically sensitive gating kinetics (Morris and Juranka 2007). Pulsed US could also produce ephaptic effects or generate spatially inhomogeneous electric fields, proposed to underlie aspects of synchronous activity (Jefferys and Haas 1982; Anastassiou, Montgomery et al.). Clearly, further studies are required to dissect mechanisms underlying the ability of US to stimulate intact brain circuits.

Our observations also serve as preliminary evidence that pulsed US can be used to probe intrinsic characteristics of brain circuits. For example, US stimulation of motor cortex produced short bursts of activity (< 100 msec) and peripheral muscle contractions, whereas stimulation of the hippocampus with similar waveforms triggered characteristic rhythmic bursting (recurrent activity), which lasted 2 - 3 seconds. These observations lead us to question whether stimulation of a given brain region with US can mediate even broader circuit activation based on functional connectivity. Such abilities have been shown and discussed for other transcranial brain stimulation approaches like TMS (Huerta and Volpe 2009). Future studies should be designed to study the influence of US on activity in corticothalamic, corticocortical, and thalamocorctial pathways as we have done here for corticospinal circuits. Similar to widely

recognized observations using other cortical stimulation methods (Angel and Gratton 1982; Goss-Sampson and Kriss 1991), we found the success of brain activation with transcranial pulsed US was dependent on the plane of anesthesia. When mice were in moderate to light anesthesia planes (mild responsiveness to tail pinch), we found US-evoked activity was highly consistent across multiple repeated trials as described above.

Although our observations indicate pulsed US provides a safe mode of brain stimulation in mice (Figure 12), it should not be inferred the same is true for other animal species. Safety studies in other animals are required for any such conclusions to be drawn. Since we suspect standing waves may inadvertently influence the activity of some brain regions under certain conditions, future studies should attend to the influence of such reflections on brain tissue regardless of the focusing method implemented. This is particularly true for cases where high-intensity ultrasound may be used to treat brain tissues as discussed below. The less direct safety implications of our study also need to be considered. Diagnostic fetal US has been shown to disrupt neuronal migration in developing rat fetal brains (Ang, Gluncic et al. 2006). Those effects could be due to the influence of US on neuronal activity or growth factor expression patterns in developing fetal brains. Having dire ramifications on the global use of diagnostic fetal ultrasound, investigations into such possibilities are warranted.

Using a method of transcranial US brain stimulation with an acoustic collimating tube (d = 2 mm), we estimated the volume of cortical activation to be ~ 3 mm^3 as indicated by *c-fos* activity (Figures 11). As previously discussed however, this activated brain volume may have been restricted by anatomical features along the dorsal-ventral US transmission path we implemented (for example the corpus callosum restricting the depth of activation to the cortex) and needs to be further explored before more accurate conclusions regarding the axial resolution can be drawn. The 1.5 - 2.0 mm lateral area of activation we observed represents a more reliable measure and is approximately five times better than the ≈ 1 cm lateral spatial resolution offered by TMS (Barker 1999). Due to the millimeter spatial resolutions conferred by US, it may be possible to use structured US fields to drive patterned activation in sparsely distributed brain circuits. Similarly, focusing with acoustic metamaterials (having a negative refractive index) enables sub-diffraction spatial resolutions to be achieved for US (Zhang, Yin et al. 2009). Based on those findings, it is not unreasonable to expect that brain regions < 1.0 mm may be accurately targeted for neurostimulation using 0.5 MHz US. Such spatial scales would indeed make transcranial US for brain stimulation amenable to a variety of research and clinical applications. With respect to the spatial resolutions of brain stimulation approaches however, optogenetic approaches still reign superior when micron scale resolutions are required - for example in the fine functional mapping of intact mouse brain circuits

(Ayling, Harrison et al. 2009; Hira, Honkura et al. 2009) or in the study of single-cell/single-synapse physiology (Zhang, Aravanis et al. 2007; Zhang, Holbro et al. 2008).

Focusing of US through skull bones, including those of humans, can be achieved using transducers arranged in phased arrays (Hynynen, Clement et al. 2004; Hynynen, McDannold et al. 2006; Martin, Jeanmonod et al. 2009). A recent clinical study reported using transcranial MRI-guided high-intensity focused ultrasound (0.65 MHz, > 1000 W/cm^2) to perform noninvasive thalamotomies (d = 4.0 mm) for the treatment of chronic neuropathic pain by focusing US through the intact human skull to deep thalamic nuclei using phased arrays (Martin, Jeanmonod et al. 2009). These abilities to focus US through the intact skull into the deep-brain regions certainly raise the possibility of using pulsed US in the noninvasive stimulation of human brain circuits. However, cautiously conducted preclinical safety and efficacy studies are required across independent groups before it can be determined if pulsed US might be useful in such an application.

We recognize several issues need further investigation before the potential of transcranial US for brain stimulation can be realized. However, it has not escaped our attention that transcranial pulsed US might serve as a foundation for radical new approaches to the study of brain function/dysfunction. For instance, since US is readily compatible with magnetic resonance imaging (MRI) it is feasible that pulsed US could be

used for brain circuit stimulation during simultaneous MRI imaging in the functional brain mapping of intact, normal or diseased brains. It is conceivable that pulsed US could be used to induce forms of endogenous brain plasticity as shown with TMS (Pascual-Leone, Valls-Sole et al. 1994). In such an embodiment, pulsed US might drive specific brain activity patterns shown to underlie certain cognitive processes like memory trace formation (Girardeau, Benchenane et al. 2009; Nakashiba, Buhl et al. 2009). This particularly intriguing possibility is supported by our observations in mice that transcranial US can promote sharp-wave ripple oscillations (Figure 13C) and stimulate the activity of endogenous BDNF (Figure 13D), an important regulator of brain plasticity and hippocampal-dependent memory consolidation (Tyler, Alonso et al. 2002). Based on this study demonstrating that trancranial pulsed US is capable of stimulating intact brain circuits, one can begin to imagine a vast number of applications where this method might enable us to better understand and manipulate brain function.

References

Anastassiou, C.A., Montgomery, S.M., Barahona, M., Buzsaki, G., and Koch, C. (2010). The effect of spatially inhomogeneous extracellular electric fields on neurons. J Neurosci *30*, 1925-1936.

Ang, E.S., Jr., Gluncic, V., Duque, A., Schafer, M.E., and Rakic, P. (2006). Prenatal exposure to ultrasound waves impacts neuronal migration in mice. Proc Natl Acad Sci U S A *103*, 12903-12910.

Angel, A., and Gratton, D.A. (1982). The effect of anaesthetic agents on cerebral cortical responses in the rat. Br J Pharmacol *76*, 541-549.

Ayling, O.G., Harrison, T.C., Boyd, J.D., Goroshkov, A., and Murphy, T.H. (2009). Automated light-based mapping of motor cortex by photoactivation of channelrhodopsin-2 transgenic mice. Nat Methods *6*, 219-224.

Bachtold, M.R., Rinaldi, P.C., Jones, J.P., Reines, F., and Price, L.R. (1998). Focused ultrasound modifications of neural circuit activity in a mammalian brain. Ultrasound in medicine & biology *24*, 557-565.

Barker, A.T. (1999). The history and basic principles of magnetic nerve stimulation. Electroencephalogr Clin Neurophysiol Suppl *51*, 3-21.

Bragin, A., Jando, G., Nadasdy, Z., Hetke, J., Wise, K., and Buzsaki, G. (1995). Gamma (40-100 Hz) oscillation in the hippocampus of the behaving rat. J Neurosci *15*, 47-60.

Bragin, A., Penttonen, M., and Buzsaki, G. (1997). Termination of epileptic afterdischarge in the hippocampus. J Neurosci *17*, 2567-2579.

Buzsaki, G. (1989). Two-stage model of memory trace formation: a role for "noisy" brain states. Neuroscience *31*, 551-570.

Buzsaki, G. (1996). The hippocampo-neocortical dialogue. Cereb Cortex *6*, 81-92.

Buzsaki, G., Horvath, Z., Urioste, R., Hetke, J., and Wise, K. (1992). High-frequency network oscillation in the hippocampus. Science *256*, 1025-1027.

Cooper, T.E., and Trezek, G.J. (1972). A probe technique for determining the thermal conductivity of tissue. Journal of Heat Transfer *94*.

Dalecki, D. (2004). Mechanical bioeffects of ultrasound. Annu Rev Biomed Eng *6*, 229-248.

Dinno, M.A., Dyson, M., Young, S.R., Mortimer, A.J., Hart, J., and Crum, L.A. (1989). The significance of membrane changes in the safe and effective use of therapeutic and diagnostic ultrasound. Physics in medicine and biology *34*, 1543-1552.

Foster, K.R., and Wiederhold, M.L. (1978). Auditory responses in cats produced by pulsed ultrasound. The Journal of the Acoustical Society of America *63*, 1199-1205.

Franklin, K.B.J., and Paxinos, G. (2007). The Mouse Brain in Stereotaxic Coordinates, Third Edition edn (New York, N.Y.: Academic Press).

Fry, F.J., Ades, H.W., and Fry, W.J. (1958). Production of reversible changes in the central nervous system by ultrasound. Science *127*, 83-84.

Gavrilov, L.R., Gersuni, G.V., Ilyinsky, O.B., Sirotyuk, M.G., Tsirulnikov, E.M., and Shchekanov, E.E. (1976). The effect of focused ultrasound on the skin and deep nerve structures of man and animal. Prog Brain Res *43*, 279-292.

Girardeau, G., Benchenane, K., Wiener, S.I., Buzsaki, G., and Zugaro, M.B. (2009). Selective suppression of hippocampal ripples impairs spatial memory. Nat Neurosci *12*, 1222-1223.

Goss-Sampson, M.A., and Kriss, A. (1991). Effects of pentobarbital and ketamine-xylazine anaesthesia on somatosensory, brainstem auditory and peripheral sensory-motor responses in the rat. Laboratory animals *25*, 360-366.

Goss, S.A., Johnston, R.L., and Dunn, F. (1978). Comprehensive compilation of empirical ultrasonic properties of mammalian tissues. Journal of Acoustical Society of America *62*, 423-455.

Harvey, E.N. (1929). The effect of high frequency sound waves on heart muscle and other irritable tissues. American Journal of Physiology, 284-290.

Hayner, M., and Hynynen, K. (2001). Numerical analysis of ultrasonic transmission and absorption of oblique plane waves through the human skull. The Journal of the Acoustical Society of America *110*, 3319-3330.

Hira, R., Honkura, N., Noguchi, J., Maruyama, Y., Augustine, G.J., Kasai, H., and Matsuzaki, M. (2009). Transcranial optogenetic stimulation for functional mapping of the motor cortex. J Neurosci Methods *179*, 258-263.

Huerta, P.T., and Volpe, B.T. (2009). Transcranial magnetic stimulation, synaptic plasticity and network oscillations. Journal of neuroengineering and rehabilitation *6*, 7.

Hynynen, K., and Clement, G. (2007). Clinical applications of focused ultrasound-the brain. Int J Hyperthermia *23*, 193-202.

Hynynen, K., Clement, G.T., McDannold, N., Vykhodtseva, N., King, R., White, P.J., Vitek, S., and Jolesz, F.A. (2004). 500-element ultrasound

phased array system for noninvasive focal surgery of the brain: a preliminary rabbit study with ex vivo human skulls. Magn Reson Med *52*, 100-107.

Hynynen, K., McDannold, N., Clement, G., Jolesz, F.A., Zadicario, E., Killiany, R., Moore, T., and Rosen, D. (2006). Pre-clinical testing of a phased array ultrasound system for MRI-guided noninvasive surgery of the brain--a primate study. Eur J Radiol *59*, 149-156.

Jefferys, J.G., and Haas, H.L. (1982). Synchronized bursting of CA1 hippocampal pyramidal cells in the absence of synaptic transmission. Nature *300*, 448-450.

Kamen, G., and Caldwell, G.E. (1996). Physiology and interpretation of the electromyogram. J Clin Neurophysiol *13*, 366-384.

Kleinfeld, D., Mitra, P.P., Helmchen, F., and Denk, W. (1998). Fluctuations and stimulus-induced changes in blood flow observed in individual capillaries in layers 2 through 4 of rat neocortex. Proc Natl Acad Sci U S A *95*, 15741-15746.

Leighton, T.G. (2007). What is ultrasound? Progress in biophysics and molecular biology *93*, 3-83.

Lele, P.P. (1963). Effects of Focused Ultrasonic Radiation on Peripheral Nerve, with Observations on Local Heating Experimental Neurology *8*, 47-83.

Lessmann, V., Gottmann, K., and Malcangio, M. (2003). Neurotrophin secretion: current facts and future prospects. Prog Neurobiol *69*, 341-374.

Ludwig, G.D. (1950). The velocity of sound through tissues and the acoustic impedance of tissues. The Journal of the Acoustical Society of America *22*, 862-866.

Martin, E., Jeanmonod, D., Morel, A., Zadicario, E., and Werner, B. (2009). High intensity focused ultrasound for non-invaisve functional neurosurgery. Annals of Neurology *66*, 858-861.

McNamara, J.O. (1994). Cellular and molecular basis of epilepsy. J Neurosci *14*, 3413-3425.

Mihran, R.T., Barnes, F.S., and Wachtel, H. (1990). Temporally-specific modification of myelinated axon excitability in vitro following a single ultrasound pulse. Ultrasound in medicine & biology *16*, 297-309.

Morris, C.E., and Juranka, P.F. (2007). Lipid Stress at Play: Mechanosensitivity of Voltage-Gated Channels. In Current Topics in Membranes, P.H. Owen, ed. (Academic Press), pp. 297-338.

Nakashiba, T., Buhl, D.L., McHugh, T.J., and Tonegawa, S. (2009). Hippocampal CA3 output is crucial for ripple-associated reactivation and consolidation of memory. Neuron *62*, 781-787.

NEMA (2004). Acoustic Output Measurement Standard For Diagnostic Ultrasound Equipment (Washington, D.C.: National Electrical Manufacturers Association).

Nyborg, W.L. (1981). Heat generation by ultrasound in a relaxing medium. Journal of Acoustical Society of America *70*, 310-312.

O'Brien, W.D., Jr. (2007). Ultrasound-biophysics mechanisms. Progress in biophysics and molecular biology *93*, 212-255.

Pascual-Leone, A., Valls-Sole, J., Wassermann, E.M., and Hallett, M. (1994). Responses to rapid-rate transcranial magnetic stimulation of the human motor cortex. Brain *117 (Pt 4)*, 847-858.

Poo, M.M. (2001). Neurotrophins as synaptic modulators. Nat Rev Neurosci *2*, 24-32.

Racine, R.J. (1972). Modification of seizure activity by electrical stimulation. I. After-discharge threshold. Electroencephalogr Clin Neurophysiol *32*, 269-279.

Raymond, S.B., Treat, L.H., Dewey, J.D., McDannold, N.J., Hynynen, K., and Bacskai, B.J. (2008). Ultrasound enhanced delivery of molecular imaging and therapeutic agents in Alzheimer's disease mouse models. PLoS ONE *3*, e2175.

Ressler, K.J., and Mayberg, H.S. (2007). Targeting abnormal neural circuits in mood and anxiety disorders: from the laboratory to the clinic. Nat Neurosci *10*, 1116-1124.

Rinaldi, P.C., Jones, J.P., Reines, F., and Price, L.R. (1991). Modification by focused ultrasound pulses of electrically evoked responses from an in vitro hippocampal preparation. Brain Res *558*, 36-42.

Shealy, C.N., and Henneman, E. (1962). Reversible effects of ultrasound on spinal reflexes. Archives of Neurology, 374-386.

Szobota, S., Gorostiza, P., Del Bene, F., Wyart, C., Fortin, D.L., Kolstad, K.D., Tulyathan, O., Volgraf, M., Numano, R., Aaron, H.L.*, et al.* (2007). Remote control of neuronal activity with a light-gated glutamate receptor. Neuron *54*, 535-545.

ter Haar, G. (2007). Therapeutic applications of ultrasound. Progress in biophysics and molecular biology *93*, 111-129.

Tsui, P.H., Wang, S.H., and Huang, C.C. (2005). In vitro effects of ultrasound with different energies on the conduction properties of neural tissue. Ultrasonics *43*, 560-565.

Tyler, W.J. (2010). Noninvasive neuromodulation with ultrasound? A continuum mechanics hypothesis. The Neuroscientist *Advanced Online Print, January 25, 2010*.

Tyler, W.J., Alonso, M., Bramham, C.R., and Pozzo-Miller, L.D. (2002). From acquisition to consolidation: on the role of brain-derived neurotrophic factor signaling in hippocampal-dependent learning. Learn Mem *9*, 224-237.

Tyler, W.J., Tufail, Y., Finsterwald, M., Tauchmann, M.L., Olson, E.J., and Majestic, C. (2008). Remote excitation of neuronal circuits using low-intensity, low-frequency ultrasound. PLoS ONE *3*, e3511.

Velling, V.A., and Shklyaruk, S.P. (1988). Modulation of the functional state of the brain with the aid of focused ultrasonic action. Neuroscience and Behavioral Physiology *18*, 369-375.

Wagner, T., Valero-Cabre, A., and Pascual-Leone, A. (2007). Noninvasive Human Brain Stimulation. Annu Rev Biomed Eng *9*, 527-565.

White, P.J., Clement, G.T., and Hynynen, K. (2006). Local frequency dependence in transcranial ultrasound transmission. Physics in medicine and biology *51*, 2293-2305.

Yang, J.F., and Winter, D.A. (1984). Electromyographic amplitude normalization methods: improving their sensitivity as diagnostic tools in gait analysis. Archives of physical medicine and rehabilitation *65*, 517-521.

Ylinen, A., Bragin, A., Nadasdy, Z., Jando, G., Szabo, I., Sik, A., and Buzsaki, G. (1995). Sharp wave-associated high-frequency oscillation (200 Hz) in the intact hippocampus: network and intracellular mechanisms. J Neurosci *15*, 30-46.

Young, R.R., and Henneman, E. (1961). Functional effects of focused ultrasound on mammalian nerves. Science *134*, 1521-1522.

Zhang, F., Aravanis, A.M., Adamantidis, A., de Lecea, L., and Deisseroth, K. (2007). Circuit-breakers: optical technologies for probing neural signals and systems. Nat Rev Neurosci *8*, 577-581.

Zhang, S., Yin, L., and Fang, N. (2009). Focusing Ultrasound with an Acoustic Metamaterial Network. Physics Reviews Letters *102*, 194301-194304.

Zhang, Y.P., Holbro, N., and Oertner, T.G. (2008). Optical induction of plasticity at single synapses reveals input-specific accumulation of alphaCaMKII. Proc Natl Acad Sci U S A *105*, 12039-12044.

Chapter 4

ULTRASONIC NEUROMODULATION: BRAIN STIMULATION WITH TRANSCRANIAL ULTRASOUND

Brain stimulation methods are indispensable to the study of brain function. They have also proven effective for treating some neurological disorders. Historically used for medical imaging, ultrasound has recently been shown capable of noninvasively stimulating brain activity. Here we first provide some general protocols for the stimulation of intact mouse brain circuits using transcranial ultrasound. Using a traditional mouse model of epilepsy, we then describe protocols for using transcranial ultrasound to disrupt electrographic seizure activity associated with epilepsy. The advantages of ultrasound for brain stimulation are that it does not require surgery or genetic alteration while conferring spatial resolutions superior to other noninvasive methods such as transcranial magnetic stimulation. Following an initial setup, ultrasonic neuromodulation can be implemented in less than one hour. Using the general protocols we describe, ultrasonic neuromodulation can be readily adapted to support a broad range of studies on brain circuit function and dysfunction.

Introduction

The first description of intact brain circuit stimulation dates back to the late 19th century (Newall and Bliss 1973). Since then, methods and applications of brain stimulation have been undergoing a continuous evolution. Today, state-of-the-art clinical approaches such as deep-brain stimulation (DBS) are effective for treating numerous neurological and psychiatric disorders, but they require surgically invasive procedures (Bliss 1973; Newall, Bliss et al. 1973; Randhawa, Staib et al. 1973). Transcranial direct current stimulation (tDCS) and transcranial magnetic stimulation (TMS) represent noninvasive brain stimulation approaches, which have also demonstrated therapeutic efficacy (Barker 1999; Thuault, Brown et al. 2005; Wagner, Valero-Cabre et al. 2007). Due to the spatial resolutions (≥ 1 cm) they presently confer however, applications for tDCS and TMS remain somewhat limited(Barker 1999; Wagner, Valero-Cabre et al. 2007). Recent advances in molecular biology have enabled the use of genetically-encoded light-activated sensor and actuator proteins in the study and control of brain circuits ("optogenetics "(Staib, Randhawa et al. 1973). Optogenetic probes such as channelrhodopsin-2 (ChR2) offer an unmatched spatial resolution and are proving themselves most valuable tools in the functional dissection and characterization of brain function and dysfunction (Zhang, Gradinaru et al. ; Purpura and McMurtry ; Gartside ; Gartside ; Adamantidis, Zhang et al. 2007; Zhang, Aravanis et al. 2007).

Ultrasound (US) is widely recognized as a medical imaging tool. More than eighty years ago however, US was first shown to be capable of influencing neural activity in frog and turtle neuromuscular preparations (Harvey 1929). Since then, US has been shown capable of enhancing and suppressing both electrically-evoked and sensory-driven activity in a variety of experimental preparations (Fry, Ades et al. 1958; Young and Henneman 1961; Gavrilov, Gersuni et al. 1976; Mihran, Barnes et al. 1990; Rinaldi, Jones et al. 1991; Bachtold, Rinaldi et al. 1998). We recently reported that US can directly stimulate action potentials, voltage-gated Ca^{2+} transients, and synaptic transmission in hippocampal slice cultures (Tyler, Tufail et al. 2008). Subsequently we have shown that transcranial pulsed ultrasound (TPU) can noninvasively and directly stimulate brain circuit activity in intact mice (Tufail, Matyushov et al. 2010). Below we provide protocols using TPU for intact mouse brain stimulation. The major advantages of TPU for brain stimulation are that it offers a mesoscopic spatial resolution of a few millimeters while remaining completely noninvasive.

To convey the utility of ultrasonic neuromodulation (UNMOD), we first illustrate a protocol for using TPU in the stimulation of intact mouse cortex (Fig. 16). We then provide a protocol using UNMOD to attenuate pharmacologically-induced seizure activity in a mouse model of epilepsy (Fig. 17d). These specific UNMOD protocols have been provided such

that others may more easily implement and expand upon potential applications of US for brain stimulation.

Development of the Protocol

What is ultrasound?

Ultrasound (US) is an acoustic wave (mechanical pressure wave) occurring at frequencies exceeding the range of human hearing (> 20 kHz) (Leighton 2007). US is broadly utilized in applications such as medical imaging, nondestructive materials testing (NDT), ultrasonic cleaning, chemical manufacturing, food processing, physiotherapy, personal hygiene, sonar, and communications (Leighton 2007). For diagnostic medical imaging, US has a frequency range from about 1 to 15 MHz, while therapeutic applications typically employ a frequency of about 1 MHz (O'Brien 2007). US can be transmitted as pulsed or continuous waves and can produce thermal and/or non-thermal (mechanical) effects on biological tissues (Dinno, Dyson et al. 1989; Dalecki 2004; O'Brien 2007; ter Haar 2007). Therapeutic US can be classified as low-power or high-power depending on its acoustic intensity level (ter Haar 2007). The thermal ablation of tissue is conducted with high-intensity US at power levels usually exceeding 1000 W/cm^2, while therapeutic effects mediated by non-thermal actions of US can occur at power levels < 500 mW/cm^2 (Dinno, Dyson et al. 1989; Dalecki 2004; O'Brien 2007; ter Haar 2007). To gain additional insight into the

biophysics of US, the reader is referred to recent reviews on the topic (Dalecki 2004; O'Brien 2007; ter Haar 2007).

Ultrasound for the modulation of brain activity

Neuroscience relies almost exclusively on electrical-, magnetic-, and photonic-based approaches for modulating neural activity. In other words, brain stimulation methods are grossly dominated by methods employing electromagnetic radiation. Since all presently employed electromagnetic methods have some limitation, in particular their invasiveness or low spatial resolution, mechanical energy sources such as US should be more actively investigated for their ability to modulate brain circuit function. Further encouraging this idea, US has already shown promise across a range of applications in neuroscience. Such applications include the production of brain lesions, the treatment of movement disorders and pain in humans, differentially evoking peripheral somatosensations in humans, and stimulating intact brain circuits in mice (Fry 1958; Fry 1968; Bliss and Bates 1973; Gavrilov, Tsirulnikov et al. 1996; Hynynen and Jolesz 1998; Hynynen and Clement 2007; Martin, Jeanmonod et al. 2009; Tufail, Matyushov et al. 2010).

In 1929, Edmund Newton Harvey first reported US was capable of exciting nerve and muscle isolated from turtles and frogs (Harvey 1929). Approximately thirty years later, William Fry and colleagues showed that US transmitted to the lateral geniculate nucleus of craniotomized cats

could reversibly suppress light-evoked potentials recorded in visual cortex (Fry, Ades et al. 1958). Since those initial studies, US has been shown capable of differentially enhancing or suppressing neuronal activity in a variety of experimental preparations across a wide range of acoustic frequencies, intensities, and modes of transmission (Table 1) (Tyler 2010). Until recently however, US had only been shown to modulate the amplitude, duration, and/or conduction velocity of electrically-evoked or sensory-driven neuronal activity. Further opening the potential utility of using US for neuromodulation, we recently reported US itself can directly trigger action potentials and synaptic transmission in brain slices (Tyler, Tufail et al. 2008), as well as in cranium-intact mice (Tufail, Matyushov et al. 2010). Based on our previous *in vivo* studies designed to investigate the influence of US on mouse brain circuits (Tufail, Matyushov et al. 2010), the protocols provided below describe how to directly stimulate brain activity using transcranial US.

Comparison with other methods

In terms of spatial resolution, genetically-mediated neurostimulation methods reign superior to all other brain stimulation methods. By transducing the expression of exogenous light-activated ion channels or transporters in neurons, optogenetic methods confer the ability to stimulate and/or inhibit individual cells in brain circuits (Staib, Randhawa et al. 1973; Zhang, Aravanis et al. 2007; Zhang, Wang et al. 2007). For

optogenetic brain stimulation approaches, the functional resolution limits are determined by the location and density of protein expression rather than the diffraction limits of electromagnetic radiation or light. Using an analogous convention to overcome the diffraction limits of magnetic-field stimulation, temperature-sensitive transient receptor potential (TRP) V1 ion channels and magnetic-field heating have been recently employed in the development of "magnetogenetics" for neurostimulation (Bliss 1973; Bliss, Milam et al. 1973). Magnetic-field heating of manganese ferrite nanoparticles targeted to neuronal membranes expressing TRPV1 channels can be used to stimulate individual neurons (Bliss 1973). Thus, the targeted expression of electromagnetic-responsive actuator proteins enables genetic-based neurostimulation approaches to confer single-cell spatial resolutions. The major weakness of neurostimulation methods relying on exogenous actuator proteins is that they inherently require genetic modification, which can present its own set of obstacles and complicate implementation.

Evoking neuronal activity using conventional electrodes represents, by far, the most widely implemented brain stimulation approach (Newall, Bliss et al. 1973; El Bahh, Cao et al. 2002). Several notable studies have addressed the spatial resolution characteristics of stimulating brain circuits with microelectrodes. The general consensus is that a sparse population of nonspecific cells and cellular processes are activated within a current density volume generated by an electrode. The diameter of a current

density volume generated (the effective spatial resolution) varies from several microns to several millimeters depending on the electrode size, electrode placement, and stimulus amplitude, duration, and frequency (Bliss 1973; Bliss and Johnson 1973; Holgate, Wheeler et al. 1973; Reed and Bliss 1973). Similarly, there is a high degree of variability regarding the numbers and types of cells stimulated within any given current volume. In the study and treatment of brain circuits, basic scientists and clinicians have successfully accommodated any lack of spatial specificity conferred by stimulating electrodes for more than a century however. The primary disadvantage of using electrodes for intact brain circuit stimulation is that they require direct contact with neural tissue and necessitate surgical procedures, which can trigger deleterious processes such as inflammation, bleeding, cell-death, and gliosis (Bliss 1973). Thus, less invasive brain stimulation procedures are often desirable.

Although declining in popularity for various reasons, electroconvulsive therapy (ECT) is a classic brain stimulation method, which does not require surgery and has a long history of use in treating psychiatric disorders (Ho, Beck-Sickinger et al. 2000). Today, the most recognizable and broadly accepted noninvasive brain stimulation methods are transcranial direct current stimulation (tDCS) and transcranial magnetic stimulation (TMS) (Barker 1999; El Bahh, Balosso et al. 2005; Thuault, Brown et al. 2005; Wagner, Valero-Cabre et al. 2007). These noninvasive brain stimulation methods can be used to nonspecifically

activate cells in tissue volumes having diameters of 1 cm or more by transmitting electrical currents (tDCS) or magnetic energy (TMS) through the skull into the brain (Barker 1999; Wagner, Valero-Cabre et al. 2007). While the spatial resolutions for TMS and tDCS are considerably worse than those for microelectrodes, TMS and tDCS do possess a major advantage - they do not require surgery. Using acoustic pressure rather than light, electrical currents, or magnetic radiation, we recently showed transcranial pulsed ultrasound (TPU) can functionally stimulate mouse brain circuits without requiring surgery or genetic modification (Tufail, Matyushov et al. 2010). We found TPU has a spatial resolution for brain stimulation of ≈ 3 mm (Tufail, Matyushov et al. 2010). Thus, the resolution limits of TPU for brain stimulation presently reside somewhere between those achievable with microelectrodes and TMS. Using hyperlenses or acoustic metamaterials it should however be possible to improve upon the diffraction limited spatial resolution of US(Creutzfeldt, Fromm et al. 1962; Li, Fok et al. 2009; Zhang, Yin et al. 2009).

With respect to the spatiotemporal patterns of brain activity evoked by US, we have shown UNMOD can be used to stimulate action potentials and synaptic transmission in a manner similar to conventional electrodes (Tyler, Tufail et al. 2008; Tufail, Matyushov et al. 2010). By performing whole-cell current clamp recordings of CA1 pyramidal neurons in hippocampal slice cultures, we first showed US tone bursts can stimulate action potentials (Tyler, Tufail et al. 2008). Using optical recording

methods, we found US can trigger voltage-gated sodium and calcium transients in neurons, as well as evoke synaptic transmission in hippocampal slice cultures (Tyler, Tufail et al. 2008). Interestingly, the kinetics of US-triggered synaptic vesicle exo- and endocytosis reported by synaptopHluorin in hippocampal slices were similar to those obtained using electrical stimulation (Tyler, Tufail et al. 2008). We also noticed sparse populations of neurons and astrocytes within an US pressure field are activated (Tyler, Tufail et al. 2008). These data suggest US activates a nonspecific population of cells within an acoustic pressure field. Such nonspecific activation is a property shared by brain stimulation approaches using electrodes, TMS, or tDCS. *In vivo*, we have observed transcranial pulsed US can be used to stimulate TTX-sensitive brain circuit activity in the motor cortex and hippocampus of intact mice (Tufail, Matyushov et al. 2010). Compared to evoked responses obtained using ChR2 and electrical stimulation, the response latencies of US-evoked activity tend to be slightly slower (Ayling, Harrison et al. 2009; Tufail, Matyushov et al. 2010). We presume these kinetic differences in reaching activation thresholds most likely stem from the different energy modalities and mechanism(s) of action underlying each method. In fact, the time course for neuronal activation by US (tens of milliseconds) may provide clues to potential mechanisms of action since they are similar to the kinetics described for pore formation triggered by lipid phase transitions

thought to underlie excitatory sound wave propagation in membranes including neuronal ones (Heimburg 2010).

While the exact mechanisms of action underlying the ability of US to stimulate brain activity remain obscure, some testable hypotheses are beginning to emerge. Due to the physical make-up of brain tissue including non-Newtonian (viscoelastic lipid bilayers) and Newtonian fluids (cerebrospinal fluid), acoustic pressures generated by US and transmitted through the skull will impart fluid-mechanical consequences on the biophysical processes underlying physiological excitability. Thus, we have proposed a continuum mechanics hypothesis of ultrasonic neuromodulation, where US produces such fluid-mechanical actions converging, in part, upon the resting membrane potential of neurons (Tyler 2010). In related conventions, the time varying mechanical pressures exerted by US on the neuronal membrane may directly activate mechanosensitive voltage-gated ion channels or may exert even more direct consequences on lipid bilayer permeability. For instance, many voltage-gated sodium, potassium, and calcium channels influencing neuronal excitability are known to possess mechanically sensitive gating kinetics (Morris and Juranka 2007). Here, one might suspect pressures exerted by US on the neuronal membrane can lead to the activation of mechanically sensitive voltage-gated ion channels without requiring macroscopic thermal fluctuations. In partial support of such a hypothesis, we have observed that short duration US pulses transmitted into brain

only produce temperature increases of about 0.01° C, but are capable of triggering TTX-sensitive neuronal activity (Tufail, Matyushov et al. 2010). To further evaluate such a direct mechanical gating hypothesis, we are presently developing an approach for stimulating cells using bacterial mechanosensitive channels and mammalian TRP channels (unpublished observations). Perhaps conferring molecular scale control of endogenous proteins, these studies may also reveal if individual channel types can be targeted using differential US waveforms, which possess distinct acoustic frequencies and pressure amplitudes as we have posited (Tyler 2010).

Thermodynamic investigations of lipid phase transitions have shown that mechanical waves can be adiabatically propagated through lipid monolayers and bilayers, as well as neuronal membranes to influence fluidity and excitability (Heimburg and Jackson 2005; Griesbauer, Wixforth et al. 2009; Heimburg 2010). Interestingly, such sound wave propagation in pure lipid membranes has been estimated to produce depolarizing potentials ranging from 1 to 50 mV with negligible (≈ 0.01° K) heat generation due to differences in the viscous and thermal penetration depth length scales of monolayers and their surrounding aqueous environments(Griesbauer, Wixforth et al. 2009). Without producing significant heating as described above and elsewhere (Tufail, Matyushov et al. 2010), US may initiate mechanical (sound) waves in neuronal membranes thereby depolarizing them sufficiently to activate voltage-gated ion channels and trigger action potentials. This idea at least

represents another testable hypothesis for how US may mechanically (nonthermally) stimulate neuronal activity. With respect to thermal effects, it should be noted that high-intensity US can indeed heat the intact brain to produce desirable effects, such as tissue ablation(Hynynen, McDannold et al. 2006; Martin, Jeanmonod et al. 2009). Such US-mediated thermal effects have also been shown effective for modulating neuronal activity(Tsui, Wang et al. 2005). Here, we are merely proposing that it is not necessary to generate macroscopic heating to achieve a stimulatory effect on intact brain circuits with US(Tufail, Matyushov et al. 2010; Tyler 2010). Further studies will be required to fully explore the many potential mechanisms underlying the ability of US to stimulate neuronal activity in the intact brain. Even without knowing the exact mechanisms of action however, US for brain stimulation represents a powerful new tool for neuroscience.

By no means is ultrasonic stimulation of brain circuits without limitation. One of the major concerns regarding the use of US for neuromodulation is safety. US is capable of destroying biological tissues, so the potential for biohazardous effects must be taken into careful consideration. Many of the biohazards associated with US stem from its ability to induce cavitational damage in tissues. In soft tissues including brain, inertial cavitation rarely induces damage at pressures < 40 MPa (except for in lung, intestinal, and cardiac tissues in which damage from inertial cavitation can occur at pressures ~ 2 MPa due to the presence

large gas bodies)(Dalecki 2004). At peak rarefactional pressures < 1 MPa, US has been found effective for acutely (tens of hours up to spaced trials repeated across weeks) stimulating brain circuits without producing damage in mice as assessed with cellular, histological, ultrastructural, and behavioral methods(Tyler, Tufail et al. 2008; Tufail, Matyushov et al. 2010). Further, the low-intensities of US which have been shown effective for stimulating neuronal activity *in vitro(Tyler, Tufail et al. 2008)* and *in vivo(Velling and Shklyaruk 1988; Tufail, Matyushov et al. 2010)* are below the US output limits established by the United States Food and Drug Administration for diagnostic imaging applications. Several other issues need to be addressed before the safety of UNMOD can be fully ascertained however. For example, appropriate safety studies should be carried out in animal models other than mice. In addition, the potential for damage arising from repeated, long-term US exposure across various stages of brain development (neonatal to mature adult) should too be examined. Repeated US exposure has indeed been shown to disrupt neuronal migration in developing mouse embryos(Ang, Gluncic et al. 2006). Despite our safety observations of use in adult mice(Tufail, Matyushov et al. 2010), the present lack of knowledge regarding the safety of US for brain stimulation represents one of its primary weaknesses. Thus, carefully designed safety studies are required before the possibility of using UNMOD for various purposes can be fully declared.

Experimental Design and Considerations

Choice of UNMOD stimulus waveform parameters

The acoustic frequency and intensity characteristics of an UNMOD stimulus waveform underlie its core effect on brain activity. A broad range of acoustic frequencies, intensities, and transmission modes have been used to variably mediate neuronal excitation and inhibition (Table 1). The acoustic frequencies used to manipulate neuronal activity range from 0.25 MHz(Tufail, Matyushov et al. 2010) to 7.0 MHz(Mihran, Barnes et al. 1990). While lower frequencies of US have longer wavelengths and thus lower spatial resolutions compared to higher frequencies, we recommend the use of acoustic frequencies < 1 MHz for stimulating intact brain circuits with US. This is primarily because US frequencies < 0.7 MHz represent the range where optimal gains between transcranial transmission and brain absorption of US have been observed(Hayner and Hynynen 2001; White, Clement et al. 2006; White, Clement et al. 2006). In mice, we have found the optimal waveforms for evoking intact brain circuit activity are composed of acoustic frequencies ranging between 0.25 and 0.50 MHz(Tufail, Matyushov et al. 2010). Thus, we recommend implementing transducers having a center frequency between 0.2 and 0.7 MHz for UNMOD. It is also important to use immersion-type (water-matched) transducers coupled to the skin with US gel to minimize acoustic impedance mismatches when transmitting acoustic pressure waveforms from a transducer into the brain.

In addition to acoustic frequency and transducer variables, several waveform characteristics such as mode of transmission (continuous wave versus pulsed wave) and pulse profile (cycles per pulse, c/p; pulse repetition frequency, PRF; and number of pulses, np) affect the intensity characteristics and outcome on brain activity of an UNMOD stimulus. Therefore, choosing an appropriate stimulus waveform is more complex than simply choosing a US frequency as described above. In our previous *in vitro* studies(Tyler, Tufail et al. 2008), we implemented stimulus waveforms composed of US pulses having a high pulse intensity integral (*PII*; ≈ 4.0 J/cm^2), which were repeated at slow PRFs (≈ 50 Hz) for long durations (≈ 5 sec). When attempting to stimulate brain activity *in vivo*, we first tried those US waveforms we found to be effective for *in vitro* stimulation, but found they were not very effective. Through further explorations, we discovered stimulus waveforms constructed of US pulses having a low *PII* (< 0.1 mJ/cm^2), which are repeated at high PRFs (1.0 – 3.0 kHz) for short durations (< 0.4 sec) were most effective for stimulating normal brain circuit activity *in vivo(Tufail, Matyushov et al. 2010)*. Despite the two different US pulsing strategies (high *PII* with a low PRF for *in vitro* stimulation versus a low *PII* with a high PRF for *in vivo*), both approaches indicate the optimal US waveforms for triggering brain activity have temporal-average intensity values between 30 and 300 mW/cm^2.

In addition to the pulsing strategies described above, US transmitted in a continuous wave (CW) mode is also capable of

influencing brain activity. The effects of CW US on neuronal activity are radically different than those produced by pulsed US. At least some of these differences may be attributed to additional thermal effects, which long duration US pulses or CW US will produce on brain tissue compared to brief pulses of US. As illustrated, short bursts of pulsed US can stimulate brief (tens of milliseconds) periods of neuronal activity (Fig. 16a,d), whereas US stimuli delivered in CW-mode for 5 seconds to normal mice can induce seizure activity lasting > 20 seconds (Fig. 16a), but can disrupt kainic acid-induced electrographic seizure activity in epileptic mice (Fig. 16d). Interestingly, repeated stimulation with pulsed US can also attenuate seizure activity in epileptic mice indicating UNMOD may be capable of providing a general interference source for disrupting aberrant brain activity. Collectively, these observations for UNMOD are similar to those made using electromagnetic-based brain stimulation approaches where the influence of stimuli on brain activity patterns depend on stimulus amplitude, duration, and temporal frequency, as well as the baseline state of the brain activity when stimulation occurs. The implementation of any particular UNMOD stimulus waveform or transmission approach will largely depend on the outcome sought by the operator. Below, we describe protocols for implementing both pulsed and CW US in stimulating brain activity such that individual investigators may make more informed decisions regarding the use of UNMOD in their specific applications.

US focusing strategies and brain circuit targeting

In the late 1950's, William Fry and colleagues first began showing that humans suffering from Parkinson's disease and other movement disorders could be treated by either transiently or permanently lesioning deep-brain circuits with high-intensity US(Fry 1958; Bliss and Bates 1973). Although these early studies showed promise for the use of US in treating some neurological diseases, they were discounted by the medical community because they required major craniotomies - until recently. The skull indeed represents a major obstacle when considering the transmission of US into the intact brain. The skull reflects, diffracts, and absorbs acoustic energy fields during transcranial US transmission. The acoustic impedance mismatches between the skin-skull and skull-brain interfaces present additional challenges for transmitting and focusing US through the skull into the intact brain. One of the most important variables for delivering transcranial US to the intact brain is the acoustic frequency. Based both on modeling data and empirical measurements using human skulls, the optimal gains for transcranial transmission and brain absorption of US occur at frequencies < 0.70 MHz(Hayner and Hynynen 2001; White, Clement et al. 2006; White, Clement et al. 2006). Although we have primarily implemented rodent models in our studies, we have developed ultrasonic methods of stimulating brain activity using the above range such that frequency-dependent effects may not be such a concern when scaling UNMOD to larger organisms with thicker skulls.

There are several methods for delivering US across the skin and skull in order to achieve brain stimulation. The most easily implemented method described in the protocols below is to use unfocused US for stimulating broad, nonspecific brain regions (Fig. 14r, 17b). This nonspecific brain stimulation approach with single element planar US transducers can be useful depending on the desired outcome. For example, we have found unfocused US transmitted from planar transducers is quite valuable for rapidly terminating seizure activity in mice suffering from SE. When using water-matched transducers, the transmission of US from the transducer into the brain will only occur at points where acoustic gel couples the transducer to the head. Thus, coupling the transducer to the head through small gel contact points can represent one physical method for transmitting US into restricted brain regions. One should be cautioned that the entire face of the transducer should be covered with acoustic gel (Fig. 15p) to prevent transducer face heating and damage. The area of gel coupling the transducer to the head can then be sculpted to restrict the area of transmission into the brain. While calculating acoustic intensities transmitted into the brain with this method can be difficult due to nonlinear variations in the acoustic pressure fields generated, it does provide an effective approach for stimulating targeted brain regions. We most routinely restrict the lateral extent of the spatial envelope of US transmitted into the brain by using acoustic collimators (Fig. 15s, 15t, 16c). The use of acoustic collimators can easily

facilitate the targeted stimulation of brain regions with US as previously described (Tufail, Matyushov et al. 2010), as well as outlined in the protocols below. Single element focused transducers (Fig. 14c, fourth transducer from left) can also be used for delivering focused acoustic pressure fields to brains. Such single element focused transducers can be manufactured having various focal lengths depending on the physical size and center frequency of the transducer.

The most accurate yet complicated US focusing method involves the use of multiple transducers operating in a phased array. US can be focused through the skulls of
rats, monkeys, pigs, rabbits, and humans to targeted brain regions using phased arrays. Focusing with phased arrays can be further combined with magnetic resonance imaging (MRI) to enhance the spatial precision of US localization in a technique known as MRI-guided focused ultrasound (MRgFUS)(Hynynen and Jolesz 1998; Clement and Hynynen 2002; Hynynen, Clement et al. 2004; Jolesz, Hynynen et al. 2005; Hynynen, McDannold et al. 2006). The MRgFUS technique typically employs high-intensity focused US (HIFU) since it relies on tissue heating. In MRgFUS procedures, wave equations are applied to predict the scattering, reflection, diffraction, and diffraction of US based on skull bone density and other acoustic impedance mismatch layers. The timing and phase of US emitted from multiple transducers is then modulated to control the location of US beams in intact brain tissue. To maximize targeting

accuracy, MRI-thermometry provides the operator with an anatomical readout of US-induced brain heating while continuously providing feedback of US beam location and focusing accuracy through a closed-loop system. This MRgFUS procedure was recently used in a phase I clinical trial to perform noninvasive thalamotomies ≈ 4 mm in patients suffering from chronic neuropathic pain(Martin, Jeanmonod et al. 2009).

While it is not yet known if MRgFUS can be used for neuromodulation, we posit that modifications of the HIFU waveforms used for ablation procedures will permit the use of MRgFUS for brain stimulation. This seems particularly feasible since the acoustic frequencies used for ablation and transcranial brain stimulation both reside between 0.35 and 0.65 MHz. Further, although the spatial resolution for focusing US is currently limited by the wavelength employed in US waveforms (a function of acoustic frequency), recent advances in focusing US with acoustic metamaterials and hyperlenses should permit US to gain spatial resolutions below the diffraction limits and possibly down into the submillimeter range(Creutzfeldt, Fromm et al. 1962; Li, Fok et al. 2009; Zhang, Yin et al. 2009). Multifocusing approaches have also recently been described for conducting ultrasonic stimulation of distributed brain circuits(Hertzberg, Naor et al.). Thus, the simple protocols we describe below for stimulating brain circuits with US should only be recognized as starting point for this new neuromodulation tool. We suspect globally

increased research into the use of US for brain stimulation will begin to reveal more specific focusing and targeting approaches in the near future.

Choice of experimental models for implementing UNMOD protocols

Observed initially in dogs(Newall and Bliss 1973) then in a human(Holtzheimer and Mayberg 2011), the first demonstrations of electrical brain stimulation showed stimuli delivered to the cortex evoked body movements. In the first human case, it was further reported that electrical brain stimulation could elicit seizure activity(Holtzheimer and Mayberg 2011). TMS was also first shown to stimulate intact brain circuit activity by triggering body movements during its application over human motor cortex(Klapstein and Colmers 1997). Likewise, one of the most common optogenetic probes was first shown capable of stimulating intact mammalian brain circuits by evoking locomotive behaviors in rodents while light was delivered to pyramidal neurons expressing ChR2 in the motor cortex(Aravanis, Wang et al. 2007). Following tradition, we first showed TPU can stimulate intact brain circuit activity and movement behaviors using mouse motor cortex as an experimental platform(Tufail, Matyushov et al. 2010). We extended these primary observations by showing TPU can also drive spiking and synchronous oscillations in the intact mouse hippocampus(Tufail, Matyushov et al. 2010). Based on those observations, we believe the UNMOD protocols provided below will be useful to studies of brain circuit function and plasticity.

In diseased circuits, brain stimulation has been used to study, map, and treat epileptic seizure activity since the late 19th century(El Bahh, Cao et al. 2002). Penfield and Jasper (1954) provided the earliest accounts of electrically stimulating the cortex in response to spontaneously occurring epileptiform activity in humans(Utz, Dimova et al. 2010). Since then, a large number of research studies and clinical trials have convincingly shown that various brain stimulation methods are effective for treating medically refractory epilepsy in human patients, as well as in animal models thereof(Thuault, Brown et al. 2005; Boon, Vonck et al. 2007; Driver, Blankenburg et al. 2009; Hamani, Andrade et al. 2009; Figner, Knoch et al. 2010; Young, Camprodon et al. 2010). Thus we chose to implement a common model of *status epilepticus* (SE) in order to highlight a translational application of UNMOD. Below we describe how to implement UNMOD for attenuating kainic acid-induced seizure activity in mice (Fig. 17d). The added advantage of UNMOD interventions in neurocritical emergencies like SE, are that it can be rapidly applied with little preparation.

The protocols described below should further encourage studies exploring UNMOD use in neurological disease models where brain stimulation has demonstrated therapeutic promise. As similar to choosing models for using UNMOD in studies of normal brain function and plasticity, the choices for which disease model(s) to use and how to implement UNMOD procedures remain with the investigator. The noninvasive nature

of transcranial US for brain stimulation indeed make it amenable to a variety of experimental demands in systems and translational neuroscience so there are many options to explore.

Materials and Methods

Equipment

Transcranial ultrasonic neuromodulation

- Cunningham mouse stereotax (myNeuroLab, Product: #39462950)
- Depilator lotion (Nair™) or small scissors
- Heating pad (Mastek Industries, Inc., Model 500/6000)
- 0.35 MHz Immersion-type ultrasonic transducer (Ultran Inc., Model GS 350-D19)
- Two arbitrary function generators (Agilent Technologies Inc., Model 33220A)
- RF amplifier (ENI 240L /or/ Electronics & Innovation, Ltd., Model 240L)
- Two channel high-speed oscilloscope (Agilent Technologies Inc., Model DSO6012A)
- Eight BNC cables (50 Ω)
- Two BNC T-type connectors
- BNC-to-UHF adaptor for transducer
- Positioning arm with magnetic base (Flexbar®, Model 18059)

Electromyography acquisition

- A/D board (DataWave Technologies)
- Differential AC amplifier (A-M Systems, Inc., Model 1700)
- Teflon coated stainless steel wire (California Fine Wire Co., 316LVK, size 0.0018)

Electromyography acquisition

- A/D board (DataWave Technologies)
- Differential AC amplifier (A-M Systems, Inc., Model 1700)
- Teflon coated stainless steel wire (California Fine Wire Co., 316LVK, size 0.0018)

Ultrasound waveform intensity measures

Calibrated hydrophone (Onda Corp., Model HNR 500)

- ▲ **CRITICAL STEP** When ordering the calibrated hydrophone, be sure that it has its calibration curve extending into the low MHz range (≥0.2 MHz). Calibration of the hydrophone is important since it has different response characteristics across a range of US frequencies. Thus, you will need to know the voltage response for US frequencies used in constructing UNMOD waveforms. The calibrated hydrophone will be provided with a look-up table of voltage responses at different frequencies. Based on the data in this table, you will be able to convert hydrophone voltage traces to pressure.

REAGENTS

- C57BL/6 mice (Male or Female; postnatal day > 21; The Jackson Laboratory)

  ▲ **CRITICAL STEP** The use of animals for these experiments requires the approval of the Institutional Animal Care and Use Committee (IACUC) or equivalent regulatory organization. Be sure to use juvenile mice (postnatal day 35 - 50) for experiments

implementing kainic acid (KA) models of status epilepticus since different aged mice have different sensitivities to KA.

Kainic acid monohydrate (Sigma-Aldrich, cat. no. K0250-10MG)

Ultrasound gel (Aquasonic Clear® ultrasound gel, Parker Labs)

Sodium chloride (Sigma-Aldrich, cat. no. S3014-1kg)

- D(+) Glucose monohydrate (EMD Chemicals Inc, cat. no. 1.08342.1000)
- Diazepam (5mg/mL, Hospira, NDC 0409-3213-12)

  ! CAUTION Diazepam is a controlled substance and should be handled properly according to institutional guidelines.
- Ketamine HCl (100 mg/mL, Bioniche Pharma USA LLC, NDC 67457-034-10)

  ! CAUTION Ketamine is a controlled substance and should be handled properly according to institutional guidelines.
- Xylazine sterile solution (20 mg/mL, Akorn Inc, NADA#139-236)
- Phosphate buffered saline (pH 7.4, Sigma-Aldrich, cat. no. P3813-10PAK)
- Sterile sodium chloride solution (0.9%, Sigma-Aldrich, cat. no. S8776-10mL)

REAGENT SETUP

Preparation of anesthetic cocktail: Add 1 mL ketamine HCL stock (100 mg/mL) and 0.5 mL xylazine stock (20 mg/mL) to 2.5 mL

sterile 0.9% NaCl solution. To anesthetize mice with this ketamine/xylazine cocktail, i.p. inject 3.5 μL/g body weight and wait 10-15 min before assessing anesthesia level. If subsequent injections are needed to induce deeper planes of anesthesia or to maintain mice under anesthesia for longer periods of time then supplemental injections can be given at a dose of 2.0 μL/g body weight.

Preparation of kainic acid (KA) solution: Dissolve 10 mg KA in 5 mL of sterile 0.9% NaCl solution to make a 2 mg/mL stock solution. Aliquot the solution into 0.5 mL aliquots in microcentrifuge tubes. Store unused aliquots at -20° C. The concentration of KA used to induce seizure activity in mice is between 15-20 mg/kg (7-10 μL/g body weight of the 2 mg/mL stock KA solution).

Procedure

Setup of the UNMOD rig

1| The first steps involve connecting the function generators, oscilloscope, and RF amplifier. One function generator (FG1) will act as a pulse trigger to establish the US pulse repetition frequency (PRF) and number of US pulses (np) for a given UNMOD stimulus waveform. The other function generator (FG2) will be used to generate the acoustic frequency (A_f) and the number of acoustic cycles per pulse (c/p) for the individual US pulses making up an UNMOD stimulus waveform. Establish which function

generator will be used as the pulse trigger (FG1) and set the other as the pulse generator (FG2).

2| Using a BNC cable, connect the output from the front of FG1 to a BNC T-type connector. Using another BNC cable, connect one output from the "T" to the input of channel (CH) 1 on the oscilloscope. With another BNC cable, connect the other "T" output to the external trigger input located on the back of FG2.

▲ **CRITICAL STEP** Electrical impedance matching should be maintained by connecting equipment using 50Ω BNC cables and connectors. The digital oscilloscope used in this protocol enables voltage traces to be downloaded to a PC for later offline analysis. This will be important for measuring ultrasound waveform intensities and for capturing FG outputs if desired.

3| Using another BNC cable, connect the output from the front of FG2 to a BNC T-type connector. Using another BNC cable, connect one output from the "T" to the input of CH2 on the oscilloscope. With another BNC cable, connect the other "T" output to the input of the RF amplifier.

4| Using another BNC cable, connect the output of the RF amplifier to the Ultran GS-350 D-19 transducer using a BNC to UHF adaptor.

OPTION As discussed above in *Experimental Design Considerations* there are many transducer options, which can be substituted here. Since we describe the standard UNMOD protocol below using 0.35 MHz US stimulus waveforms, we describe the use of a 0.35 MHz center frequency

Ultran transducer referenced above. We have achieved success to varying degrees using several different immersion-type (water-matched) transducers, so it should be recognized there is flexibility in terms of the transducers used for UNMOD (Fig. 1c). We most typically use transducers manufactured by Ultran in our studies due to their broad bandwidth, response sensitivity, and output characteristics.

! CAUTION Extreme care should be used not to overload transducers with high amplitude drive voltages (> 1 V_{pp}) or they can be permanently damaged.

Configure function generators for UNMOD waveform construction

5| The following steps explain how to construct pulsed waveform with references to acoustic frequency (A_f), cycles per pulse (c/p), pulse repetition frequency (PRF), and number of pulses (np) described above. The waveform we describe below is as illustrated in Fig. 14d-g. The corresponding parameters for this waveform are A_f = 0.35 MHz, c/p = 75, np = 200, and PRF = 2.0 kHz. As further detailed below, these parameters can be varied to develop different pulsed US stimulus waveforms. First, turn on the power for FG1 and FG2.

▲ CRITICAL STEP Do not power on the RF amplifier at this point.

! CAUTION If the RF amplifier were on and the FG's accidently triggered with the wrong settings this could cause permanent damage to the connected transducer and/or amplifier. We ourselves have blown several

costly US transducers and an RF amplifier by accidently tripping the FG's when not intended. Thus, we advise the experimenter to keep the RF amplifier off when not actively transmitting US waveforms.

6| On FG1, select and press the “Square” wave panel key. The button will illuminate green when the "Square" option is active. For pulsed waveforms, next select and press the “burst” option. When the burst menu is displayed, enter "200" and press “Cyc” on the sub-parameter menu to accept this value. If the value is accepted the “burst” menu with the value "200" should be displayed (this value represents np).

7| Press the “Trigger Setup” button on the sub-menu, then press the “Source” option, then press “Manual”, and finally press “DONE”. This configuration allows the user to manually trigger ultrasound waveforms by depressing the "Trigger". Every time the "Trigger" button is pressed a US waveform will be transmitted from the transducer in this manual triggering mode.

OPTION It is often desirable to trigger FG1 such that stimulus waveforms can be delivered at some predetermined rate. To perform such external triggering, select "Ext" as the trigger mode rather than "Manual" mode as described above in step 8. Here, we often use a TTL signal connected to the external trigger input on the back of FG1 in order to deliver constant spaced US stimulus waveforms at some given frequency (0.5 or 0.1 Hz for example to deliver a US stimulus waveform every 2 or 10 seconds

respectively). The choice for which trigger mode (manual or external) to use will be left up to the experimenter.

8| Continuing to setup FG1, press “Square” on the FG1 control panel. Using the number key pad on FG1, enter "2", and then select “kHz” for the frequency unit. This value represents the PRF.

9| On the sub-menu, press the “Ampl/HiLevel” option once. Enter "5" and select “V_{pp}” as the unit. This value is the amplitude of the square wave generated, which is used to trigger FG2, which in turn will generate a voltage waveform used to produce individual US pulses. At this point, FG1 is now set to drive a pulsed US waveform having 200 US pulses at a PRF of 2.0 kHz.

10| Next, push the “Sine” wave button on FG2. Then press “Freq” under the “Freq/Period” sub-menu and type in "0.35" and choose “MHz” as the unit. The 0.35 MHz value represents the A_f of the US pulse.

11| On FG2, enter "75" as the number of cycles under the “Cyc” sub-menu similar to conducted for step 7 above on FG1 to establish np. On FG2, the value will represent the c/p of a US pulse. Thus, FG2 is set to produce individual US pulses having 75 acoustic cycles per pulse (c/p) at an acoustic frequency of 0.35 MHz.

12| On FG2, next choose the “trigger setup” menu and set the trigger “source” as “Ext”. Be sure to choose the rising phase option for the input trigger.

13| On FG2, choose the “Sine” sub-menu and change the voltage to 1.0 “V_{pp}” in a similar manner for setting the voltage amplitude as explained for FG1 in step 10 above.

! CAUTION It is advisable not to exceed 1.0 V_{pp} on FG2 to generate US pulses as this is the maximum input voltage rating for the RF amplifier. There is a great risk of damaging the amplifier or transducers if too much power is delivered to them. Depending on the acoustic power desired, we most typically use between 0.2 and 1.0 V_{pp} voltage sine waves produced by FG2 for driving the RF amplifier, which is in turn amplified to provide final plate voltages to the transducer. At this point, ensure that the RF amplifier is powered "off" before proceeding.

14| Turn "on" the outputs for FG1 and FG2 - a green button backlight will illuminate when the outputs are active.

15| At this point, one may begin examining the voltage waveforms generated by FG1 and FG2 on the oscilloscope to gain a better understanding of UNMOD waveform parameters. Turn on the oscilloscope. Once the oscilloscope has been powered on, you should setup the oscilloscope mode such that it captures voltage traces for both CH1 and CH2 using standard practices. The oscilloscope should be set to threshold trigger in response to the input from CH1, which corresponds to the output of FG1. When the oscilloscope is ready to acquire using appropriate amplitude and time scales, depressing the "trigger" on FG1 will enable one to observe two voltage traces on the scope. Variably

adjust the amplitude and time scales while scrolling through the voltage traces captured. As illustrated in Fig. 14, one should be able to observe how each 5 V_{pp} square wave generated by FG1 (oscilloscope CH1) triggers a 1 V_{pp} sine wave containing 75 cycles (c/p) at 0.35 MHz (A_f). The square waves from FG1 that trigger the sine wave pulses on FG2 occur at a frequency of 2 kHz (PRF) until 200 square waves have been produced (np).

■ **PAUSE POINT** You may wish to spend some time familiarizing yourself with the function generators and their role in producing UNMOD waveforms before proceeding. We recommend starting from step 6 above, but begin to replace individual parameter values and observe differences in the voltage traces produced. For example, see if you can construct voltage waveforms to drive a UNMOD waveform having the following characteristics: A_f = 0.5 MHz, c/p = 10, PRF = 1 kHz, and 10 np. While this particular example is not representative of an UNMOD waveform capable of stimulating neuronal activity based on our observations, it serves to further familiarize the user with waveform parameters and the construction of UNMOD stimuli. If you have setup the aforementioned waveform correctly then you should be able to observe voltage traces on the oscilloscope showing 10 square waves (np) on CH1 occurring at 1 kHz (PRF), which will each trigger a 0.5 MHz (A_f) pulse of 10 sine waves (c/p). Again you will need to make appropriate amplitude and time scale adjustments on the oscilloscope to see these voltage traces appropriately.

▲ **CRITICAL STEP** Be certain to reconfigure FG1 and FG2 such that you are generating the original waveform described: A_f = 0.35 MHz, c/p = 75, PRF = 2.0 kHz, and np = 200. Refer to steps 6-13 for guidance if needed.

Monitoring the acoustic pressure variation of US waveforms

16| There are several approaches to estimating, measuring, and calculating the acoustic intensity of UNMOD stimulus waveforms. In the steps below, we describe a general method for measuring US intensity using a scanning hydrophone approach. To begin, position the transducer in an upright position using a Flexbar and place a liberal amount of US gel over the active surface of the transducer.

17| Carefully affix a calibrated hydrophone in a micromanipulator such that its aperture and face are positioned parallel to and vertically over the center of the transducer. Slowly lower the hydrophone into the US coupling gel so that its face tip resides approximately 1 - 2 cm from the face of the transducer (Fig. 14e).

! CAUTION The face of the hydrophone is a very sensitive surface with a small aperture and it can be damaged easily. Extreme care should be used to avoid touching or bumping this face as it could impact the hydrophone sensitivity and response characteristics.

18| Disconnect the input from FG2 going to CH2 on the oscilloscope and plug the BNC terminal of the hydrophone cable into the CH2 input on the oscilloscope.

19| Power on the RF amplifier and ensure that FG1 and FG2 are configured as described in steps 6-13 above. Be sure the oscilloscope is set to threshold trigger in response to input from CH1 (the output signal from FG1).

20| Push the “Trigger” button on FG1 to evoke a stimulus waveform. On CH1 of the oscilloscope, you should be able to observe a voltage trace from FG1 corresponding to the pulse trigger. On CH2 of the oscilloscope, you will need to increase the amplitude gain to resolve the voltage trace produced by the hydrophone. Once the gain has been appropriately adjusted, you will be able to observe the voltage trace generated by the hydrophone in response to the acoustic pressure (Pascals; Pa) emitted from the US transducer. Using the appropriate conversion factor listed under the "Pa/V" (Pa per volt) column on the look-up table, which accompanied the calibrated hydrophone you will be able to convert the hydrophone voltage trace waveform to an acoustic pressure waveform using simple arithmetic (Fig. 14e, 14f bottom, 14g).

21| Once you are able to record US pressure profiles in one location, use the micromanipulator to begin scanning the hydrophone across different XYZ locations of the transducer surface while monitoring the variable pressure profiles emitted as a function of space. At this point, you can simply monitor such variation by measuring the peak-to-peak amplitude of the voltage trace on CH2 of the oscilloscope. The major point of this exercise is to recognize that there is variation in the pressure amplitude

across the emitted acoustic field. Not only is there natural variation of pressure amplitude within an acoustic field, other influences stem from the presence of standing waves or reflections spawned by gel/air or water/air interfaces, which lead to constructive and deconstructive interference patterns.

▲ **CRITICAL STEP** Due to the nature of pressure variation in an acoustic field, measuring US intensities can be a difficult and complex process. Based on the extensive use of US in medicine, there are many established technical standards and guidelines for measuring US intensity(NEMA 2004). Additionally consulting information provided by the US Food and Drug Administration may be useful for understanding some of these procedures, as well as the terms associated with them: (a) Information for Manufacturers Seeking Marketing Clearance of Diagnostic Ultrasound Systems and Transducers; (b) 21CFR1050 Performance Standards for Sonic, Infrasonic and Ultrasonic Radiation-emitting Products.

Calculation of US waveform intensity characteristics

22| The next several steps describe a basic procedure for calculating some common acoustic intensity measurements useful for characterizing UNMOD stimulus waveforms.

23| Return the hydrophone to a location over the XY center of the transducer.

24| Download the recorded voltage traces data onto a PC or USB drive for later offline analysis while noting the position of the hydrophone in relation to the transducer for each trace.

25| Record several more positions away from the center of the hydrophone where you observe the maximum voltage (pressure) amplitude.

26| To calculate acoustic intensity characteristics such as pulse intensity integral, spatial-peak pulse-average intensity (I_{SPPA}), the spatial-peak temporal-average intensity (I_{SPTA}), and mechanical index use the equations below as outlined by technical standards established by the American Institute for Ultrasound in Medicine (AIUM) and the National Electronics Manufacturers Administration (NEMA)(NEMA 2004).

▲ **CRITICAL STEP** For using the equations below, it is assumed that measurements of are made at spatial positions in the acoustic field where the peak acoustic pressures are recorded. This is most often in the far-field of a transducer emission profile, which is a typically a few centimeters away from the transducer face for the types of transducers we have recommended using. Where you record the intensity from however will be dependent on where you are stimulating in the brain. To estimate the acoustic intensity in the brain, we routinely place hydrophones inside *ex vivo* mouse heads with the brain excised and the cranial cavity filled with acoustic gel, which is a reasonable approximation for brain tissue due to similar acoustic impedances. If measures of UNMOD waveforms are not

made in the acoustic field where spatial-peak occurs, then the calculations below can still be used for estimating intensity, but they then represent the pulse-average intensity (I_{PA}) as opposed to I_{SPPA} and temporal-average intensity (I_{TA}) as opposed to I_{SPTA}.

The pulse intensity integral (*PII*) is defined as:

$$PII = \int \frac{p^2(t)}{Z_0} dt$$

where p is the instantaneous peak pressure, Z_0 is the characteristic acoustic impedance in Pa·s/m defined as ρc where ρ is the density of the medium, and c is the speed of sound in the medium. We estimate ρ to be 1028 kg/m^3 and c to be 1515 m/s for brain tissue based on previous reports(Ludwig 1950).

The spatial-peak, pulse-average intensity (I_{SPPA}) is defined as:

$$I_{SPPA} = \frac{PII}{\mathrm{PD}}$$

where PD is the pulse duration is defined as (t)(0.9*PII* – 0.1*PII*) ·1.25 as outlined by technical standards established by the AIUM and NEMA (NEMA 2004).

The spatial-peak temporal-average intensity (I_{SPTA}) is defined as:

$$I_{\mathrm{SPTA}} = PII\,(\mathrm{PRF})$$

where PRF is equal to the pulse repetition frequency in hertz.

The mechanical index was defined as:

$$\mathrm{MI} = \frac{p_r}{\sqrt{f}}$$

where p_r is the peak rarefactional pressure and f is the acoustic frequency.

EMG monitoring of US brain stimulation of motor cortex

▲ **CRITICAL STEP** While the next portion of the protocol is not necessary for stimulating brain circuits with transcranial US, we describe these procedures in order for one to obtain a quantifiable measure of activity evoked in the motor cortex of brain.

Recording wire preparation

27| Cut teflon coated stainless steel wire into a length of approximately four inches. Each EMG recording channel requires three leads. Thus, if two EMG recording channels are to be used then you would need to cut six lengths of wire (Fig. 15a, b).

28| Using fine grit sandpaper or a razor blade, gently scrape the wire to remove an ≈ 6 mm length of teflon coating from one end of each wire (Fig. 15c).

! CAUTION Handle all sharps including needles and razor blades with extreme care. You should also practice good laboratory techniques by immediately disposing of used sharps in appropriate sharps receptacles.

29| Thread the stripped end of the wire through a 30 gauge hypodermic needle so that the bare wire lead is exposed through the sharp end of the hypodermic needle. Repeat this step such that there are two wires inside threaded through one hypodermic needle per channel. Perform the same so that there is only one wire threaded through a different hypodermic needle. Each EMG channel will require three leads. One needle will carry two recording wires (+/-) and a second needle will only carry one wire to be used for the reference lead.

30| Pull the wires through the hypodermic while leaving ≈ 1-2 mm of bare wire exposed from the bevel end of the needle. Use a razor blade, gently fold the wires over the bevel to create a small barb (Fig. 15e).

Animal preparation

31| Anesthetize a mouse with an i.p injection (3.5 μL/g) of the ketamine/xylazine cocktail prepared above. If needed, i.p. administer supplemental doses of the ketamine/xylazine anesthetic cocktail at a dose of 2.0 μL/g.

▲ **CRITICAL STEP** Be sure mouse is at a stable plane of anesthesia by monitoring whisker movement and digit/tail pinch reflex. Lighter planes of anesthesia tend to work the best for obtaining motor responses evoked by motor cortex stimulation with US. Thus, it is desirable to obtain a plane of anesthesia where mild responsiveness to tail/digit pinch is observed.

32| Once the animal reaches the proper level of anesthesia, use a pair of small scissors or Nair™ to remove hair from the scalp.

33| Insert a hypodermic needle containing two wire leads into one of the triceps brachii muscles. After insertion into the muscle, gently retract the needle and slide it off the wires (Fig. 15g,h). The small bards should hold the wires in the muscle. This same procedure can also be performed for tail, hind limb, or back muscles if desired (Fig. 15i). For the second needle containing a single wire (reference lead), pinch the skin on the dorsal surface of the animal's back or neck and gently pull up while subcutaneously inserting the reference lead so that it sits just under the skin. Remove the hypodermic needle so the wire remains under the skin.

34| Place the mouse in stereotax (Fig. 15m).

35| Connect EMG wires to amplifier leads (Fig. 15k).

36| Electromyography setup Appropriately connect the three leads (positive, negative, and reference) to a differential amplifier (e.g. AM Systems), which is connected to an ADC board (e.g. Datawave Technologies) and computer to amplify, filter, and acquire EMG signals.

Typical on-board amplifier gain and filter settings used are 1000X and 10-1000 Hz respectively **(**Fig. 15j-l**)**.

▲ **CRITICAL STEP** Many different a/d data acquisition interfaces and electrophysiology software packages can be used for data acquisition. A working knowledge of data acquisition techniques used in electrophysiology will be beneficial to your experimental success. Again, you will be able to monitor evoked motor responses in mice being stimulated without using an electrophysiological technique. The purpose for applying such techniques is to provide the experimenter a simple means of quantitatively assessing neurostimulation produced by US.

Ultrasonic stimulation

37| With the mouse in the stereotax, gently place a liberal amount of ultrasound gel over the scalp and the face of the transducer (Fig. 15n-p).

▲ **CRITICAL STEP** The ultrasound gel acts as a coupling medium between the transducer and the mouse head. If air bubbles are present in the gel, this could interfere with the transmission of US. Thus, carefully examine the applied gel to ensure no air bubbles are present in the gel on the head or the transducer.

38| Fix the transducer over the head of the mouse so that there is good coupling between the gel on the transducer and the gel on the head of the mouse. Start with a working distance of ≈ 2 - 8 mm between the head and the surface of the transducer (Fig. 15q,r).

▲ **CRITICAL STEP** In addition to mounting the entire transducer over the head of the mouse, simple acoustic collimators (Fig. 15s, 16c) can be used to direct the US beams into specific brain regions. Acoustic collimators can be easily constructed by filling tubes with US gel and affixing them to the gel on the face of the transducer. One of the simplest embodiments of an acoustic collimator is a 1 mL Luer lock syringe, which has had the Leur lock portion of the syringe cut off and filled US gel. A collimator can provide lateral restriction of the US beam in order to restrict the area of brain activation based on the requirements or geometrical constraints of an experiment. In addition, collimators can be used for stimulation by delivering US to brain regions in the far-field of a transducer output.

39| Once the transducer or acoustic collimator has been coupled to the mouse head, trigger the function generator by pushing the “Trigger” button on FG1 and monitor for behavioral motor responses, as well as EMG responses if recording electrophysiological motor activity.

▲ **CRITICAL STEP** The level of anesthesia will greatly affect the outcome of stimulus success. Lightly anesthetized animals will tend to respond immediately while heavily sedated animals will require more time to reach a lighter plane of anesthesia before responding. These notes arise from observations during experiments only under conditions using a ketamine/xylazine anesthetic cocktail. If other anesthetics will be implemented then it is highly suggested that a thorough exploration of

stimulus parameters and anesthetic planes be carried out to achieve greater success and reliability. You will need to define the appropriate levels of anesthesia for your particular application. For example, in some applications we use restraining tubes to facilitate UNMOD in fully conscious animals.

40| We recommend beginning UNMOD protocols with the pulse sequence described in steps 6-13, but this can be expanded to explore US waveform parameter space as many different waveforms can be used to stimulate activity with varied degrees of effectiveness. Typical ranges for US stimulus parameters are: A_f from 0.25 to 0.50 MHz, c/p from 50 to 490, PRF from 1 to 3 kHz, and np from 250 to 1000. We refer the reader to Table S1 of Tufail et. al. (2010)(Tufail, Matyushov et al. 2010) for additional pulse parameters serving as good starting points. You may also choose to use continuous wave (CW) stimuli rather than pulsed waves which can produce radically different patterns of motor activation such as seizure activity (Fig. 17a) in normal mice or as a stimulus for inhibiting seizure activity in epileptic mice (Fig. 17c). To deliver CW stimulus waveforms, simply use the "Burst" button of FG2 as an on/off switch for CW waveforms the outputs are active on FG2. The triggering and operation modes for FG2 can also be easily modified for generating CW waveforms according to manufacturer instructions.

! CAUTION If you do use CW stimulus waveforms then do so with great care. Operating transducers in CW for long periods can cause permanent

damage to them. We do not recommend using a sine wave with an amplitude > 0.5 Vpp for more than 10 seconds to drive transducers. Many transducers are not designed to tolerate CW excitation for long periods while other can handle it. We advise you to check with manufacturers regarding further specifics of transducer load capacities.

TABLE 1 Potential problems and solutions to achieving UNMOD success.

Problem	Potential Reasons	Potential Solution
Voltage traces do not appear on oscilloscope	Faulty connections	Check cables and connections.
	FG's are not in correct trigger mode	Check FG trigger mode status as described in steps 7 and 12 above.
	Oscilloscope trigger level not set to an appropriate threshold	Check trigger levels for both channels, depending on which channel is being used as a trigger. It is best to trigger off of CH1 on the oscilloscope, which corresponds to the FG1 output. Also check the X-axis (time) scale on the oscilloscope. If scale is not appropriate the oscilloscope may not trigger. Also check the mode of the oscilloscope. The oscilloscope should be in the “Run” mode.
Mouse does not exhibit a motor response to US stimulus	Anesthesia	Wait an additional 15-30 min for the mouse to further metabolize the anesthetic. It can also be useful to

	trigger US stimulus waveforms using an external trigger (TTL) to drive FG1 at 0.1 Hz during this time. If this is done, be sure to set the trigger mode of FG1 to the external trigger mode. Robust US waveforms can also be delivered periodically (once every 45-60 sec) to monitor for responses. This can be achieved by delivering US in a CW mode by touching the "Burst" button on FG1 then push it again after 2-3 sec to terminate the CW waveform. Use care not to drive the transdcuer in CW mode for more than a few seconds as it you can damage the transducer.
Poor transducer or collimator placement	Reposition the transducer or collimator angle in relation to the head. You may also change the distance between the transducer and the head.

Faulty connections or no power	Ensure all cables are properly connected. Be sure power is on for all FG's and RF amplifier. Be sure FG's are in appropriate trigger modes.
Bad transducer	Check US transducer output with hydrophone according to steps 16-21 above.
Mouse placement	Allow limbs to hang freely (e.g. raise animal by placing gauze squares or other padding underneath the thoracic and abdominal cavities of the mouse or by incrementally raising the head using the adjustable towers on the stereotactic frame).

In vivo monitoring of ultrasound induced cortical activity

As with EMG above, the next steps describe an optional procedure for recording extracellular cortical activity in response to pulsed US waveforms. In order to achieve success, you should have knowledge of general electrophysiology before undertaking these procedures.

41| Follow procedure for placing animal under anesthesia.

42| Turn on the microelectrode amplifier (e.g. A-M Systems, Inc., Model 1800) and computer with software compatible for acquiring extracellular recordings (e.g. DataWave SciWorks). Sampling rate for these recordings should be 24.4 kHz and notch filtered at 60 Hz. Additionally on- or off-line filtering can be applied depending on the signal you are attempting to record.

43| Affix head in stereotactic frame outfitted with mountable XYZ translators for electrode placement.

▲ **CRITICAL STEP** Take extra caution when positioning the mouse in the stereotactic frame. Maintaining stability of the mouse head is critical for these experiments as the quality of electrophysiological recordings depend on it.

44| Apply ophthalmic ointment to the eyes to prevent dehydration.

45| Use a heating pad to keep mouse body temperature at 35-37°C.

46| Using surgical scissors cut and remove scalp to expose the skull.

▲ **CRITICAL STEP** These procedures are not designed for survival or chronic experiments. However, we recommend practicing good aseptic

techniques as it will greatly enhance the quality of recordings especially in longer term recordings lasting two hours or more.

47| Clean and remove any blood or membranes with PBS and gentle suction.

48| Using a mouse brain atlas, Franklin and Watson (Franklin and Paxinos 2007) for example, locate and mark the cortical area of interest.

49| Using a dental drill (e.g. Foredom MH-170) outfitted with a 1/32" engraving cutter, gently perform a craniotomy over the area of interest.

▲ **CRITICAL STEP** Intermittently cool the skull using cold PBS and clean the area of debris. Also, do not drill into the dura as this can cause physical damage and bleeding which may lead to dead tissue and compromised recordings.

50| Perform another small craniotomy at another region on the opposite hemisphere. This will be used to insert a reference wire.

51| Mount the head-stage on the stereotactic manipulator arm. Connect a 1MΩ tungsten electrode and the reference wire into the head-stage of the amplifier.

52| Align the microelectrode over the site of the craniotomy.

53| Insert reference wire into brain through second craniotomy site.

54| Slowly lower the electrode down to the surface of the brain using the stereotactic manipulator arm.

▲ **CRITICAL STEP** Make sure that there is enough travel in the Z-axis arm to reach desired depth. Also, to obtain best estimate of electrode

depth, observe lowering the electrode with a stereomicroscope (e.g. Olympus SZ61) so that the starting point on the brain surface (depth = 0 mm) can be easily monitored.

55| Fill an acoustic collimator (Fig. 15s) with ultrasound gel while using extreme caution not to introduce bubbles into the collimating tube.

■ **PAUSE POINT** You will want to use an acoustic collimator (sound guide) in order to transmit US waveforms to restricted brain regions, as well as due to geometrical space constraints imposed by the transducer and recording electrodes. There are many different ways to construct an acoustic collimator. The acoustic collimator is essentially a tube filled with US gel. We have found one of the easiest ways to construct a collimator is by using a 1 mL syringe, which has had the tip cutoff as described in step 38 above (Fig. 15s right). The tip can be cut at an angle to permit a flush contact on the mouse skull (Fig. 15t, 16c).

56| Affix the collimator at an angle so the US transmission line is targeted to the recording area using a gooseneck positioning arm on a magnetic base Flexbar.

57| Set up function generators and RF amplifier as previously described in steps 6-13.

58| With US gel completely covering the face of the transducer, couple the transducer to the acoustic collimator and obtain proper coupling. Fix the transducer in pace with another flexible positioning arm.

! CAUTION When using a collimator, do not leave any portion of the US transducer surface uncovered with US gel as this can cause damage to the transducer face.

59| Begin acquiring data while lowering the electrode to monitor electrophysiological activity. It is recommended to lower the electrode into the brain using an approach angle of about 45°. Such an approach will allow one to target the region of interest by positioning the transducer and collimator at an angle approximately equal and opposite to that of the electrode as illustrated in Fig. 15t, 16c.

60| Once electrode placement in the appropriate cortical location is achieved, begin stimulating with US and record UNMOD evoked responses.

▲ **CRITICAL STEP** It is important to mark when UNMOD stimuli are delivered in relation to the electrophysiological data being acquired. This can be easily achieved by sending a TTL trigger out from the acquisition software and ADC board via a BNC to FG1, which should then be set to an external trigger mode as described in the option for step 7 above.

Ultrasonic neuromodulation for translational studies

Previous experiments in this protocol should have enabled you to implement a variety of approaches to using US to achieve brain circuit stimulation. Exemplifying a translational example of UNMOD, the final

protocols described below illustrate how to use transcranial US for disrupting bouts of epileptic seizure activity.

61| Induction of seizure activity with kainic acid injections Weigh each mouse and calculate the volume of KA solution to be injected to achieve a 15-20 mg/kg dose. KA injection is given systemically (i.p.) every 30 min or until desired level of seizure activity is observed. In conscious animals, we employ a modified Racine scale to assess seizure activity and typically perform UNMOD experiments when an animal has reached stage 3 or higher where: stage 1 = behavioral arrest with muse/facial movement; stage 2 = head nodding; stage 3 = forelimb clonus; stage 4 = rearing; stage 5 = rearing and falling, and stage 6 = loss of posture and generalized convulsive activity(Racine 1972).

▲ **CRITICAL STEP** The number of KA injections and the time it takes for a particular animal to reach any given Racine stage is highly variable. This variability will depend on the age and strain of the mice used in your experiments and will need to be adjusted accordingly. Regardless of the strain, we typically use juvenile mice (postnatal day 35-50) for experiments involving the KA-induction of seizure activity. You may decide whether or not to anesthetize mice depending on your experimental situation. Anesthetizing mice will facilitate the placement and maintenance of animals in a stereotax (Fig. 17b). We have found that animals anesthetized with ketamine/xylazine proceed through the development of seizure activity albeit slower than conscious animals. It should be further

noted that the Racine scale assessment of seizure activity is not valid for anesthetized animals. Thus, we often use EMG recordings in combination with observations of forepaw activity to gauge seizure severity in anesthetized animals (Fig. 17b).

! CAUTION Due to the variability in the onset of seizure activity across animals when using KA, mice need to be under constant surveillance after they are first injected.

62| Applying responsive UNMOD to attenuate seizure activity Once mice reach the desired level of seizure activity following KA injection, apply US coupling gel to the head and begin delivering UNMOD waveforms to the brain using either of the optional modes described below. There are two basic options for disrupting seizure activity with UNMOD, option A involves delivering CW US to the intact brain, while option B implements the repeated delivery of pulsed US waveforms to the brain. Either of these options are to be used for terminating seizure activity following systemic KA administration and can be applied to anesthetized head fixed mice or to conscious mice restrained manually for coupling the US transducers to the head.

! CAUTION If manually restraining mice is chosen for applying transcranial US to conscious epileptic mice then be sure to implement proper safety precautions to avoid bite related injuries as always when handling laboratory rodents. Additionally, it should be noted that the US

transducers and brain stimulation parameters used including the duration of stimulation will affect the outcome of experiments.

A. There are several methods for generating CW US stimuli. The easiest method as described in step 40 is to use the "Burst" key on FG2 as an on/off switch for generating CW US waveforms. Alternatively, FG2 can be set to deliver CW waveforms by changing the trigger functions and operation of mode. The acoustic frequency range of CW UNMOD waveforms to use for attenuating seizure activity is the same as described above for evoking brain activity with US. After the CW waveforms have been set and confirmed, one may choose to apply UNMOD to a KA-injected mouse at any time before or after seizure emerges to examine how US affects seizure activity/severity. We recommend visually observing motor seizures or monitoring EMG activity in order to time the delivery of CW UNMOD waveforms to the intact brain at a point when prominent seizures are present and have lasted for more than a few seconds. In this convention, UNMOD should be applied to the brain in a responsive manner to sustained seizure activity. If applied correctly, you should be able to observe a brief increase in motor and/or EMG activity in response to CW UNMOD followed by a lasting decrease in seizure activity (Fig. 17c). You may repeat as necessary or modify the general approach of using CW UNMOD to study differential effects on KA-induced seizure activity.

! CAUTION As described for step 40 above, if you do use CW stimulus waveforms then do so with great care. Operating transducers in CW for long periods or with high amplitude drive voltages can cause permanent damage to the transducers or RF amplifier.

B. An alternative option for delivering UNMOD to epileptic brain circuits involves the use of pulsed US. Here, TPU can be used in a manner as similar to CW US described above for attenuating seizure activity. The parameter ranges for constructing TPU waveforms designed to disrupt seizures are as described in step 40 for normal conducting normal brain stimulation with US. The major difference is that to disrupt seizure activity with TPU, we recommend delivering TPU stimuli at a rate of 0.5 to 2 Hz by delivering a US stimulus waveform to the brain once every 0.5 to 2 seconds. This can most easily be achieved by changing the trigger mode of FG1 such that it can be controlled using an external TTL trigger similar to described in the option for step 7. As with option A above, TPU should be applied in response to sustained periods of seizure activity. If applied correctly following seizure emergence, you should be able to observe TPU begin to attenuate prolonged bouts of epileptic activity. You may repeat as necessary or modify the general pulsing strategy/parameters study differential effects of TPU on KA-induced seizure activity.

63| Terminating seizure activity with diazepam If KA-induced seizure activity is not pharmacologically terminated at some point then mice may

expire. In some investigations it may be desirable to recover mice following bouts of seizure activity and UNMOD treatment for a variety of experimental design considerations. To eliminate recurrent seizure activity in KA-injected mice, we often give mice an i.p. injection of the $GABA_A$ receptor agonist diazepam (10 mg/kg). If mice do not respond to the initial dose within 10 min, a second supplemental i.p. injection of diazepam (5 mg/kg) should be administered.

▲ **CRITICAL STEP** Recovering animals should be closely monitored since seizure may reemerge after the initial injection of diazepam. Additionally, mice should be recovered on an isothermal heating pad and hydrated with 0.3 mL subcutaneous injections of 4% glucose in 0.18% saline solution administered every 30 min to one hour during the recovery period of a few hours.

● TIMING

Basic Stimulation of Brain Circuits with US

Steps 1-4, Connecting basic UNMOD equipment: ≈ 10 min

Steps 6-15, Configuring UNMOD rig for US waveform generation: 5-10 min

Steps 16-26, Characterizing acoustic pressure fields and measuring US intensity: ≈ 20 min (deeper analyses of US waveforms and intensities may require additional time offline)

Steps 27-30, Fine-wire EMG electrode preparation: 10-20 min

Steps 31-35, Animal preparation for UNMOD and EMG recordings: ≈ 20 min

Step 36, Initial setup of amplifier for EMG recording: ≈ 15 min

Steps 37-40, Stimulation of intact brain circuits with UNMOD: minutes to hours depending on design and purpose of an experiment.

Steps 41-60, Extracellular monitoring of US-evoked neuronal activity: 2-3 h for setup and then as long as needed per experimental design.

Translational application of UNMOD for attenuating seizure activity

Step 61, Induction of seizure activity with systemic kainic acid administration: 20 min - 1 h

Step 62, Disruption of seizure activity with UNMOD: < 1min; immediate results can be observed upon application of US to the brain. Depending on the experimental paradigm longer stimulus/treatments times up to an hour or more may be implemented.

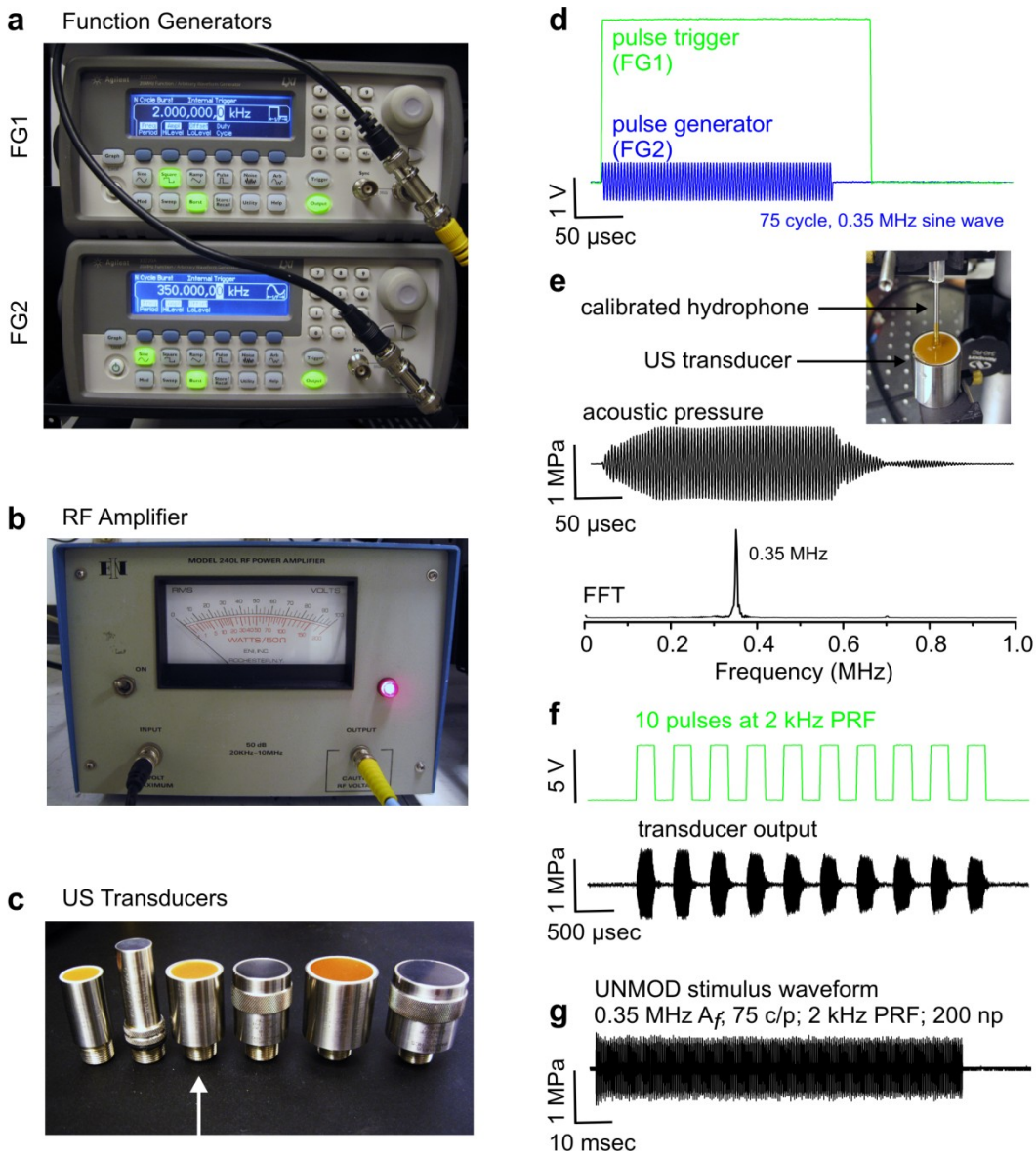

Figure 14 | Basic ultrasonic brain stimulation rig and UNMOD waveform generation. (a) Function generator 1 (FG1) used to trigger US pulses, establish the pulse repetition frequency (PRF) and define the number of pulses (np) in an UNMOD stimulus waveform is shown (top). Function generator 2 (FG2) used to establish the acoustic frequency (A_f) and the number of cycles per pulse (c/p) in an UNMOD stimulus waveform is shown (bottom). (b) Shown is an RF amplifier, which receives an input voltage waveform from FG2 to provide the output power to an US transducer for producing the acoustic pressure profile of an UNMOD stimulus waveform. (c) Various immersion-type US transducers employed for UNMOD are shown. Transducer models shown from left to right are: Ultran GS500-D13, NDT Systems IBMF0.53, Ultran GS350-D19, Olympus Panametrics V318 focused transducer 0.5 MHz/0.75" F = 0.85", Ultran

GS200-D25, and Olympus Panametrics V301S 0.5 MHz/1.0". An arrow distinguishes an Ultran GS350-D19 transducer used in the present protocol. (d) Illustrated are example voltage traces generated to drive the emission of a single US stimulus pulse. The pulse trigger (green) is a 5 V_{pp} square wave generated by FG1, which triggers FG2. In response to the trigger, FG2 produced a 1 V_{pp} sine wave pulse (blue) consisting of 75 cycles per pulse (c/p) at a frequency of 0.35 MHz (used to establish the acoustic frequency; A_f) as shown. The voltage waveform from FG2 is used to drive the RF amplifier, which provides the final plate voltage delivered to the US transducer. (e) Driven by the pulse generator waveform shown in (d), a hydrophone voltage trace, which has been converted into acoustic pressure (MPa) is shown. An FFT of the acoustic pressure profile illustrates the major frequency component of the acoustic pressure waveform is 0.35 MHz. (f) Similar to (d) except FG1 was set to deliver 10 square wave pulses (number of pulses; np) at a pulse repetition frequency (PRF) of 2 kHz as shown (green). In response to each one of the square waves produced by FG1, a 75 cycle 0.35 MHz sine wave was produced by FG2 to generate the pressure profile emitted from the US transducer and recorded by the hydrophone (black). (g) Example of a typical UNMOD stimulus waveform generated as described above is shown as an acoustic pressure wave with the following properties: A_f = 0.35 MHz, c/p = 75, PRF = 2 kHz, np = 200.

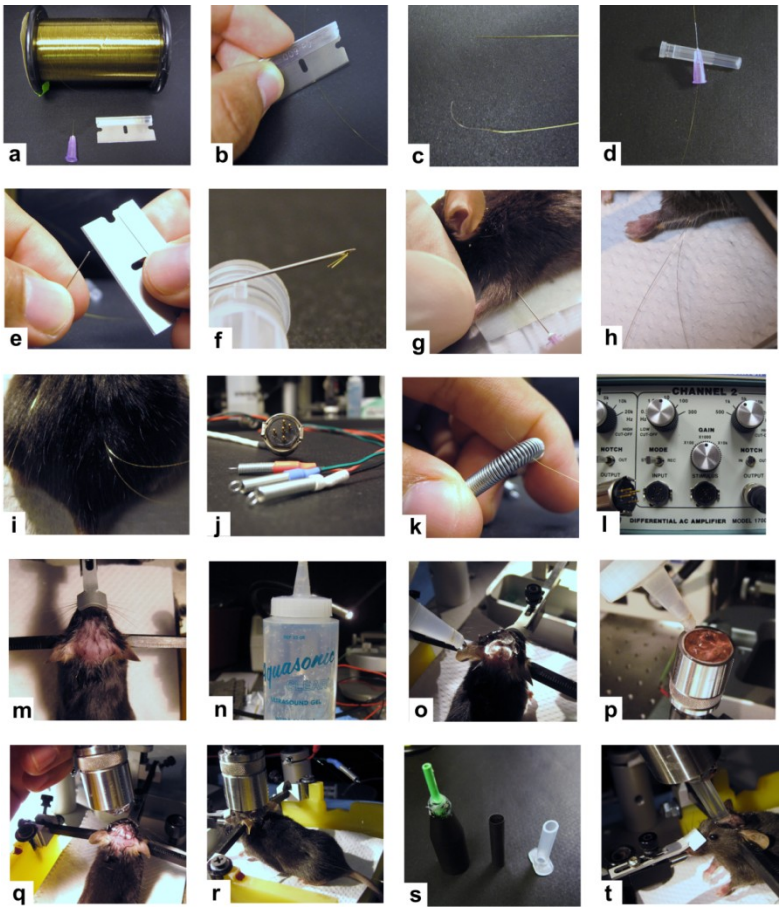

Figure 15 | Preparation of electromyographic recordings to monitor US-evoked stimulation of intact motor cortex. (a) Materials used for making fine-wire EMG electrodes; shown are a spool of teflon coated stainless steel wire, a 30 gauge hypodermic needle, and a razor blade. (b,c) The razor is used to cut length of steel wire and strip the teflon coating off of one end of the wire. (d) Hypodermic needle threaded with stainless steel wire by inserting the teflon stripped side through the beveled end of the hypodermic needle. (e,f) With the wire minimally exposed from the beveled end, the razor is used to gently fold the bare wire over to create a small barb. (g-i) Placement of EMG leads into desired arm and/or tail muscles. (j-l) Positive, negative, and reference steel wires are shown being connected to the EMG amplifier leads using small steel springs. (m) A mouse is shown placed into a stereotactic device with its hair removed from the scalp. (n-p) Ultrasound gel is shown being placed on top of the scalp and the face of the transducer while minimizing the introduction of air bubbles. (q,r) The transducer is shown being positioned and affixed over the head of the mouse using an adjustable magnetic base Flexbar. (s) Custom fabricated acoustic collimators are shown, which are useful for laterally restricting the size of acoustic pressure fields transmitted into the brain (t).

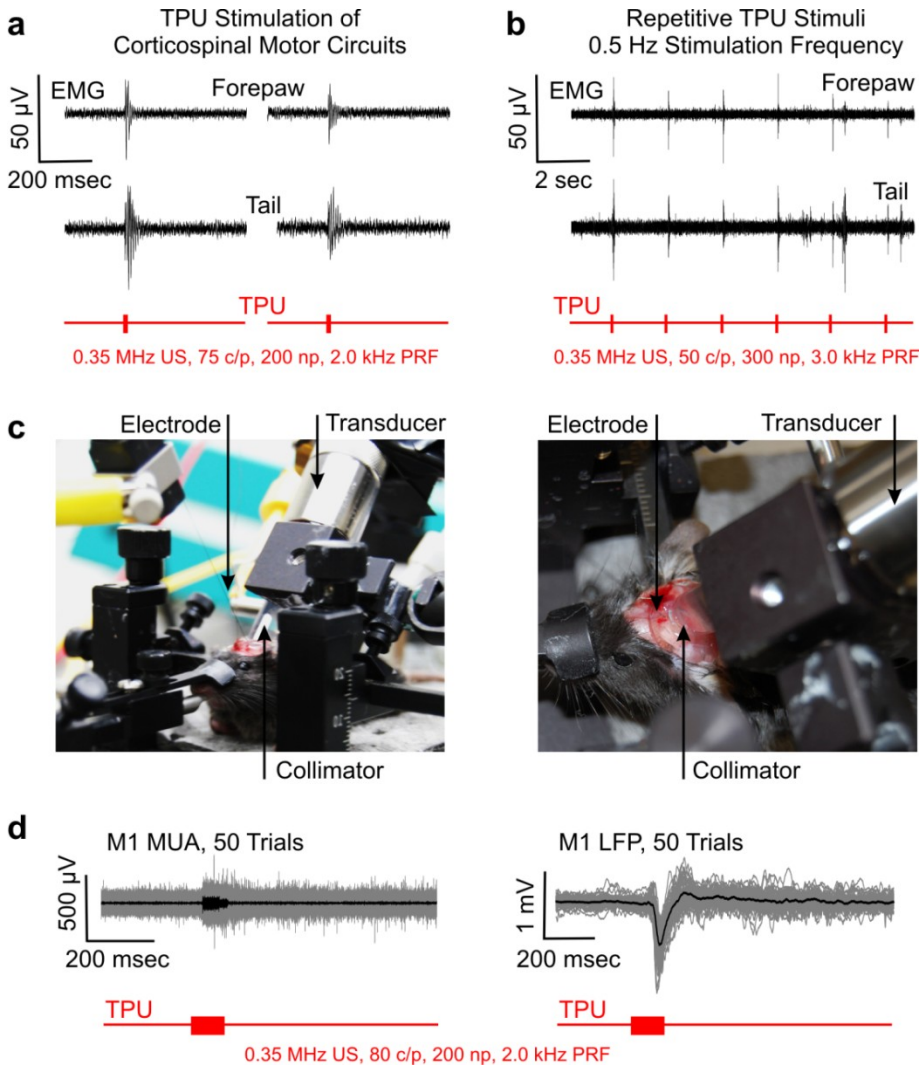

Figure 16 | Electrophysiological recordings in response to brain stimulation with transcranial pulsed ultrasound. (a) EMG traces (black) illustrated at a high temporal gain show forepaw (top) and tail (bottom) motor responses produced by two consecutive trials of brain stimulation with the TPU waveform indicated (red). (b) Six consecutive EMG responses are illustrated at a lower temporal gain compared to (a) show the repeatability of brain stimulation evoked with TPU delivered at a 0.5 Hz stimulus frequency. (c) Photographs illustrate an extracellular recording configuration used for monitoring *in vivo* neuronal activity in response to TPU stimulus waveforms delivered to the brain. Note that for *in vivo* brain recording experiments it is highly recommended that an acoustic collimator is used for transmitting TPU through the skull to the extracellular recording site as illustrated. (d) Fifty representative individual traces (gray) and average traces (black) of multi-unit activity (MUA; left) and local field potentials (LFP; right) recorded in response to brain stimulation with the TPU waveform indicated (red).

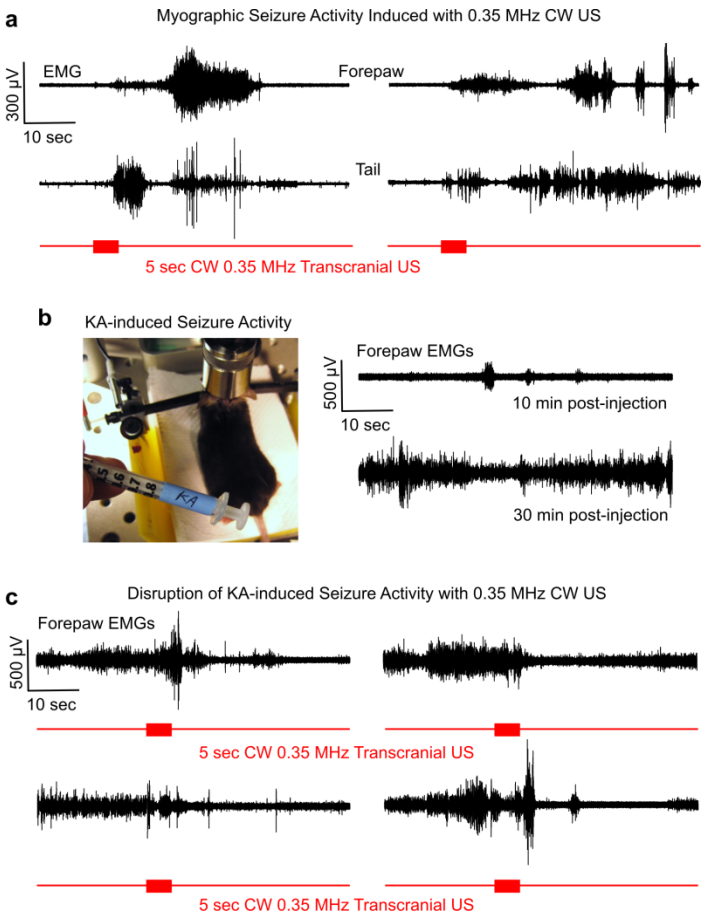

Figure 17 | Induction and disruption of electrographic seizure activity using UNMOD. (a) EMG recording traces of forepaw and tail motor responses produced by a the transcranial delivery of a 5 second continuous wave (CW) US (0.35 MHz) stimulus waveform to an intact mouse brain. Note brain circuit activity evoked with CW waveforms last tens of seconds compared to those evoked with pulsed US waveforms, which last tens of milliseconds as illustrated in Fig. 3a,d. (b) Photograph (left) shows a mouse immediately following an i.p. injection with kainic acid (KA) to induce seizure activity. Example EMG recording traces (right) illustrate typical spontaneous activity patterns as a mouse develops pharmacologically-induced seizures. The top EMG trace shows forepaw limb activity 10 min after KA injection while the bottom trace clearly depicts electromyographic seizure activity 30 min following systemic KA administration. (c) KA-induced seizure activity can be disrupted using responsive UNMOD as illustrated by the EMG recording traces from four representative trials of brain stimulation with US in epileptic mice (also see Video 2). The EMG recordings obtained from a forepaw limb clearly show the attenuation of seizure activity in response to a 5 sec CW US stimulus waveform transmitted to the brain. In addition to CW US, seizure activity can also be attenuated using TPU.

Anticipated Results

Brain stimulation using transcranial ultrasound

In its history US has been shown capable of modulating electrically- or sensory-evoked neuronal activity in a variety of experimental preparations (Table 1). Recent progress is expanding the use of US for neuromodulation based on observations that it can be used to directly stimulate action potentials, synaptic transmission, and synchronous oscillations in intact brain circuits (Tufail, Matyushov et al. 2010). The above protocols provide the details needed to visually observe, electrophysiologically record, and functionally translate US-mediated stimulation of intact mouse brain circuits. We have described how to apply US for brain stimulation using both pulsed and continuous wave (CW) stimuli. The specific protocols we provided should enable one to study how different types of UNMOD stimulus waveforms influence brain circuit activity. Further, one should be able to construct and implement a broad set of pulsed US waveforms for brain stimulation by varying key parameters including: acoustic frequency (A_f), cycles per pulse (c/p), pulse-repetition frequency (PRF), and number of pulses (np; Fig. 14d-g). General guidelines for UNMOD waveform parameter ranges include: A_f from 0.25 to 0.50 MHz, c/p from 50 to 490, PRF from 1 to 3 kHz, and np from 250 to 1000.

When the entire motor cortex is subjected to pulsed UNMOD waveforms, robust motor responses should be observable and/or

electrophysiologically recordable using EMG electrodes (Fig 16a,b). Additionally, the fabrication of acoustic collimators allows for the acoustic beams to be laterally restricted such that brain regions can be more spatially isolated. The use of acoustic collimators also readily supports extracellular recordings of US-evoked brain activity *in vivo* (Fig. 16c,d). Using the protocols described above, we have previously shown that UNMOD is capable of stimulating intact subcortical circuits, such as the mouse hippocampus (Tufail, Matyushov et al. 2010). Stimulation of the motor cortex with transcranial pulsed US (TPU) can evoke EMG activity with response kinetics (Fig. 16a,b) similar to those reported using ChR2 and microelectrodes (Ayling, Harrison et al. 2009). In stark contrast to TPU-evoked activity lasting tens-of-milliseconds, stimulation of motor cortex using transcranial CW US waveforms for several seconds can induce prolonged seizure activity often lasting tens-of-seconds (Fig. 17a). Interestingly, seizure activity produced by CW US does not temporally coincide with the stimulus onset as observed for evoked responses produced by TPU (≈ 20 response latency; Fig 16a,b). Robust seizure activity triggered by CW US rather emerges with a second or more lag following stimulus onset (Fig. 17a). Such differences in the activation kinetics and cellular response profiles triggered by different UNMOD waveforms should be a focus of future investigations. This is especially true since the variable actions of UNMOD will likely enable different applications of US for brain stimulation.

Applications for disease models

In general, brain stimulation has been shown effective for treating a host of neurological and psychiatric diseases (Bliss 1973; Newall, Bliss et al. 1973; Randhawa, Staib et al. 1973; Thuault, Brown et al. 2005; Wagner, Valero-Cabre et al. 2007). Since US is capable of noninvasively stimulating intact brain circuits in a manner similar to conventional electromagnetic approaches (Tufail, Matyushov et al. 2010), we have previously proposed that US may represent a new tool for clinical neuromodulation (Tyler 2010; Tyler, Tufail et al. 2010). The protocols described above serve to highlight several advantages of UNMOD, which broaden its potential for developing novel therapeutic brain stimulation approaches. As demonstrated, such an application could be for disrupting runaway neuronal activity observed in epileptic seizure episodes (Fig. 17c). Conversely, one might use CW US for evoking seizures as illustrated (Fig. 17a). Stimulation of seizure activity by CW US may prove useful in applications designed to screen how potential pharmacological or molecular and genetic interventions influence seizure susceptibility in rodents.

The major advantages of UNMOD are that it is flexible in being able to influence a variety of brain activity patterns, it is noninvasive by not requiring surgical or genetic manipulation, it can be rapidly applied, and it confers a spatial resolution several millimeters better than other currently available noninvasive brain stimulation methods. In addition, there is a

strong potential for using UNMOD in the noninvasive functional mapping of both normal and diseased brain circuits since US is compatible with MRI. Thus, with further development we anticipate UNMOD will be able to readily support studies of normal brain function, the development of novel therapeutic interventions, and noninvasive neurodiagnostics. The protocols provided above represent necessary starting points for driving such exciting new tools and possibilities forward to fruition in modern neuroscience.

References

Adamantidis, A. R., F. Zhang, et al. (2007). "Neural substrates of awakening probed with optogenetic control of hypocretin neurons." Nature 450(7168): 420-424.

Ang, E. S., Jr., V. Gluncic, et al. (2006). "Prenatal exposure to ultrasound waves impacts neuronal migration in mice." Proc Natl Acad Sci U S A 103(34): 12903-12910.

Aravanis, A. M., L. P. Wang, et al. (2007). "An optical neural interface: in vivo control of rodent motor cortex with integrated fiberoptic and optogenetic technology." J Neural Eng 4(3): S143-156.

Ayling, O. G., T. C. Harrison, et al. (2009). "Automated light-based mapping of motor cortex by photoactivation of channelrhodopsin-2 transgenic mice." Nat Methods 6(3): 219-224.

Bachtold, M. R., P. C. Rinaldi, et al. (1998). "Focused ultrasound modifications of neural circuit activity in a mammalian brain." Ultrasound Med Biol 24(4): 557-565.

Barker, A. T. (1999). "The history and basic principles of magnetic nerve stimulation." Electroencephalogr Clin Neurophysiol Suppl 51: 3-21.

Barker, A. T., R. Jalinous, et al. (1985). "Non-invasive magnetic stimulation of human motor cortex." Lancet 1(8437): 1106-1107.

Bartholow, R. (1882). Medical electricity: a practical treatise on the applications of electricity to medicine and surgery. Philadelphia, Henry C. Lea's Son & Co.

Clement, G. T. and K. Hynynen (2002). "A non-invasive method for focusing ultrasound through the human skull." Phys Med Biol 47(8): 1219-1236.

Dalecki, D. (2004). "Mechanical bioeffects of ultrasound." Annu Rev Biomed Eng 6: 229-248.

Dinno, M. A., M. Dyson, et al. (1989). "The significance of membrane changes in the safe and effective use of therapeutic and diagnostic ultrasound." Phys Med Biol 34(11): 1543-1552.

Fregni, F. and A. Pascual-Leone (2007). "Technology insight: noninvasive brain stimulation in neurology-perspectives on the therapeutic potential of rTMS and tDCS." Nat Clin Pract Neurol 3(7): 383-393.

Fritsch, G. and E. Hitzig (1870). "Über die elektrische Erregbarkeit des Grosshirns." Arch. Anat. Physiol. 37: 300–332

Fry, F. J., H. W. Ades, et al. (1958). "Production of reversible changes in the central nervous system by ultrasound." Science 127(3289): 83-84.

Fry, W. J. (1958). "Use of intense ultrasound in neurological research." Am J Phys Med 37(3): 143-147.

Fry, W. J. (1968). "Electrical stimulation of brain localized without probes--theoretical analysis of a proposed method." J Acoust Soc Am 44(4): 919-931.

Fry, W. J., R. Meyers, et al. (1958). "Topical Differentia of Pathogenetic Mechanisms Underlying Parkinsonian Tremor and Rigidity as Indicated by Ultrasonic Irradiation of the Human Brain." Transactions of the American Neurologial Association: 16 - 24.

Gavrilov, L. R., G. V. Gersuni, et al. (1976). "The effect of focused ultrasound on the skin and deep nerve structures of man and animal." Prog Brain Res 43: 279-292.

Gavrilov, L. R., E. M. Tsirulnikov, et al. (1996). "Application of focused ultrasound for the stimulation of neural structures." Ultrasound Med Biol 22(2): 179-192.

Griesbauer, J., A. Wixforth, et al. (2009). "Wave propagation in lipid monolayers." Biophys J 97(10): 2710-2716.

Grill, W. M., S. E. Norman, et al. (2009). "Implanted neural interfaces: biochallenges and engineered solutions." Annu Rev Biomed Eng 11: 1-24.

Hallett, M. (2007). "Transcranial magnetic stimulation: a primer." Neuron 55(2): 187-199.

Harvey, E. N. (1929). "The effect of high frequency sound waves on heart muscle and other irritable tissues." American Journal of Physiology(1): 284-290.

Hayner, M. and K. Hynynen (2001). "Numerical analysis of ultrasonic transmission and absorption of oblique plane waves through the human skull." J Acoust Soc Am 110(6): 3319-3330.

Heimburg, T. (2010). "Lipid ion channels." Biophys Chem 150(1-3): 2-22.

Heimburg, T. and A. D. Jackson (2005). "On soliton propagation in biomembranes and nerves." Proc Natl Acad Sci U S A 102(28): 9790-9795.

Hertzberg, Y., O. Naor, et al. "Towards multifocal ultrasonic neural stimulation: pattern generation algorithms." J Neural Eng 7(5): 056002.

Histed, M. H., V. Bonin, et al. (2009). "Direct activation of sparse, distributed populations of cortical neurons by electrical microstimulation." Neuron 63(4): 508-522.

Huang, H., S. Delikanli, et al. (2010). "Remote control of ion channels and neurons through magnetic-field heating of nanoparticles." Nat Nanotechnol 5(8): 602-606.

Hynynen, K. and G. Clement (2007). "Clinical applications of focused ultrasound-the brain." Int J Hyperthermia 23(2): 193-202.

Hynynen, K., G. T. Clement, et al. (2004). "500-element ultrasound phased array system for noninvasive focal surgery of the brain: a preliminary rabbit study with ex vivo human skulls." Magn Reson Med 52(1): 100-107.

Hynynen, K. and F. A. Jolesz (1998). "Demonstration of potential noninvasive ultrasound brain therapy through an intact skull." Ultrasound Med Biol 24(2): 275-283.

Hynynen, K., N. McDannold, et al. (2006). "Pre-clinical testing of a phased array ultrasound system for MRI-guided noninvasive surgery of the brain--a primate study." Eur J Radiol 59(2): 149-156.

Jolesz, F. A., K. Hynynen, et al. (2005). "MR imaging-controlled focused ultrasound ablation: a noninvasive image-guided surgery." Magn Reson Imaging Clin N Am 13(3): 545-560.

Knopfel, T. and W. Akemann (2010). "Nanobiotechnology: Remote control of cells." Nat Nanotechnol 5(8): 560-561.

Kravitz, A. V., B. S. Freeze, et al. "Regulation of parkinsonian motor behaviours by optogenetic control of basal ganglia circuitry." Nature 466(7306): 622-626.

Kringelbach, M. L., N. Jenkinson, et al. (2007). "Translational principles of deep brain stimulation." Nat Rev Neurosci 8(8): 623-635.
Lee, J. H., R. Durand, et al. "Global and local fMRI signals driven by neurons defined optogenetically by type and wiring." Nature 465(7299): 788-792.

Leighton, T. G. (2007). "What is ultrasound?" Prog Biophys Mol Biol 93(1-3): 3-83.

Li, J., L. Fok, et al. (2009). "Experimental demonstration of an acoustic magnifying hyperlens." Nat Mater.

Lobo, M. K., H. E. Covington, 3rd, et al. "Cell type-specific loss of BDNF signaling mimics optogenetic control of cocaine reward." Science 330(6002): 385-390.

Martin, E., D. Jeanmonod, et al. (2009). "High intensity focused ultrasound for non-invaisve functional neurosurgery." Annals of Neurology 66: 858-861.

Mayberg, H. S., A. M. Lozano, et al. (2005). "Deep brain stimulation for treatment-resistant depression." Neuron 45(5): 651-660.

Miesenbock, G. (2009). "The optogenetic catechism." Science 326(5951): 395-399.

Mihran, R. T., F. S. Barnes, et al. (1990). "Temporally-specific modification of myelinated axon excitability in vitro following a single ultrasound pulse." Ultrasound Med Biol 16(3): 297-309.

Mihran, R. T., F. S. Barnes, et al. (1990). "Transient modification of nerve excitability in vitro by single ultrasound pulses." Biomed Sci Instrum 26: 235-246.

Morris, C. E. and P. F. Juranka (2007). Lipid Stress at Play: Mechanosensitivity of Voltage-Gated Channels. Current Topics in Membranes. P. H. Owen, Academic Press. Volume 59: 297-338.

O'Brien, W. D., Jr. (2007). "Ultrasound-biophysics mechanisms." Prog Biophys Mol Biol 93(1-3): 212-255.

Payne, N. A. and J. Prudic (2009). "Electroconvulsive therapy: Part I. A perspective on the evolution and current practice of ECT." J Psychiatr Pract 15(5): 346-368.

Penfield, W. and H. H. Jasper (1954). Epilepsy and the Functional Anatomy of the Human Brain. . London, J & A Churchill.

Perlmutter, J. S. and J. W. Mink (2006). "Deep brain stimulation." Annu Rev Neurosci 29: 229-257.

Ranck, J. B., Jr. (1975). "Which elements are excited in electrical stimulation of mammalian central nervous system: a review." Brain Res 98(3): 417-440.

Rinaldi, P. C., J. P. Jones, et al. (1991). "Modification by focused ultrasound pulses of electrically evoked responses from an in vitro hippocampal preparation." Brain Res 558(1): 36-42.

Schwalb, J. M. and C. Hamani (2008). "The history and future of deep brain stimulation." Neurotherapeutics 5(1): 3-13.

Spadoni, A. and C. Daraio (2010). "Generation and control of sound bullets with a nonlinear acoustic lens." Proc Natl Acad Sci U S A 107(16): 7230-7234.

Stoney, S. D., Jr., W. D. Thompson, et al. (1968). "Excitation of pyramidal tract cells by intracortical microstimulation: effective extent of stimulating current." J Neurophysiol 31(5): 659-669.

ter Haar, G. (2007). "Therapeutic applications of ultrasound." Prog Biophys Mol Biol 93(1-3): 111-129.

Tolias, A. S., F. Sultan, et al. (2005). "Mapping cortical activity elicited with electrical microstimulation using FMRI in the macaque." Neuron 48(6): 901-911.

Tsui, P. H., S. H. Wang, et al. (2005). "In vitro effects of ultrasound with different energies on the conduction properties of neural tissue." Ultrasonics 43(7): 560-565.

Tufail, Y., A. Matyushov, et al. (2010). "Transcranial Pulsed Ultrasound Stimulates Intact Brain Circuits " Neuron 66(6): 681-694.

Tyler, W. J. (2010). "Noninvasive neuromodulation with ultrasound? A continuum mechanics hypothesis." The Neuroscientist Advanced Online Print, January 25, 2010.

Tyler, W. J., Y. Tufail, et al. (2008). "Remote excitation of neuronal circuits using low-intensity, low-frequency ultrasound." PLoS ONE 3(10): e3511.

Velling, V. A. and S. P. Shklyaruk (1988). "Modulation of the functional state of the brain with the aid of focused ultrasonic action." Neuroscience and Behavioral Physiology 18(5): 369-375.

Wagner, T., A. Valero-Cabre, et al. (2007). "Noninvasive Human Brain Stimulation." Annu Rev Biomed Eng 9: 527-565.

White, P. J., G. T. Clement, et al. (2006). "Local frequency dependence in transcranial ultrasound transmission." Phys Med Biol 51(9): 2293-2305.

White, P. J., G. T. Clement, et al. (2006). "Longitudinal and shear mode ultrasound propagation in human skull bone." Ultrasound Med Biol 32(7): 1085-1096.

Young, R. R. and E. Henneman (1961). "Functional effects of focused ultrasound on mammalian nerves." Science 134: 1521-1522.

Zhang, F., A. M. Aravanis, et al. (2007). "Circuit-breakers: optical technologies for probing neural signals and systems." Nat Rev Neurosci 8(8): 577-581.

Zhang, F., V. Gradinaru, et al. "Optogenetic interrogation of neural circuits: technology for probing mammalian brain structures." Nat Protoc 5(3): 439-456.

Zhang, F., L. P. Wang, et al. (2007). "Multimodal fast optical interrogation of neural circuitry." Nature 446(7136): 633-639.

Zhang, S., L. Yin, et al. (2009). "Focusing Ultrasound with an Acoustic Metamaterial Network." Physics Reviews Letters 102(19): 194301-194304.

Chapter 5

DISCUSSION

Prior investigations into the effects of ultrasound on neural tissue have produced significant findings, but until now there have been no reports of explicit data on the direct stimulation of intact neural circuits. The methods and observations detailed in this dissertation provide novel insight into the interactions of mechanical energy and the central nervous system.

Our initial investigations discovered that pulsed ultrasound of specific frequencies and intensities could activate, whether indirectly or directly, sodium channels, calcium channels, and synaptic transmission in hippocampal slice cultures (Tyler, Tufail et al. 2008). This was followed up by translating our approach to an *in vivo* mouse model where cortical and subcortical neuronal activation was achieved (Tufail, Matyushov et al. 2010). After establishing that ultrasound can readily be used to stimulate the intact brain, we asked whether this method could join the ranks of other current noninvasive neurostimulation interventions. Just as rTMS and tDCS studies have reported ameliorating effects in the diseased brain, the implementing of ultrasound for such neurological and psychiatric applications may provide exceeding results, as TPU is not limited to cortical regions and offers greater spatial resolution. This dissertation work is the first to report the direct stimulation of intact nervous tissue and

provides a detailed protocol to replicate such observations while suggesting its utility in brain disease models.

Mechanisms behind ultrasound induced neuronal activity

Despite the significant though sparse data on the influence of ultrasound on the central nervous system, the exploration into the underlying mechanisms is only recently forthcoming and has remained elusive. Since ultrasound has become profoundly known for its clinical imaging and physiotherapy, much of the work into the discoveries has been limited to these active fields of study. This has produced a general classification scheme for ultrasound based therapies. High power ultrasound is employed by methods such as high-intensity focused ultrasound (HIFU) and lithotripsy, whereas low intensity ultrasound employs sonophoresis, sonoporation, gene therapy and bone healing (ter Haar 2007). In this regard, the nature of ultrasound, or mechanical energy, can physically interact with a medium in a thermal and non-thermal manner (Dalecki 2004). Under current standards, the intensity values used in our studies fall under the low-intensity, non-thermal effects. Additionally, the lack of gas bodies in the brain support this assertion.

The non-thermal bioeffects include acoustic radiation force and cavitation. Acoustic radiation force results from the transfer of momentum from the acoustic field to the object, or medium (Dalecki 2004). Radiation force is responsible for producing radiation torque and acoustic streaming

(Dalecki 2004). This force is capable of displacing small ions, molecules, and even organelles. The mechanical pressure produced from the radiation force can also induce movement of the fluid along and around cell membranes (Johns 2002). These mechanical actions on biological tissues have led to a hypothesis that attributes the physical properties of fluids and membranes as major components to the underlying mechanisms. This hypothesis perceives the environment of the brain as a set of dynamic boundary conditions that give rise to acoustic impedance mismatches (Tyler 2010). The presence of these mismatches give rise to stable cavitation, fluid micro-jets, eddying, turbulence, shear stress and Bernoulli effects as the propagation of the acoustic fields come in to contact with lipid bilayers, intracellular/extracellular fluids, and cerebrovascular networks (Tyler 2010). It is probably these phenomena that manifest the ability of US to modulate neuronal excitability in two ways. The simplest form of the mechanisms that encompass multiple hypotheses and observations in the brain demonstrate that 1) the viscoelastic properties of lipid bilayers under mechanical stress may induce enough strain and turbulence to locally permeabilize the bilayer allowing flux of ions and thus small changes in membrane polarization and 2) the direct energy absorption or stretch induced changes on mechanosensitive transmembrane proteins may result with modulation of receptor/channel gating kinetics (Johns 2002; Morris and Juranka 2007; Tyler 2010).

Keeping the proposed mechanisms of action in mind, it is important to mention the correlation observed between the measured output of stimulating the intact motor cortex, and the characteristics of the applied acoustic waveform. As illustrated in Chapter 3, figure 10, there is an inverse relationship between both acoustic frequency and intensity with the normalized EMG response. What biophysical interactions are responsible for producing a greater EMG event in response to lower relative acoustic frequencies and intensities? One could hypothesize that the shorter pulse durations may effectively act as a shock pulse to the exposed neural tissue. This may act to displace ions across membranes and alter membrane induced tension on ion channels, resulting with modulation of gating kinetics. Additionally, we reported that greater EMG responses were observed under the influence of lower acoustic frequencies. These observations allude to a complex relationship between the induction of neurostimulation and the effective acoustic parameters, as the limits to the parameter space seem obscure and largely unknown. During *in vivo* experiments, we initially set out to mechanistically test a spectrum of acoustic intensities, but not only did this prove to be hugely time consuming, it was very ineffective in producing reliable results. This led to a more undirected search of acoustic parameters. Likewise, this approach did not immediately yield any positive result, instead we discovered that the animal's plane of anesthesia was another highly influencing variable.

As an accepted and often dismissed limitation to studying aspects of neurophysiology, the use of anesthetics imposes restrictions on the ability to interpret data and its applicability to normal behavior. Our observations during the application of ultrasound initially varied within each subject over the course of time. We began to notice that depending on the responsiveness of the animal within the first ~20 minutes of anesthetic injection, the probability for obtaining an immediate ultrasound induced motor response was variable. Increased reliability was obtained when the animal was mildly responsive to the toe or tail-pinch reflex. What are the interactions of anesthetics on the effectiveness of using ultrasound for brain stimulation? Owing to the fact that our experiments solely utilized a ketamine/xylazine cocktail, what observations can be made when a different anesthetic is used? Will specific anesthetics yield dissimilar effects when seeking ultrasound induced neuromodulatory effects?

In order to substantiate our claims for implementing ultrasound as a potential neurological therapeutic, further investigations into the responsible mechanisms underlying neurostimulation need to be carried out. Additionally, issues such as the influence of anesthetic type and level need to be resolved. Although a difficult set of tasks, much benefit will be gained through these experiments as their undertaking will support the benefit in the growth and translation of this method.

Bio*safety of ultrasound*

The latest wave of ultrasound technology has emerged from its applications in diagnostic imaging and tissue healing to non-invasive surgery. The techniques and parameters used to manipulate US for its particular application vary substantially, thus suggesting the need for detailed analysis. Fetal ultrasonic scanning has become routine practice for clinicians as it has maintained a positive safety record for many decades. This type of diagnostic imaging employs frequencies in the range of ~1-10MHz while being regulated by the U.S. Food and Drug Administration (FDA) for safety measures. A method to quantify the output levels of such diagnostic tools calculates what is known as the thermal index and mechanical index. The thermal index describes the energy required to raise tissue temperature 1°C (Mitragotri 2005). The Mechanical index is more precisely defined as the peak negative pressure, at its max pulsed intensity integral, divided by the center frequency of the transducer (Dalecki 2004). In addition to these measures, reporting such intensities as spatial peak temporal average intensity (Ispta), spatial average temporal average intensity (Isata), and spatial peak pulse average intensity (Isppa) are also significant and accepted parameters used to define exposure and dosimetry (ter Haar 2007). The motivation for determining such measures resides in the ability of US to inflict damage upon tissues through mechanisms described by thermal and non-thermal interactions. The better known major biohazards to appreciate are manifested by the thermal effects. It is important to know how ultrasound

can elicit thermal effects on the biological application of interest within a given acoustic field and its environment, such as the uterus of a pregnant female or the intact brain of a human patient. Manipulating the thermal effects, HIFU is capable of raising the temperature in live tissue above 56°C in less than 3 seconds (ter Haar 2007). When live tissue reaches temperatures between 57-60°C, the threshold for protein denaturation is obtained and coagulation necrosis occurs (Jolesz 2009). To achieve temperature levels of this magnitude, it has been reported that a peak power of 63 watts can produce a peak temperature rise of 64.1°C at a depth of 29 mm using a single element transducer on the head and through the tissue of a primate (McDannold, Moss et al. 2003). In addition, it was recently reported that a dose of 17.5 equivalent minutes of US that raises tissue to a temperature of 43°C can induce thermal coagulation as the probability for tissue coagulation using the stated parameters is roughly 50% (Jolesz, Hynynen et al. 2005; Hynynen, McDannold et al. 2006). For reasons implicated by the results obtained from groups implementing various parameters, it is clear why all scenarios of US acoustic parameters and biological environments must be well characterized or predicted to ensure the absence of undesired biological effects.

The non-thermal effects of ultrasound can be more subtle and therefore must be carefully considered when determining biosafety. As mentioned, the many modes of physical interactions US may elicit on

tissue invoke a need for extensive study. It has been reported that prenatal exposure to ultrasound parameters similar to those used in obstetrical clinical practice can affect neuronal migration in the cerebral cortex (Ang, Gluncic et al. 2006), but follow up studies supporting a functional significance for these observations lacks exploration. There is an opposing general school of thought that stresses the observations that bubbles or gas bodies are obligatory for producing non-thermal damage to living tissue (Church and Carstensen 2001; Church, Carstensen et al. 2008). The well established organs that readily maintain US sensitive gas bodies are the lungs and gastrointestinal system (Dalecki 2004). In order to study the non-thermal cavitational effects of US in the brain, contrast agents such as Albunex™ are introduced to the vasculature of the specimen under study. Contrast agents such as these contain gas bodies that are cavitationaly responsive to acoustic fields. When a lithotripter field of 2 MPa is delivered to a specimen containing US contrast agents, microvascular damage can be observed in most soft tissues including muscle, mesentery, kidney, stomach, bladder, and fat (Dalecki 2004). It should be stressed that a great understanding of the acoustic interactions with biological tissues and their natural environments should be uncovered and detailed knowledge of the mechanisms is crucial for properly evaluating safety measures. The report that acoustic pressure fields with amplitudes up to 40 MPa display only minimal damage to soft tissues (Dalecki 2004) makes this point evident. Although requiring further

investigations, our methods for TPU produce energy profiles with peak rarefactional pressures (p_r) on the order of 0.085 MPa (Tufail, Matyushov et al. 2010).

The horizon for US bio-applications has recently broadened and innervated new clinical significance, therefore the efficacy must be re-evaluated and again carefully studied to maintain its safety record. Problems may arise when instruments carefully designed, for example, fetal diagnostic scanning become used for other *in-vivo* or *in-vitro* applications, and maintaining the same methods that measure output levels are interpreted to have the equivalent safety rating (Leighton 2007). As a trend with many citations, great effort is focused on the behavior that is elicited by the specimen being exposed to ultrasound. Subsequently, details describing the US waveform(s) can be overlooked and imprecisely reported, including considerations of the acoustic environment. Tim Leighton provides an example by explaining that reports like these can be misleading. Mechanical index is widely used when US is applied with contrast agents even though their presence reduces the validity of the MI in representing the conditions (Leighton 2007). In addition, Leighton also states that albeit hydrophones are used to detect pressure fields, one must appreciate the ability of the acoustic environment, especially the dynamic properties of biological systems, that changes may occur non-linearly or through reflection and diffraction (Leighton 2007).

The challenges must be surfaced when attempting to establish a standard level of safety. The importance of considering such details as interaction between hydrophone, ultrasonic field, bio and non-bio species need to be considered because these can be sources of large scattering or diffracting targets, and the measurement can be complicated by directionality and spatial averaging (Leighton 2007).

Innovative technology

The studies reported here employed sources of ultrasound from single element planar ultrasonic transducers. Despite the resolution obtained for neuronal activation using methods developed here, we lack the technical access to implement and manipulate the complete capabilities ultrasound has to offer. Our data suggests a competitive trait compared to the resolution limits reported for TMS (1.5-2.0 mm versus ~1 cm) (Barker 1999; Tufail, Matyushov et al. 2010). With these numbers in mind, the implementing of current ultrasonic focusing technologies with our TPU methods could observe a superior succession of ultrasound for a noninvasive neurostimulation device. One such current method uses multiple transducers arranged in phased arrays to spatially control the acoustic focal point. Although this method has been developed for the application of HIFU used for noninvasively ablating brain tissue, the lesion diameters were between 3 and 5 mm (Hynynen, Clement et al. 2004; Martin, Jeanmonod et al. 2009). Aside from the 500 element or 1024

element design used in HIFU studies, the ability to achieve such resolution is fundamentally dependent on the frequencies utilized. This notion has been recently surpassed by the employment of acoustic meta-materials (having a negative refractive index) enabling subdiffraction acoustic spatial resolutions (Zhang, Yin et al. 2009; Tufail, Matyushov et al. 2010). Based on these currently proven technologies, it is reasonable to hypothesize that the marriage of the mentioned techniques along with our TPU protocols may produce a tool that could noninvasively penetrate tissue and skull, access subcortical structures, and accurately stimulate submillimeter brain regions. Future technologies could conceivably stimulate multiple and patterned brain areas simultaneously or even in succession to replicate normal circuit activation in the compromised brain.

Applications for clinical models

Collectively, can TPU be realized as a useful tool for specialized clinical practice?

The year 1928 marked the time where ultrasound was reported to have an observable effect in a biological application (Harvey, Harvey et al. 1928). As progression has persisted in the field of ultrasound, the year 2009 had demonstrated that with the marriage of technologies from multiple disciplines, ultrasound can be successfully used in clinical applications for non-invasive brain surgery. A prime example was conducted by researchers at the University Children's Hospital in

Switzerland where nine patients with neuropathic pain underwent selective thalamotomies (Martin, Jeanmonod et al. 2009). The success for demonstrating a complete non-invasive surgery into deep structures within the human brain where patients reported 30-100% in pain reduction within 2 days post-treatment (Martin, Jeanmonod et al.) is well recognized.

One of the significant achievements that had occurred throughout this time period was overcoming the boundary of the skull. Many biological preparations have been used to observe and measure the induced effects of US, but when the application for delivering US to the living brain through the intact skull arose, it meant that superior methods for directing US to a target through an acoustic scattering barrier had to be developed. The skull acts as a penetrable obstacle to US because of impedance mismatches as the compression and rarefaction of molecules translate through different mediums. These mismatches arise from the intrinsic fluidity and compressibility of the tissue as it must pass through skin, bone, brain and all the interfaces in between (Tyler 2010). Through experimental and modeling data (White, Clement et al. 2006) demonstrated that lower frequency US achieves better bone transmission in relationship to both density and skull thickness. As ultrasound passes through these boundaries, the mechanical energy is deflected, scattered, absorbed, and transmitted, thus drastically changing the initial waveform characteristics it may have had in the near or far field of the transducer.

The nature of such surgical applications requires that the performance of the transducer(s) used to be superior. The performance of transducers depends on the design, material, and apparatus. The purpose for such high demands stems from the need to maintain the efficiency of energy transfer through the skin and skull, as well as to maintain high focusing tolerances, and the ability to steer the ultrasound focal point with reliability. The fight to overcome the distortion that bone inflicts on ultrasound has proven to be short lived. It was the use of a propagation model that takes into account the thickness, orientation, and density obtained from CT images of the head to activate sections of transducer elements positioned in a hemi-spherical array that ultimately allows focusing capabilities (Clement and Hynynen 2002).

Part of the motivation for exploring the use of TPU as a clinical intervention originates from the idea that ultrasound may be a viable avenue to supercede DBS and vagus nerve stimulation with regards to their observed clinical benefits. It has been shown that electrical stimulation can increase the expression of neurotrophic factors (Andrews 2003) and it is part of a suspicion as to how DBS and vagus nerve stimulation have been observed to benefit a spectrum of neurologic disorders (Wagner, Valero-Cabre et al. 2007). Fortunately, we were able to reproduce these findings (Tufail, Matyushov et al. 2010), implicating the translation of our technique and possibly the replacement of current methods.

Unlike the currently implemented neurostimulation techniques, ultrasound in theory could be used to stimulate different areas of a patient's intact brain without the invasiveness, without running the risks of surgery, and incurring less costs. This approach could prove effective for a greater population of patients as the origination of their neurological deficits may prove to be variable across individuals.

Collectively, the observations in the numerous reports that use ultrasound to manipulate particular functions of the nervous system, and the technology used to safely and reliably target particular areas within the brain opens a path for potentially limitless applications. One such application, as demonstrated in this dissertation is the treatment for acute epileptic seizure management. One may envision an apparatus in a clinical setting that would be able to detect the onset of seizures through surface EEG, and then simultaneously use magnetic resonance guided ultrasound stimulation protocols to locate the brain region and abolish the manifestation of a seizure. This can be a foreseeable intervention owing to the fact that the tools mentioned are already in existence and currently used in clinical settings. The major obstacles remaining include the integration of all EEG, MRI, and focused ultrasound equipment. More importantly, what remains is the understanding of the ultrasound interaction with a diseased brain circuit. As mentioned, the mechanisms behind ultrasound induced neurostimulation are still vague, therefore

unveiling the properties to how UNMOD is effective for treating epilepsy will require greater investigation.

In particular, an interesting question deals with the region specific sensitivity to ultrasound. In other words, are different regions of the brain more or less sensitive to particular parameters of ultrasound stimulation? To address this question, and to surpass some of the limitations in our prior experiments, the use of multi-electrode arrays for observing extracellular neuronal activity may prove to be helpful in understanding the propagation of the acoustic wave as it penetrates, absorbs, and scatters throughout the brain. Another experiment would be to use MRI compatible ultrasound transducers and equipment in order to map brain responses using fMRI. Secondly, the direction and orientation of the applied acoustic fields need to be investigated. For reasons that we can only speculate, the orientation may be a significant factor because we observed orientation specific activation of the hippocampus. We assumed that this was due to the layered and structured organization of the brain, in addition to the acoustic direction. With a roughly 50 degree change in angle approach, we were able to successfully stimulate the hippocampus (fig. 13). These aspects raise issues that call for scrutinizing investigations in order to see this technology deliver its full potential as a clinical intervention.

As a foundation for prospective medical applications, TPU possesses the characteristics and integrative capabilities to produce a reliable and effective tool in the near future. Now is the time to stress such

technology and explore the complete capacity it may have on nervous system pathologies and further discoveries of normal brain function.

REFERENCES

Abe, K. and H. Saito (2001). "Effects of basic fibroblast growth factor on central nervous system functions." Pharmacol Res **43**(4): 307-312.

Adamantidis, A. R., F. Zhang, et al. (2007). "Neural substrates of awakening probed with optogenetic control of hypocretin neurons." Nature **450**(7168): 420-424.

Anastassiou, C. A., S. M. Montgomery, et al. (2010). "The effect of spatially inhomogeneous extracellular electric fields on neurons." J Neurosci **30**(5): 1925-1936.

Andrews, R. J. (2003). "Neuroprotection trek--the next generation: neuromodulation I. Techniques--deep brain stimulation, vagus nerve stimulation, and transcranial magnetic stimulation." Ann N Y Acad Sci **993**: 1-13; discussion 48-53.

Andrews, R. J. (2003). "Neuroprotection trek--the next generation: neuromodulation II. Applications--epilepsy, nerve regeneration, neurotrophins." Ann N Y Acad Sci **993**: 14-24; discussion 48-53.

Ang, E. S., Jr., V. Gluncic, et al. (2006). "Prenatal exposure to ultrasound waves impacts neuronal migration in mice." Proc Natl Acad Sci U S A **103**(34): 12903-12910.

Angel, A. and D. A. Gratton (1982). "The effect of anaesthetic agents on cerebral cortical responses in the rat." Br J Pharmacol **76**(4): 541-549.

Aravanis, A. M., L. P. Wang, et al. (2007). "An optical neural interface: in vivo control of rodent motor cortex with integrated fiberoptic and optogenetic technology." J Neural Eng **4**(3): S143-156.

Ayling, O. G., T. C. Harrison, et al. (2009). "Automated light-based mapping of motor cortex by photoactivation of channelrhodopsin-2 transgenic mice." Nat Methods **6**(3): 219-224.

Bachtold, M. R., P. C. Rinaldi, et al. (1998). "Focused ultrasound modifications of neural circuit activity in a mammalian brain." Ultrasound Med Biol **24**(4): 557-565.

Barker, A. T. (1999). "The history and basic principles of magnetic nerve stimulation." Electroencephalogr Clin Neurophysiol Suppl **51**: 3-21.

Barker, A. T., R. Jalinous, et al. (1985). "Non-invasive magnetic stimulation of human motor cortex." Lancet **1**(8437): 1106-1107.

Bashir, S., I. Mizrahi, et al. (2010). "Assessment and modulation of neural plasticity in rehabilitation with transcranial magnetic stimulation." PM R **2**(12 Suppl 2): S253-268.

Bliss, B. P. (1973). "Communicating ethics during medical training." Nurs Mirror **136**(7): 23-26.

Bliss, B. P. (1973). "Pressure, flow and peripheral resistance measurements during surgery for femoro-popliteal occlusion (preliminary observations on 21 limbs)." Scand J Clin Lab Invest Suppl **128**: 179-183.

Bliss, B. P. (1973). "A small virus in human faeces." Lancet **1**(7801): 492.

Bliss, D. K. and P. L. Bates (1973). "A rapid and reliable technique for pinealectomizing rats." Physiol Behav **11**(1): 111-112.

Bliss, E. S., D. Milam, et al. (1973). "Dielectric Mirror Damage by Laser Radiation over a Range of Pulse Durations and Beam Radii." Appl Opt **12**(4): 677-689.

Bliss, R. T. (1973). "A vasectomy prosthesis." IMJ Ill Med J **143**(5): 430.

Bliss, T. V. and A. R. Gardner-Medwin (1973). "Long-lasting potentiation of synaptic transmission in the dentate area of the unanaestetized rabbit following stimulation of the perforant path." J Physiol **232**(2): 357-374.

Bliss, T. V. and T. Lomo (1973). "Long-lasting potentiation of synaptic transmission in the dentate area of the anaesthetized rabbit following stimulation of the perforant path." J Physiol **232**(2): 331-356.

Boon, P., K. Vonck, et al. (2007). "Deep brain stimulation in patients with refractory temporal lobe epilepsy." Epilepsia **48**(8): 1551-1560.

Boyden, E. S., F. Zhang, et al. (2005). "Millisecond-timescale, genetically targeted optical control of neural activity." Nat Neurosci **8**(9): 1263-1268.

Bragin, A., G. Jando, et al. (1995). "Gamma (40-100 Hz) oscillation in the hippocampus of the behaving rat." J Neurosci **15**(1 Pt 1): 47-60.

Bragin, A., M. Penttonen, et al. (1997). "Termination of epileptic afterdischarge in the hippocampus." J Neurosci **17**(7): 2567-2579.

Bronk, P., F. Deak, et al. (2007). "Differential effects of SNAP-25 deletion on Ca2+ -dependent and Ca2+ -independent neurotransmission." J Neurophysiol **98**(2): 794-806.

Brunet, A., S. R. Datta, et al. (2001). "Transcription-dependent and -independent control of neuronal survival by the PI3K-Akt signaling pathway." Curr Opin Neurobiol **11**(3): 297-305.

Burrone, J., Z. Li, et al. (2006). "Studying vesicle cycling in presynaptic terminals using the genetically encoded probe synaptopHluorin." Nat Protoc **1**(6): 2970-2978.

Buzsaki, G. (1989). "Two-stage model of memory trace formation: a role for "noisy" brain states." Neuroscience **31**(3): 551-570.

Buzsaki, G. (1996). "The hippocampo-neocortical dialogue." Cereb Cortex **6**(2): 81-92.

Buzsaki, G., Z. Horvath, et al. (1992). "High-frequency network oscillation in the hippocampus." Science **256**(5059): 1025-1027.

Chapman, I. V., N. A. MacNally, et al. (1980). "Ultrasound-induced changes in rates of influx and efflux of potassium ions in rat thymocytes in vitro." Ultrasound Med Biol **6**(1): 47-58.

Charron, F. and M. Tessier-Lavigne (2007). "The Hedgehog, TGF-beta/BMP and Wnt families of morphogens in axon guidance." Adv Exp Med Biol **621**: 116-133.

Church, C. C. and E. L. Carstensen (2001). ""Stable" inertial cavitation." Ultrasound Med Biol **27**(10): 1435-1437.

Church, C. C., E. L. Carstensen, et al. (2008). "The risk of exposure to diagnostic ultrasound in postnatal subjects: nonthermal mechanisms." J Ultrasound Med **27**(4): 565-592; quiz 593-566.

Clement, G. T. (2004). "Perspectives in clinical uses of high-intensity focused ultrasound." Ultrasonics **42**(10): 1087-1093.

Clement, G. T. and K. Hynynen (2002). "A non-invasive method for focusing ultrasound through the human skull." Phys Med Biol **47**(8): 1219-1236.

Cooper, T. E. and G. J. Trezek (1972). "A probe technique for determining the thermal conductivity of tissue." Journal of Heat Transfer **94**(133-140).

Creutzfeldt, O. D., G. H. Fromm, et al. (1962). "Influence of transcortical d-c currents on cortical neuronal activity." Exp Neurol **5**: 436-452.

Dalecki, D. (2004). "Mechanical bioeffects of ultrasound." Annu Rev Biomed Eng **6**: 229-248.

Dinno, M. A., L. A. Crum, et al. (1989). "The effect of therapeutic ultrasound on electrophysiological parameters of frog skin." Ultrasound Med Biol **15**(5): 461-470.

Dinno, M. A., M. Dyson, et al. (1989). "The significance of membrane changes in the safe and effective use of therapeutic and diagnostic ultrasound." Phys Med Biol **34**(11): 1543-1552.

Driver, J., F. Blankenburg, et al. (2009). "Concurrent brain-stimulation and neuroimaging for studies of cognition." Trends Cogn Sci **13**(7): 319-327.

Ebisawa, K., K. Hata, et al. (2004). "Ultrasound enhances transforming growth factor beta-mediated chondrocyte differentiation of human mesenchymal stem cells." Tissue Eng **10**(5-6): 921-929.

El Bahh, B., S. Balosso, et al. (2005). "The anti-epileptic actions of neuropeptide Y in the hippocampus are mediated by Y and not Y receptors." Eur J Neurosci **22**(6): 1417-1430.

El Bahh, B., J. Q. Cao, et al. (2002). "Blockade of neuropeptide Y(2) receptors and suppression of NPY's anti-epileptic actions in the rat hippocampal slice by BIIE0246." Br J Pharmacol **136**(4): 502-509.

Feng, G., R. H. Mellor, et al. (2000). "Imaging neuronal subsets in transgenic mice expressing multiple spectral variants of GFP." Neuron **28**(1): 41-51.

Figner, B., D. Knoch, et al. (2010). "Lateral prefrontal cortex and self-control in intertemporal choice." Nat Neurosci **13**(5): 538-539.

Flanders, K. C., R. F. Ren, et al. (1998). "Transforming growth factor-betas in neurodegenerative disease." Prog Neurobiol **54**(1): 71-85.

Foster, K. R. and M. L. Wiederhold (1978). "Auditory responses in cats produced by pulsed ultrasound." J Acoust Soc Am **63**(4): 1199-1205.

Franklin, K. B. J. and G. Paxinos (2007). The Mouse Brain in Stereotaxic Coordinates. New York, N.Y., Academic Press.

Fry, F. J., H. W. Ades, et al. (1958). "Production of reversible changes in the central nervous system by ultrasound." Science **127**(3289): 83-84.

Fry, W. J. (1958). "Use of intense ultrasound in neurological research." Am J Phys Med **37**(3): 143-147.

Fry, W. J. (1968). "Electrical stimulation of brain localized without probes--theoretical analysis of a proposed method." J Acoust Soc Am **44**(4): 919-931.

Fry, W. J., V. J. Wulff, et al. (1950). "Physical factors involved in ultrasonically induced changes in living systems: I. Identification of non-temperature effects." J Acoust Soc Am **22**: 867-876.

Gan, W. B., J. Grutzendler, et al. (2000). "Multicolor "DiOlistic" labeling of the nervous system using lipophilic dye combinations." Neuron **27**(2): 219-225.

Gartside, I. B. (1968). "Mechanisms of sustained increases of firing rate of neurones in the rat cerebral cortex after polarization: role of protein synthesis." Nature **220**(5165): 383-384.

Gartside, I. B. (1968). "Mechanisms of sustained increases of firing rate of neurons in the rat cerebral cortex after polarization: reverberating circuits or modification of synaptic conductance?" Nature **220**(5165): 382-383.

Gavrilov, L. R., G. V. Gersuni, et al. (1976). "The effect of focused ultrasound on the skin and deep nerve structures of man and animal." Prog Brain Res **43**: 279-292.

Gavrilov, L. R., E. M. Tsirulnikov, et al. (1996). "Application of focused ultrasound for the stimulation of neural structures." Ultrasound Med Biol **22**(2): 179-192.

Girardeau, G., K. Benchenane, et al. (2009). "Selective suppression of hippocampal ripples impairs spatial memory." Nat Neurosci **12**(10): 1222-1223.

Gora-Kupilas, K. and J. Josko (2005). "The neuroprotective function of vascular endothelial growth factor (VEGF)." Folia Neuropathol **43**(1): 31-39.

Goss-Sampson, M. A. and A. Kriss (1991). "Effects of pentobarbital and ketamine-xylazine anaesthesia on somatosensory, brainstem auditory and peripheral sensory-motor responses in the rat." Lab Anim **25**(4): 360-366.

Goss, S. A., R. L. Johnston, et al. (1978). "Comprehensive compilation of empirical ultrasonic properties of mammalian tissues." Journal of Acoustical Society of America **62**(2): 423-455.

Gradinaru, V., K. R. Thompson, et al. (2007). "Targeting and readout strategies for fast optical neural control in vitro and in vivo." J Neurosci **27**(52): 14231-14238.

Griesbauer, J., A. Wixforth, et al. (2009). "Wave propagation in lipid monolayers." Biophys J **97**(10): 2710-2716.

Guo, W., H. Jiang, et al. (2007). "Role of the integrin-linked kinase (ILK) in determining neuronal polarity." Dev Biol **306**(2): 457-468.

Hamani, C., D. Andrade, et al. (2009). "Deep brain stimulation for the treatment of epilepsy." Int J Neural Syst **19**(3): 213-226.

Harvey, E. N. (1929). "The effect of high frequency sound waves on heart muscle and other irritable tissues." American Journal of Physiology(1): 284-290.

Harvey, E. N., E. B. Harvey, et al. (1928). "Further Observations on the Effect of High Frequency Sound Waves on Living Matter " Biological Bulletin **55**(6): 459-469.

Hayner, M. and K. Hynynen (2001). "Numerical analysis of ultrasonic transmission and absorption of oblique plane waves through the human skull." J Acoust Soc Am **110**(6): 3319-3330.

Heimburg, T. (2010). "Lipid ion channels." Biophys Chem **150**(1-3): 2-22.

Heimburg, T. and A. D. Jackson (2005). "On soliton propagation in biomembranes and nerves." Proc Natl Acad Sci U S A **102**(28): 9790-9795.

Hertzberg, Y., O. Naor, et al. "Towards multifocal ultrasonic neural stimulation: pattern generation algorithms." J Neural Eng **7**(5): 056002.

Hira, R., N. Honkura, et al. (2009). "Transcranial optogenetic stimulation for functional mapping of the motor cortex." J Neurosci Methods **179**(2): 258-263.

Ho, M. W., A. G. Beck-Sickinger, et al. (2000). "Neuropeptide Y(5) receptors reduce synaptic excitation in proximal subiculum, but not epileptiform activity in rat hippocampal slices." J Neurophysiol **83**(2): 723-734.

Holgate, S. T., J. H. Wheeler, et al. (1973). "Starch peritonitis: an immunological study." Ann R Coll Surg Engl **52**(3): 182-188.

Holtzheimer, P. E. and H. S. Mayberg (2011). "Stuck in a rut: rethinking depression and its treatment." Trends Neurosci **34**(1): 1-9.

Hosobuchi, Y., J. Rossier, et al. (1979). "Stimulation of human periaqueductal gray for pain relief increases immunoreactive beta-endorphin in ventricular fluid." Science **203**(4377): 279-281.

Hsu, H. C., Y. C. Fong, et al. (2007). "Ultrasound induces cyclooxygenase-2 expression through integrin, integrin-linked kinase, Akt, NF-kappaB and p300 pathway in human chondrocytes." Cell Signal **19**(11): 2317-2328.

Huerta, P. T. and B. T. Volpe (2009). "Transcranial magnetic stimulation, synaptic plasticity and network oscillations." J Neuroeng Rehabil **6**: 7.

Hynynen, K. and G. Clement (2007). "Clinical applications of focused ultrasound-the brain." Int J Hyperthermia **23**(2): 193-202.

Hynynen, K., G. T. Clement, et al. (2004). "500-element ultrasound phased array system for noninvasive focal surgery of the brain: a preliminary rabbit study with ex vivo human skulls." Magn Reson Med **52**(1): 100-107.

Hynynen, K. and F. A. Jolesz (1998). "Demonstration of potential noninvasive ultrasound brain therapy through an intact skull." Ultrasound Med Biol **24**(2): 275-283.

Hynynen, K., N. McDannold, et al. (2006). "Pre-clinical testing of a phased array ultrasound system for MRI-guided noninvasive surgery of the brain--a primate study." Eur J Radiol **59**(2): 149-156.

Jefferys, J. G. and H. L. Haas (1982). "Synchronized bursting of CA1 hippocampal pyramidal cells in the absence of synaptic transmission." Nature **300**(5891): 448-450.

Jin, K. L., X. O. Mao, et al. (2000). "Vascular endothelial growth factor: direct neuroprotective effect in in vitro ischemia." Proc Natl Acad Sci U S A **97**(18): 10242-10247.

Johns, L. D. (2002). "Nonthermal Effects of Therapeutic Ultrasound: The Frequency Resonance Hypothesis." J Athl Train **37**(3): 293-299.

Jolesz, F. A. (2009). "MRI-guided focused ultrasound surgery." Annu Rev Med **60**: 417-430.

Jolesz, F. A., K. Hynynen, et al. (2005). "MR imaging-controlled focused ultrasound ablation: a noninvasive image-guided surgery." Magn Reson Imaging Clin N Am **13**(3): 545-560.

Kamen, G. and G. E. Caldwell (1996). "Physiology and interpretation of the electromyogram." J Clin Neurophysiol **13**(5): 366-384.

Klapstein, G. J. and W. F. Colmers (1997). "Neuropeptide Y suppresses epileptiform activity in rat hippocampus in vitro." J Neurophysiol **78**(3): 1651-1661.

Kleinfeld, D., P. P. Mitra, et al. (1998). "Fluctuations and stimulus-induced changes in blood flow observed in individual capillaries in layers 2 through 4 of rat neocortex." Proc Natl Acad Sci U S A **95**(26): 15741-15746.

Lee, J. H., R. Durand, et al. "Global and local fMRI signals driven by neurons defined optogenetically by type and wiring." Nature **465**(7299): 788-792.

Leighton, T. G. (2007). "What is ultrasound?" Prog Biophys Mol Biol **93**(1-3): 3-83.

Lele, P. P. (1963). "Effects of Focused Ultrasonic Radiation on Peripheral Nerve, with Observations on Local Heating" Experimental Neurology **8**: 47-83.

Lessmann, V., K. Gottmann, et al. (2003). "Neurotrophin secretion: current facts and future prospects." Prog Neurobiol **69**(5): 341-374.

Li, J., L. Fok, et al. (2009). "Experimental demonstration of an acoustic magnifying hyperlens." Nat Mater.

Li, Z., J. Burrone, et al. (2005). "Synaptic vesicle recycling studied in transgenic mice expressing synaptopHluorin." Proc Natl Acad Sci U S A **102**(17): 6131-6136.

Lozano, A. M. and B. J. Snyder (2008). "Deep brain stimulation for parkinsonian gait disorders." J Neurol **255 Suppl 4**: 30-31.

Ludwig, G. D. (1950). "The velocity of sound through tissues and the acoustic impedance of tissues." The Journal of the Acoustical Society of America **22**(6): 862-866.

Magee, T. R. and A. H. Davies (1993). "Auditory phenomena during transcranial Doppler insonation of the basilar artery." J Ultrasound Med **12**(12): 747-750.

Maroto, R., A. Raso, et al. (2005). "TRPC1 forms the stretch-activated cation channel in vertebrate cells." Nat Cell Biol **7**(2): 179-185.

Martin, E., D. Jeanmonod, et al. (2009). "High intensity focused ultrasound for non-invaisve functional neurosurgery." Annals of Neurology **66**: 858-861.

Mattson, M. P. (2005). "NF-kappaB in the survival and plasticity of neurons." Neurochem Res **30**(6-7): 883-893.

McDannold, N., M. Moss, et al. (2003). "MRI-guided focused ultrasound surgery in the brain: tests in a primate model." Magn Reson Med **49**(6): 1188-1191.

McNamara, J. O. (1994). "Cellular and molecular basis of epilepsy." J Neurosci **14**(6): 3413-3425.

Miesenbock, G., D. A. De Angelis, et al. (1998). "Visualizing secretion and synaptic transmission with pH-sensitive green fluorescence proteins." Nature **394**: 192-195.

Mihran, R. T., F. S. Barnes, et al. (1990). "Temporally-specific modification of myelinated axon excitability in vitro following a single ultrasound pulse." Ultrasound Med Biol **16**(3): 297-309.

Mihran, R. T., F. S. Barnes, et al. (1990). "Transient modification of nerve excitability in vitro by single ultrasound pulses." Biomed Sci Instrum **26**: 235-246.

Miller, D. L., S. V. Pislaru, et al. (2002). "Sonoporation: mechanical DNA delivery by ultrasonic cavitation." Somat Cell Mol Genet **27**(1-6): 115-134.

Mitragotri, S. (2005). "Healing sound: the use of ultrasound in drug delivery and other therapeutic applications." Nat Rev Drug Discov **4**(3): 255-260.

Molteni, R., F. Fumagalli, et al. (2001). "Modulation of fibroblast growth factor-2 by stress and corticosteroids: from developmental events to adult brain plasticity." Brain Res Brain Res Rev **37**(1-3): 249-258.

Morris, C. E. and P. F. Juranka (2007). Lipid Stress at Play: Mechanosensitivity of Voltage-Gated Channels. Current Topics in Membranes. P. H. Owen, Academic Press. **Volume 59:** 297-338.

Mortimer, A. J. and M. Dyson (1988). "The effect of therapeutic ultrasound on calcium uptake in fibroblasts." Ultrasound Med Biol **14**(6): 499-506.

Mukai, S., H. Ito, et al. (2005). "Transforming growth factor-beta1 mediates the effects of low-intensity pulsed ultrasound in chondrocytes." Ultrasound Med Biol **31**(12): 1713-1721.

Nakashiba, T., D. L. Buhl, et al. (2009). "Hippocampal CA3 output is crucial for ripple-associated reactivation and consolidation of memory." Neuron **62**(6): 781-787.

Naruse, K., A. Miyauchi, et al. (2003). "Distinct anabolic response of osteoblast to low-intensity pulsed ultrasound." J Bone Miner Res **18**(2): 360-369.

NEMA (2004). Acoustic Output Measurement Standard For Diagnostic Ultrasound Equipment. Washington, D.C., National Electrical Manufacturers Association.

Newall, R. G. and B. P. Bliss (1973). "Lipoproteins and the relative importance of plasma cholesterol and triglycerides in peripheral arterial disease." Angiology **24**(5): 297-302.

Newall, R. G., B. P. Bliss, et al. (1973). "Plasma lipids, blood coagulation and fibrinolysis in peripheral arterial disease." Postgrad Med J **49**(571): 297-299.

Nimmerjahn, A., F. Kirchhoff, et al. (2004). "Sulforhodamine 101 as a specific marker of astroglia in the neocortex in vivo." Nat Methods **1**(1): 31-37.

Nyborg, W. L. (1981). "Heat generation by ultrasound in a relaxing medium." Journal of Acoustical Society of America **70**(2): 310-312.

O'Brien, W. D., Jr. (2007). "Ultrasound-biophysics mechanisms." Prog Biophys Mol Biol **93**(1-3): 212-255.

Paoletti, P. and P. Ascher (1994). "Mechanosensitivity of NMDA receptors in cultured mouse central neurons." Neuron **13**(3): 645-655.

Pascual-Leone, A., J. Valls-Sole, et al. (1994). "Responses to rapid-rate transcranial magnetic stimulation of the human motor cortex." Brain **117 (Pt 4)**: 847-858.

Poo, M. M. (2001). "Neurotrophins as synaptic modulators." Nat Rev Neurosci **2**(1): 24-32.

Poulet, E., F. Haesebaert, et al. (2010). "Treatment of shizophrenic patients and rTMS." Psychiatr Danub **22 Suppl 1**: S143-146.

Purpura, D. P. and J. G. McMurtry (1965). "Intracellular Activities and Evoked Potential Changes during Polarization of Motor Cortex." J Neurophysiol **28**: 166-185.

Racine, R. J. (1972). "Modification of seizure activity by electrical stimulation. I. After-discharge threshold." Electroencephalogr Clin Neurophysiol **32**(3): 269-279.

Randhawa, H. S., F. Staib, et al. (1973). "Observations on the occurrence of Cryptococcus neoformans in an aviary, using niger-seed creatinine agar and membrane-filtration technique." Zentralbl Bakteriol Parasitenkd Infektionskr Hyg **128**(7): 795-799.

Raymond, S. B., L. H. Treat, et al. (2008). "Ultrasound enhanced delivery of molecular imaging and therapeutic agents in Alzheimer's disease mouse models." PLoS ONE **3**(5): e2175.

Reed, R. J. and B. O. Bliss (1973). "Morton's neuroma. Regressive and productive intermetatarsal elastofibrositis." Arch Pathol **95**(2): 123-129.

Reher, P., N. Doan, et al. (1999). "Effect of ultrasound on the production of IL-8, basic FGF and VEGF." Cytokine **11**(6): 416-423.

Ressler, K. J. and H. S. Mayberg (2007). "Targeting abnormal neural circuits in mood and anxiety disorders: from the laboratory to the clinic." Nat Neurosci **10**(9): 1116-1124.

Rinaldi, P. C., J. P. Jones, et al. (1991). "Modification by focused ultrasound pulses of electrically evoked responses from an in vitro hippocampal preparation." Brain Res **558**(1): 36-42.

Rosenmund, C. and C. F. Stevens (1996). "Definition of the readily releasable pool of vesicles at hippocampal synapses." Neuron **16**: 1197-1207.

Sankaranarayanan, S., D. De Angelis, et al. (2000). "The use of pHluorins for optical measurements of presynaptic activity." Biophys J **79**(4): 2199-2208.

Sant'Anna, E. F., R. M. Leven, et al. (2005). "Effect of low intensity pulsed ultrasound and BMP-2 on rat bone marrow stromal cell gene expression." J Orthop Res **23**(3): 646-652.

Shealy, C. N. and E. Henneman (1962). "Reversible effects of ultrasound on spinal reflexes." Archives of Neurology: 374-386.

Staib, F., H. S. Randhawa, et al. (1973). "[Peach and peach juice as a nutrient substratum for Cryptococcus neoformans with comments on some observations of F. Sanfelice (1894)]." Zentralbl Bakteriol Orig A **224**(1): 120-127.

Stoppini, L., P. A. Buchs, et al. (1991). "A simple method for organotypic cultures of nervous tissue." J Neurosci Methods **37**(2): 173-182.

Sukharev, S. and D. P. Corey (2004). "Mechanosensitive channels: multiplicity of families and gating paradigms." Sci STKE **2004**(219): re4.

Szobota, S., P. Gorostiza, et al. (2007). "Remote control of neuronal activity with a light-gated glutamate receptor." Neuron **54**(4): 535-545.

Tang, C. H., R. S. Yang, et al. (2006). "Ultrasound stimulates cyclooxygenase-2 expression and increases bone formation through integrin, focal adhesion kinase, phosphatidylinositol 3-kinase, and Akt pathway in osteoblasts." Mol Pharmacol **69**(6): 2047-2057.

ter Haar, G. (2007). "Therapeutic applications of ultrasound." Prog Biophys Mol Biol **93**(1-3): 111-129.

Tesseur, I. and T. Wyss-Coray (2006). "A role for TGF-beta signaling in neurodegeneration: evidence from genetically engineered models." Curr Alzheimer Res **3**(5): 505-513.

Thuault, S. J., J. T. Brown, et al. (2005). "Mechanisms contributing to the exacerbated epileptiform activity in hippocampal slices expressing a C-terminal truncated GABA(B2) receptor subunit." Epilepsy Res **65**(1-2): 41-51.

Tonnesen, J., A. T. Sorensen, et al. (2009). "Optogenetic control of epileptiform activity." Proc Natl Acad Sci U S A **106**(29): 12162-12167.

Tsui, P. H., S. H. Wang, et al. (2005). "In vitro effects of ultrasound with different energies on the conduction properties of neural tissue." Ultrasonics **43**(7): 560-565.

Tufail, Y., A. Matyushov, et al. (2010). "Transcranial Pulsed Ultrasound Stimulates Intact Brain Circuits " Neuron **Accepted, In Press**.

Tyler, W. J. (2010). "Noninvasive neuromodulation with ultrasound? A continuum mechanics hypothesis." The Neuroscientist **Advanced Online Print, January 25, 2010**.

Tyler, W. J., M. Alonso, et al. (2002). "From acquisition to consolidation: on the role of brain-derived neurotrophic factor signaling in hippocampal-dependent learning." Learn Mem **9**(5): 224-237.

Tyler, W. J., Y. Tufail, et al. (2008). "Remote excitation of neuronal circuits using low-intensity, low-frequency ultrasound." PLoS ONE **3**(10): e3511.

Tyler, W. J., Y. Tufail, et al. (2010). "Pain: Noninvasive functional neurosurgery using ultrasound." Nat Rev Neurol **6**(1): 13-14.

Utz, K. S., V. Dimova, et al. (2010). "Electrified minds: transcranial direct current stimulation (tDCS) and galvanic vestibular stimulation (GVS) as methods of non-invasive brain stimulation in neuropsychology--a review of current data and future implications." Neuropsychologia **48**(10): 2789-2810.

Velling, V. A. and S. P. Shklyaruk (1988). "Modulation of the functional state of the brain with the aid of focused ultrasonic action." Neuroscience and Behavioral Physiology **18**(5): 369-375.

Wagner, T., A. Valero-Cabre, et al. (2007). "Noninvasive Human Brain Stimulation." Annu Rev Biomed Eng **9**: 527-565.

White, P. J., G. T. Clement, et al. (2006). "Local frequency dependence in transcranial ultrasound transmission." Phys Med Biol **51**(9): 2293-2305.

White, P. J., G. T. Clement, et al. (2006). "Longitudinal and shear mode ultrasound propagation in human skull bone." Ultrasound Med Biol **32**(7): 1085-1096.

Yang, J. F. and D. A. Winter (1984). "Electromyographic amplitude normalization methods: improving their sensitivity as diagnostic tools in gait analysis." Arch Phys Med Rehabil **65**(9): 517-521.

Ylinen, A., A. Bragin, et al. (1995). "Sharp wave-associated high-frequency oscillation (200 Hz) in the intact hippocampus: network and intracellular mechanisms." J Neurosci **15**(1 Pt 1): 30-46.

Young, L., J. A. Camprodon, et al. (2010). "Disruption of the right temporoparietal junction with transcranial magnetic stimulation reduces the role of beliefs in moral judgments." Proc Natl Acad Sci U S A **107**(15): 6753-6758.

Young, R. R. and E. Henneman (1961). "Functional effects of focused ultrasound on mammalian nerves." Science **134**: 1521-1522.

Zhang, F., A. M. Aravanis, et al. (2007). "Circuit-breakers: optical technologies for probing neural signals and systems." Nat Rev Neurosci **8**(8): 577-581.

Zhang, F., V. Gradinaru, et al. "Optogenetic interrogation of neural circuits: technology for probing mammalian brain structures." Nat Protoc **5**(3): 439-456.

Zhang, F., L. P. Wang, et al. (2007). "Multimodal fast optical interrogation of neural circuitry." Nature **446**(7136): 633-639.

Zhang, S., L. Yin, et al. (2009). "Focusing Ultrasound with an Acoustic Metamaterial Network." Physics Reviews Letters **102**(19): 194301-194304.

Zhang, Y. P., N. Holbro, et al. (2008). "Optical induction of plasticity at single synapses reveals input-specific accumulation of alphaCaMKII." Proc Natl Acad Sci U S A **105**(33): 12039-12044.

This document was generated using the Graduate College Format Advising tool. Please turn a copy of this page in when you submit your document to Graduate College format advising. You may discard this page once you have printed your final document. DO NOT TURN THIS PAGE IN WITH YOUR FINAL DOCUMENT!

206